THE ROLE OF OBESITY-ASSOCIATED EXTRACELLULAR MATRIX REMODELING IN MACROPHAGE ACTIVATION AND POTENTIAL IMPLICATIONS TO BREAST CANCER

A Dissertation

Presented to the Faculty of the Graduate School

of Cornell University

In Partial Fulfillment of the Requirements for the Degree of

Doctor of Philosophy

by

Nora L. Springer

December 2019

THE ROLE OF OBESITY-ASSOCIATED EXTRACELLULAR MATRIX REMODELING IN MACROPHAGE ACTIVATION AND POTENTIAL IMPLICATIONS TO BREAST CANCER

Nora L. Springer, D.V.M, Ph. D.

Cornell University 2019

Obesity is associated with adipose inflammation, defined by macrophages encircling dead adipocytes, as well as extracellular matrix (ECM) remodeling and increased risk of breast cancer. Whether obesity-associated ECM-remodeling affects macrophage phenotype is uncertain. A better understanding of this relationship could be strategically important to reduce cancer risk or improve outcomes in people with obesity. Utilizing clinical samples, computational approaches and *in vitro* models, this study quantified the relative abundance of pro (M1)- and anti (M2)-inflammatory macrophages in human breast adipose tissue, determined molecular similarities between obesity and tumor-associated macrophages, and assessed the regulatory effect of obese versus lean ECM on macrophage phenotype. Our results suggest that breast adipose tissue contains more M2-biased than M1-biased macrophages across all body mass index (BMI) categories. Obesity further increased M2-biased macrophages but did not affect M1-biased macrophage density. Gene Set Enrichment Analysis (GSEA) suggested that breast tissue macrophages from obese versus lean women are more similar to tumor-associated macrophages (TAMs). These changes positively correlated with adipose tissue interstitial fibrosis, and *in vitro* experiments indicated that obesity-dependent ECM remodeling directly stimulate M2-biased macrophage functions.

However, mammographic density cannot be used as a clinical indicator of these changes. Collectively, our data suggest that obesity-associated interstitial fibrosis promotes a macrophage phenotype similar to TAMs, which may contribute to the link between obesity and breast cancer.

BIOGRAPHICAL SKETCH

Nora Lynn Springer is a graduate of Marietta College in Marietta, OH where she majored in Biology and minored in Chemistry. After her undergraduate studies, Nora worked full time at West Chelsea Veterinary Hospital in New York, NY while pursuing training to become a licensed veterinary technician at LaGuardia Community College in Long Island City, NY. In 2002, Nora obtained an Applied Associates Degree (AAS) with highest academic honors. She continued to work at West Chelsea Veterinary Hospital as a licensed veterinary technician until 2004 when she was accepted and enrolled at Kansas State University College of Veterinary Medicine. During her veterinary training, Nora participated in the competitive Merck/Merial Veterinary Research Scholars Program where she completed a project, supervised by Thomas Schermerhorn, VMD, DACVIM, focused on feline glucose metabolism. Nora was inducted into Phi Zeta, the veterinary honor society in 2008. After obtaining her Doctorate of Veterinary Medicine (DVM), Nora completed a companion animal internship in medicine and surgery at Louisiana State University School of Veterinary Medicine. Subsequently, she joined the Clinical Pathology Laboratory at the New York State Veterinary College at Cornell University as a Veterinary Clinical Pathology Resident. During her residency, Nora pursued research in the field of equine coagulation, under the mentorship of Tracy Stokol, BVSc, Ph.D., DACVP. This project was awarded the American Society for Clinical Pathology Share the Future Research Award in 2010. Nora achieved Diplomate status in the American College of Veterinary Pathologists (Clinical Pathology) in 2013. Post-residency, Nora elected to pursue advanced research training in a Ph.D. program through the field of Biological and Biomedical Sciences and the School of Biomedical Engineering at Cornell University under the mentorship of Claudia Fischbach, Ph.D. During her graduate work, Nora mentored two Masters of Engineering students, one

undergraduate student, one Veterinary Leadership Program student, and one dual degree (DVM/Ph.D) rotation student. She also actively participated in science communication and outreach via a partnership between Cornell University cancer researchers and the Cancer Resource Center of the Finger Lakes. In July 2017, Nora returned to her alma mater, Kansas State University College of Veterinary Medicine, as an Assistant Professor in the Department of Diagnostic Medicine and Pathobiology.

This work is dedicated to my father, Joel H. Springer, whose faith in me is unwavering.

ACKNOWLEDGMENTS

Like many people, serendipity and taking advantage of opportunities that have presented themselves have greatly influenced my successes. I was fortunate to be born into a family where curiosity, learning, and education were encouraged and valued. My mother, Nancy Connor, father, Joel Springer, and brother Jonathan Springer have always cheered me on while being somewhat bemused by my state as a "professional student" for the past nearly 40 years. More recently, my stepfather Jaime Pinto and sister-in-law Kristin Reign Springer have joined the cheering squad.

I have been fortunate to have extraordinary mentors throughout my professional training. Before working with Tom Schermerhorn I never considered that a veterinarian could be a research scientist, too. Tracy Stokol and John Parker recognized potential in me that I did not see in myself and their constant support and encouragement gave me the courage to pursue the Ph.D degree. Claudia Fischbach has been an extraordinary mentor during my PhD studies. The highest compliment I can pay her is that I will strive to emulate her constant professionalism and sharp analytical mind. My committee members, Cynthia Leifer and Rick Cerione have also added invaluable input during my Ph.D training for which I owe them my gratitude.

The Ph.D. process is often described as a roller coaster with frequent ups and downs, but it is also a marathon with stretches of agony. Without my tribe of dear friends, I am certain I would not have made it through. Rebecca Weger, Angharad Waite, Erika Gruber, Tammy Kubinec, Chris Kitchen, Maureen Lynch, Michele Keyerleber, Ryan Fitzgerald, Douglas Marthaler, Tyler Suelter, Katie Jordan, and Laura Constance were the people I laughed and cried with these past seven years and made this whole crazy ride worth it.

TABLE OF CONTENTS

Biographical Sketch v
Dedication vi
Acknowledgements vii
List of Figures xi
List of Tables xii
List of Abbreviations xiii
Introduction 15
Chapter 1: Characterization of macrophage populations in breast adipose tissue in the lean and obese state 23
1.1 Introduction 24
1.2 Materials and Methods 25
1.3 Study population 28
1.4 Obesity-associated structural and compositional changes to breast adipose tissue 28
1.5 Macrophage polarization 30
1.6 Spatial organization of macrophages in human breast tissue 31
1.7 Confirmation of macrophage phenotype via computational biology methodology 34
1.8 Interstitial fibrosis of human samples correlates to M2-biased macrophage polarization state 35
1.9 Mammographic and histological breast density are not predictive of interstitial fibrosis or macrophage content 37
1.10 Discussion 39
Chapter 2: Extracellular matrix-macrophage interactions in obesity regulate macrophage activation and function 44
2.1 Introduction 45
2.2 Materials and Methods 46
2.3 Decellularized extracellular matrix model to study macrophage-ECM interactions in obesity 49
2.4 Preparation and validation of bone marrow-derived macrophages 52
2.5 Assessment of ECM-mediated macrophage morphology 52
2.6 Assessment of ECM-mediated macrophage proliferation 54
2.7 ECM-mediated macrophage polarization 54
2.8 Discussion 57
Chapter 3: Obese extracellular matrix-macrophage signaling promotes a Phenotype similar to pro-angiogenic tumor-associated macrophages 60
3.1 Introduction 61
3.2 Materials and Methods 62
3.3 Transcriptional identification of TAM 65
3.4 Obesity-primed macrophages promote angiogenesis 70
3.5 Osteopontin and TIMP-1 are potential mediators of obese ECM proangiogenic stimulus of macrophages 72

3.6 Discussion 73
Chapter 4: Discussion and Future Directions 76
4.1 Biomaterials approaches to modeling ECM-macrophage interactions 76
4.2 Comprehensive characterization of obesity-associated ECM and macrophage populations 81
4.3 Obese adipose tissue as a depot for tumor-promoting immune cells 86
4.4 The cumulative effect and reversibility of obesity-associated ECM remodeling on cancer risk 87
4.5 Broader impacts and concluding remarks 88
Appendix: Collaborative in vivo studies investigating the stromal microenvironment in gastric and breast cancer pathogenesis 91
A.1 Introduction 93
A.2 CD44v6 increases gastric cancer malignant potential by modulating adipose stromal cell-mediated ECM remodeling 93
A.3 Hydroxyapatite mineral enhances malignant potential in a tissue-Engineered model of ductal carcinoma in situ (DCIS) 100
A.4 Obesity-associated extracellular matrix promotes malignancy by Increasing stem-like properties in breast cancer cells 104
References 108

LIST OF FIGURES

Figure 1: Structural changes to breast adipose tissue during obesity 30
Figure 2: Macrophage polarization 31
Figure 3: Aperio ImageScope positive pixel algorithm methodology 32
Figure 4: CD11c and CD206 immunohistochemistry on breast tissue 33
Figure 5: CD206 density is independent of CLS presence 33
Figure 6: CIBERSORT M1 and M2 score on breast adipose tissue 34
Figure 7: Interstitial fibrosis and correlations to M1 versus M1 macrophages 36
Figure 8: BMI correlations to interstitial fibrosis and CD11c 37
Figure 9: Histological and mammographic breast density across BMI 38
Figure 10: Mammographic density is not predictive of interstitial fibrosis 39
Figure 11: Schematic of decellularized ECM methodology 50
Figure 12: Decellularized ECM mimics *in vivo* interstitial fibrosis 51
Figure 13: Validation of *in vitro* macrophage polarization protocols 52
Figure 14: Macrophage alignment on lean and obese ECM 53
Figure 15: Macrophage aspect ratio on lean and obese ECM 54
Figure 16: Macrophage proliferation on lean and obese ECM 55
Figure 17: Macrophage polarization (CD206 and arginase-1) on lean and obese ECM 56
Figure 18: Macrophage polarization (iNOS) on lean and obese ECM 56
Figure 19: Gene set enrichment analysis comparison of macrophages from obese breast tissue versus TAM 66
Figure 20: Venn diagram comparing TAM gene profile to human macrophage genes 66
Figure 21: Heatmap of differential expression of macrophage genes in lean versus obese women 68
Figure 22: Assessment of gene function in macrophage genes differentially Expressed between lean versus obese women 70
Figure 23: Correlation between CD206 and CD31 in breast adipose tissue 71
Figure 24: HUVEC transwell migration and tube formation assays 72
Figure 25: Angiogenesis protein microarray 73
Figure 26: Mechanosignaling regulation of macrophage phenotype 77
Figure 27: CD44v6 alters tumor growth and architecture *in vitro* 96
Figure 28: CD44v6 expression enhances desmoplasia in tumor xenografts 97
Figure 29: CD44v6 enhances tumor xenograft growth and proliferation 99
Figure 30: Exposure of DCIS cells to hydroxyapatite mineral in scaffolds Promotes features of increased malignancy *in vivo*. 103
Figure 31: Obese ASCs promote co-localization of NANOG positive cells and fibrotic ECM 107

LIST OF TABLES

Table 1: Demographic and clinicopathological features of study cohort 29
Table 2: Genes upregulated in TAM and obese vs. lean adipose tissue 69

LIST OF ABBREVIATIONS

ANOVA	Analysis of variance
ASC	Adipose stromal cell
BMDM	Bone marrow-derived macrophages
BMI	Body mass index
BRCA	breast cancer 1, early onset gene
BrdU	Bromodeoxyuridine
CAF	Cancer-activated fibroblast
CLS	Crown-like structure
CD	Cluster of differentiation
CM	Conditioned medium
COX-2	Cyclooxygenase 2
DAPI	4′,6-diamidino-2-phenylindole
DCIS	Ductal carcinoma in situ
DMEM	Dulbecco's modified Eagle's medium
DNA	Deoxyribonucleic acid
DXA	Dual-energy x-ray absorbitometry
ECM	Extracellular matrix
EGF	Epidermal growth factor
ELISA	Enzyme-linked immunosorbent assay
ER	Estrogen receptor
FAK	Focal adhesion kinase
FBS	Fetal bovine serum
FFPE	Formalin fixed paraffin embedded
Fn	Fibronectin
GC	Gastric carcinoma
GSEA	Gene set enrichment analysis
GTP	Guanosine-5'-triphosphate
H&E	Hematoxylin and eosin stain
HA	Hydroxyapetite
HER2	Human epidermal growth factor receptor 2
HUVEC	Human umbilical vein endothelial cells
IFNγ	Interferon gamma
IHC	Immunohistochemistry
IL	Interleukin
iNOS	Inducible nitric oxide synthase
LPS	Lipopolysaccharide
MC	Microcalcification
M-CSF	Macrophage colony stimulating factor
MMP	Matrix metalloproteinase
MMTV	Mouse mammary tumor virus
OPN	Osteopontin
PA	Polyacrylamide

PBS	Phosphate-buffered saline
PEG	Polyethylene glycol
PFA	Paraformaldehyde
PI3K	Phospatidylinositol 3-kinase
PLG	Poly (lactide-*co*-glycolide)
PR	Progesterone receptor
PyMT	Polyoma virus middle T antigen
RGD	Arginylglycylaspartic acid
RNA	Ribonucleic acid
ROCK	Rho-associated protein kinase
SD	Standard deviation
SPP-1	Secreted phosphoprotein-1
TAM	Tumor-associated macrophage
TGFβ	Transforming growth factor beta
TIMP	Tissue inhibitor of matrix metalloproteinase
UV	Ultraviolet
WAT	White adipose tissue
WATi	White adipose tissue inflammation
WT	Wild type

INTRODUCTION

Obesity is a known preventable risk factor for 12 kinds of cancer, including breast cancer, and an estimated 20% of cancer mortalities are attributable to obesity. Obesity is the most significant risk factor for breast cancer development in postmenopausal women and is associated with a worse clinical prognosis and increased mortality in breast cancer patients independent of subtype or menopausal status[1,2]. The mechanisms underlying the link between obesity and breast cancer are multifactorial. Alterations to hormonal status, energy balance, and systemic metabolic derangements due to excessive adiposity have been implicated in the obesity and breast cancer connection and have been reviewed elsewhere[3–7]. As breast tissue is partially composed of adipose tissue, localized changes to the physicochemical properties of the adipose tissue microenvironment might be similarly important in breast cancer development.

Both normal and cancerous tissues are composed of multiple cell types and support structures, termed the microenvironment, that work together to achieve homeostasis and when perturbed can result in pathology. The microenvironment is an active participant in cancer initiation, growth, and metastasis through such functions as angiogenesis, cancer-activated fibroblasts that provide growth signals and deposit excess extracellular matrix (ECM), and an anti-inflammatory cytokine milieu secreted, in part, by tumor-associated macrophages (TAM) to dampen tumoricidal effector cells of the immune system. Interestingly, the microenvironment of obese versus lean adipose tissue shares common features with the breast cancer microenvironment including increased fibrosis and chronic inflammation. Based on these similarities, it is plausible that the obese adipose tissue microenvironment is a fertile soil for future breast cancer development or promotes tumor growth and metastasis after breast

cancer initiation. Below, I will give a brief overview of the shared microenvironmental features of breast cancer and adipose tissue followed by a discussion of known contributions of obese adipose tissue to breast cancer development.

The breast cancer microenvironment is fibrotic, which is associated with TAM density and tumor aggressiveness

Increased mammographic density, which correlates to the stromal component of breast tissue, is a strong independent risk factor for breast cancer[8]. The biological basis for how mammographic density, or fibrosis, raises breast cancer risk is not fully understood, but mechanical perturbations to epithelial cell morphogenesis[9] likely play a role. After tumor initiation, a robust deposition of extracellular matrix, termed desmoplasia, occurs. The mediators of this stromal remodeling in the breast cancer microenvironment are cancer-activated fibroblasts (CAF). CAF share features of fibroblasts and smooth muscle cells (otherwise known as myofibroblasts) and produce and crosslink ECM proteins such as collagens and proteoglycans and also produce growth factors and cytokines[10]. This deposition of ECM results in tissue stiffening that can be used to detect a tumor via palpation versus the adjacent softer, non-neoplastic tissue.

Studies assessing the structure of ECM remodeling associated with breast cancer illustrate more significant remodeling, characterized by thicker, linearized fibers perpendicular to the tumor bulk, as neoplasms progress from pre-malignant ductal carcinoma in situ (DCIS), to malignant invasive carcionoma[11,12]. Indeed, collagen fiber arrangement surrounding DCIS lesions at the time of initial surgical excision is predictive of which lesions will recur,[13] indicating a coupling of ECM remodeling to cancer aggressiveness. This is not entirely surprising as these parallel

fibers have been shown to be densest at the invading front[11] and facilitate tumor cell migration and invasion via contact guidance directional cues[12,14].

Interestingly, this ECM remodeling is also coupled to the presence and density of TAM in the tumor. Acerbi et al. found that the number of cluster of differentiation (CD) 68+ macrophages correlated to ECM stiffness, as measured by atomic force microscopy, and both CD68+ macrophages and ECM stiffness correlated to more aggressive breast cancer subtypes, both basal and human epidermal growth factor receptor (HER) 2+ versus less aggressive luminal A or luminal B. Huo and colleagues assessed macrophage content in high mammographic density versus low mammographic density samples and, although they did not see a difference in macrophages labeled with the pan-macrophage marker CD68, they did see a significant increase in macrophages that were CD206+, corresponding to an M2 anti-inflammatory/pro-fibrotic macrophage phenotype[15], common with TAM.

A higher density of TAM is associated with a poorer prognosis in breast cancer[16,17]. TAMs are a heterogenous cell population with multifaceted functions. TAM recruitment is primarily through Ly6C^{hi} inflammatory monocytes that extravasate in response to tumor production of macrophage chemoattractants, of which the chemokine ligand CCL2 is an important mediator[18,19]. Once arriving at the tumor microenvironment, these inflammatory monocytes usually adopt a pro-tumoral phenotype, similar to an anti-inflammatory or pro-fibrotic M2-biased phenotype, and promote tumor growth and metastasis[20,21]. Indeed, high densities of TAM have been identified on the invading front of tumors, where intravital imaging has identified interactions between tumor cells, TAMs, and blood vessels,[22] supporting a role for TAMs in tumor cell migration and metastasis, similar to collagen remodeling mentioned above. The relationship between collagen remodeling and macrophage density is likely reciprocal where macrophages provide key matrix-remodeling

enzymes and, based on recent discoveries in mechanical regulation of macrophage behaviors[23], the altered tumor ECM may modulate macrophage migration and function.

Obese adipose tissue is fibrotic and inflamed

White adipose tissue (WAT) is a dynamic organ that rapidly expands and contracts based on bodily nutrient requirements. WAT consists of the parenchymal cell, the adipocyte, as well as the stromal vascular fraction, which is a conglomerate of precursor cells (adipose stromal cells, herein referred to as ASCs), immune cells, extracellular matrix, and vascular components. Remodeling of adipose tissue is maintained in homeostasis in the lean state but physiologically accelerates in the obese state where the adipocyte mass rapidly outgrows angiogenic capabilities[24]. Hypoxia response elements in WAT upregulate profibrotic gene expression[25] and adipocyte cell death is proposed to lead to an influx of inflammatory cells[26,27]. These tissue perturbations of fibrosis and inflammation result in reduction of adipocyte plasticity ultimately leading to adipocyte dysfunction. Systemic manifestations of this adipocyte dysfunction and secondary inflammation are alterations in lipid handling and hormonal regulation of adipokines as well as increased circulating levels of pro-inflammatory cytokine and acute phase protein reactants[28].

The mediators of fibrotic remodeling in WAT are myofibroblasts differentiated ASCs. ASCs are multipotential cells that share characteristics with mesenchymal stromal cells. Under homeostasis, ECM deposition in WAT is part of the normal remodeling process; however, in the case of obesity, the stimuli for ECM remodeling, including hypoxia and inflammation, are persistent resulting in enhanced myofibroblast differentiation. The ECM components deposited by the myofibroblasts consist predominantly of collagen I, collagen III, collagen VI, and fibronectin[29–32].

Collagen VI, in particular, is highly enriched in obese WAT ECM and appears to have a profound effect on the secondary metabolic consequences associated with WAT fibrosis[30,31]. In a genetic mouse model of obesity (*ob/ob* mice lacking leptin) crossed with collagen VI knockout mice (*Col6KO*) had improved glucose tolerance and lipid clearance despite similar body size and larger adipocyte area[30]. Notably, *Col6KOob/ob* mice had decreased inflammation on histological sections, suggesting that fibrosis and inflammation in obese WAT are not completely independent processes.

White adipose tissue inflammation (WATi) is thought to accumulate secondary to the release of adipocyte cellular contents, such as lipid or damage-associated molecular patterns, into the environment through necrosis[33]. These signals are triggers for macrophage accumulation through both extravasation of circulating monocytes[34] and local proliferation of tissue resident macrophages[35,36]. These macrophages encircle the dead or dying adiopocytes,[33] where they are histologically recognized and termed crown-like structures (CLS)[34,37]. These macrophages are exquisitely pro-inflammatory due to activation of macrophage pattern recognition receptors and downstream activation of the inflammasome,[38,39] contributing to insulin resistance and metabolic dysfunction. Indeed, ablation of adipose tissue macrophages with clodronate liposomes[40] results in improved metabolic status. Macrophages in obesity also reside in the interstitial spaces between adipocytes and are phenotypically different than the cells that reside in CLS[28], being more similar to M2, anti-inflammatory/pro-fibrotic macrophages[35]. Very little is known about the role of this macrophage population within obese adipose and this is the population of macrophages that is the focus of the work presented within this dissertation.

Known contributions of the obese adipose tissue microenvironment on breast tumorigenesis

Although the mechanisms underlying the obesity-cancer relationship are not fully understood, there are several aspects of the obese WAT microenvironment that have been determined to contribute to breast cancer and will be briefly outlined below.

Adipose stromal cells have been identified as mediators of breast tumorigenesis through myofibroblast differentiation with resultant ECM deposition, crosslinking, and tissue stiffening[41]. Obese WAT contains an enriched proportion of myofibroblasts relative to lean WAT[42]. In an orthotopic mouse model of breast tumorigenesis, ASCs from obese WAT co-implanted with breast cancer cells enhance tumor growth and invasion versus cancer cells mixed with control ASCs[43]. ASCs from obese WAT also assemble ECM that is partially unfolded and stiffer than the lean counterpart, which contributes to tumorigenesis[42].

Similar to the breast tumor microenvironment, obesity-associated fibrosis perturbs epithelial cells and promotes malignant behaviors. ECM deposited by ASCs from obese versus lean mice promoted breast epithelial cellular growth and migratory capability, two features used as indicators of potential malignant behavior[42]. Deletion of collagen VI in a MMTV-PyMT mouse model of cancer led to reduced epithelial hyperplasia and tumor growth,[44] indicating a direct role of ECM remodeling on breast tumorigenesis.

Adipose tissue inflammation, in the form of CLS, is probably the best studied component of the WAT microenvironment within the context of breast cancer. CLS have been described in subcutaneous[34], visceral[45], and breast[46] WAT. CLS have been utilized as a biomarker in breast tissue biopsies as these histological structures are found in a greater density in breast tissue from people with obesity and are associated with both an increased risk of breast cancer and shorter relapse-free survival in women

with recurrent metastatic breast cancer[46–48]. WATi has been shown to be reversible with weigh loss in mouse models of obesity[49]. However, despite body weight, the presence of WATi, in itself, might have negative prognostic implications as a subset of women with normal BMI but histological evidence of breast inflammation[4] or increased adiposity when measured via dual-energy x-ray absorbitometry (DXA)[3] are at increased risk for breast cancer development, similar to obese individuals.

At the whole tissue level, obese adipose tissue contains macrophages that display activation of cancer-related pathways, based on gene expression analysis[50]. Additionally, obesity has been shown to recruit and activate macrophages through the CCL2 signaling axis[51], the same signaling pathway that is critical to TAM recruitment activation. These macrophages help mediate angiogenic remodeling in the obese WAT microenvironment that then facilitate more rapid tumor growth after implantation[51]. Taken together, these findings suggest that macrophages present in WAT contribute to a tumor-permissive microenvironment. However, neither of the cited studies evaluated macrophage subsets or spatial distribution, so it is unknown whether macrophages present in CLS or the interstitial macrophages, briefly mentioned above, contribute to this process.

Evaluating adipose tissue interstitial macrophages in the context of breast cancer

Macrophages, specifically M2-biased or anti-inflammatory macrophages are pivotal regulators of fibrosis, inflammation, and angiogenesis. Because of these relationships and recent evidence that macrophage function can be regulated by the physical environment[23,52–54] we pursued the global hypothesis that obesity-associated extracellular matrix remodeling promotes a macrophage polarization state similar to TAM. In the work presented herein we assessed the spatial distribution of M1 versus M2-biased macrophages in relationship to adipose interstitial fibrosis in breast tissue

(Chapter 1). We also evaluated the ability of obesity-associated ECM to modulate macrophage polarization *in vitro* (Chapter 2) and assessed the similarity of obesity-associated macrophages to TAM with supportive *in vitro* functional assessment (Chapter 3). Results from this work are broadly applicable to other obesity-associated cancers, as discussed in Chapter 4, future directions.

CHAPTER 1

CHARACTERIZATION OF MACROPHAGE POPULATIONS IN BREAST ADIPOSE TISSUE IN THE LEAN AND OBESE STATE

Chapter written using content modified from the following publication:

Nora L. Springer[1,2,3], Neil M. Iyengar[4,5], Rohan Bareja[6], Akanksha Verma[6], Maxine Jochelson[7], Dilip D. Giri[4], Xi Kathy Zhou[8], Olivier Elemento[6], Andrew J. Dannenberg[5], and Claudia Fischbach[2,9] Obesity-associated extracellular matrix remodeling promotes a macrophage phenotype similar to tumor-associated macrophages. *Am J Path* 2019;189(10);2019-2035. PMID: 31323189

[1]Biological and Biomedical Sciences, Cornell University, Ithaca, NY

[2]Meinig School of Biomedical Engineering, Cornell University, Ithaca, NY

[3]Department of Diagnostic Medicine/Pathobiology, Kansas State University, Manhattan, KS

[4]Department of Medicine, Memorial Sloan Kettering Cancer Center, New York, NY

[5]Department of Medicine, Weill Cornell Medicine, New York, NY

[6]Institute for Computational Biomedicine, Caryl and Israel Englander Institute for Precision Medicine, Weill Cornell Medicine, New York, NY

[7]Department of Radiology, Memorial Sloan Kettering Cancer Center, New York, NY

[8]Department of Healthcare Policy and Research, Weill Cornell Medicine, New York, NY

[9]Kavli Institute at Cornell for Nanoscale Science, Cornell University, Ithaca, NY

N.L.S performed all histological and in vitro experiments unless otherwise indicated. N.M.I and A.J.D provided clinical samples and demographic data, X.K.Z provided biostatistical support, D.D.G performed initial CLS assessment, M.J. provided

mammographic interpretation. R.B., A.V, and O.E. performed transcriptomic and computational analysis. N.L.S, and C.F. designed the project and wrote the paper. All authors provided input on the manuscript.

1.1 Introduction

Excess body weight has been associated with both an increased risk of cancer and worse prognosis for some tumor types[55]. In particular, obesity has been linked with the development of both hormone receptor positive postmenopausal[56–58] and triple negative breast cancer[59]. Furthermore, obesity contributes to a worse clinical outcome in both pre- and post-menopausal breast cancer patients[2,60]. Historically, the link between obesity and breast cancer has been attributed to metabolic dysregulation, altered secretion of adipokines, elevated levels of estrogen, and inflammation[61–64]. Yet experimental evidence suggests that obesity-dependent interstitial fibrosis of breast adipose tissue may also be important[42].

Fibrosis is a hallmark of obese white adipose tissue that is characterized by excess amounts of ECM of varying composition, structure, and mechanical properties being deposited within the stromal-vascular fraction between adipocytes, herein referred to as interstitial fibrosis[27,42,65]. Given that myofibroblasts are considered key players in mediating fibrosis, it is not surprising that these cells are also increased in white adipose tissue. More specifically, ASCs isolated from the stromal vascular fraction (SVF) of obese versus lean mice are enriched in myofibroblasts that lay down abundant ECM. The resulting ECM contains increased amounts of aligned collagen type I and fibronectin fibers and is mechanically stiffer, ultimately promoting malignant tumor cell behavior due to increased mechanosignaling[42]. This finding is directly relevant to humans as demonstrated by analysis of human breast adipose tissue and cancer samples[42] and because ECM remodeling genes are highly enriched

in the transcriptomic signature of subcutaneous white adipose tissue in obese individuals[66]. While the pathophysiology underlying obesity-associated interstitial fibrosis is complex, it is commonly linked to WATi, another hallmark of obesity[34,37,66].

WATi has been identified in breast tissue from women with obesity and is associated with both an increased risk of breast cancer and shorter relapse-free survival in women with recurrent metastatic breast cancer[46–48]. Histologically, WATi appears as a grouping of macrophages surrounding dead or dying adipocytes, termed crown-like structures (CLS). CLS have been described in subcutaneous[34], visceral [45], and breast [46] adipose tissue and are considered to consist of pro-inflammatory (M1) macrophages as their presence correlates with increased circulating levels of pro-inflammatory cytokines and positive acute phase proteins[4,67]. Nevertheless, recent experimental evidence in mice and people indicates that anti-inflammatory (M2) macrophages may also be increased with obesity[35,50,68]. Whether similar findings apply to human breast adipose tissue remains unclear.

Here, in order to investigate the hypothesis that interactions between obesity-associated interstitial fibrosis and macrophages promote an anti-inflammatory phenotype, we first investigated the spatial distribution of pro- and anti-inflammatory macrophages and relationship of these macrophage phenotypes with interstitial fibrosis in tumor-free regions of breast adipose tissue via immunohistochemistry (IHC). We further analyzed these sections with picrosirius red staining to highlight interstitial fibrosis between adipocytes, and clinical mammographic imaging findings to correlate findings to global or bulk fibrosis of breast tissue.

1.2 Materials and Methods

Clinical data, biospecimen collection, and breast tissue assessment

Clinical data and archived formalin-fixed and paraffin embedded (FFPE) samples were obtained from a cohort of women who underwent mastectomy for breast cancer risk reduction or treatment between January 2011 and August 2013 at Memorial Sloan Kettering Cancer Center (MSKCC) in New York, NY. In this cohort, non-tumor-containing breast white adipose tissue, from either the contralateral breast, or a breast quadrant unaffected by the tumor, was prospectively collected at the time of surgery. CLS presence in breast adipose tissue had been previously classified in this cohort[47]. Samples were randomly selected based on a power analysis estimating 80% power to detect a correlation of 0.4 using a two-sided hypothesis test with a significance level of 0.05. Macrophage polarization states in breast white adipose tissue were evaluated via IHC on the FFPE breast tissue. Five-micrometer sections were probed with rabbit polyclonal anti-mannose receptor (CD206) (Abcam, Cambridge, MA, ab64693) or rabbit monoclonal anti-CD11c (Abcam ab52623). The signal was amplified using Vectastain ABC universal kit (Vector Laboratories, Burlingame, CA) and detected with peroxidase substrate and DAB chromogen (ThermoFisher, Waltham, MA) and hematoxylin counter stain. Tissue sections were also stained with hematoxylin and eosin (H&E) or picrosirius red. Samples with repeatable severe sectioning artifact were excluded from analysis. Stained slides were digitally archived with an Aperio CS2 microscope (Leica Biosystems, Buffalo Grove, IL) and were analyzed with the ImageScope software positive pixel count algorithm v9. Picrosirius red-stained sections were imaged under crossed polarized light[69] with a Nikon (Melville, NY) TE2000-S microscope and an RTKE (Spot Imaging Solutions, Inc., Sterling Heights, MI) color camera and images analyzed with Image J software (NIH, Bethesda, MD, v1.48, https://imagej.nih.gov/ij/download.html) using an algorithm for positive pixel counts. Mammographic data were retrieved from the patient medical record, when available (n=26), and anonymized prior to use.

Mammographic density pattern was determined by a radiologist (MJ). Histological density of breast tissue was determined by evaluating the ratio of fibroglandular tissue to adipose tissue per section, as previously described[15].

Breast tissue transcriptomic and computational analysis

At the time of collection, fresh tissue specimens were snap-frozen, stored in RNAlater (Ambion, Foster City, CA) and total RNA was extracted for RNA-seq using the RNeasy Mini Kit (Qiagen, Valencia, CA). Polyadenylated RNA-seq was performed using the standard Illumina (San Diego, CA) Truseq kits and samples were sequenced using the HiSeq2000 platform. All reads were independently aligned with STAR_2.4.0f1 for sequence alignment against the human genome build hg19, downloaded via the UCSC genome browser, and SAMTOOLS v0.1.19 for sorting and indexing reads. The resultant transcripts were analyzed with the LM22 CIBERSORT signature[70] to estimate macrophage polarization subsets, based on a signature matrix from 547 genes that effectively differentiate 22 distinct human hematopoietic cell populations, in lean versus obese breast tissue.

Statistical Analysis

All statistical analysis was performed using Prism v7.0 (GraphPad Software, La Jolla, CA) and R v3.4.3. Differences in patient characteristics across BMI categories were examined using ANOVA for continuous variables and Fisher's exact test for categorical variables. Normality assumption of the parametric method was assessed by the Shapiro-Wilk test. Continuous data are represented as the mean ± standard deviation (SD) or the median and interquartile range. Categorical data were summarized in terms of counts and percentages. Correlations between two continuous variables were assessed using Spearman's method. Specific statistical tests used and

number of independent samples and replicates per experiment are listed in the figure legends. A Tukey's post-hoc test was used when needed to account for multiple comparisons. Significance was set at $P < 0.05$.

1.3 Study population

Demographic data for the 50 women selected for this study are presented in Table 1. Based on body mass index (BMI), women were stratified into lean (BMI < 25), overweight (BMI 25-29.9), and obese (BMI ≥ 30) groups. No differences were found between groups with respect to age, race, breast cancer 1, early onset gene (BRCA) mutation, or subtype of breast cancer (such as hormone receptor positive versus triple negative breast cancer). Menopausal status and breast inflammation in the form of histologically identified CLS were significantly different between groups. Women with obesity (66.7%) were more likely to be postmenopausal than lean (17.4%) women. The incidence of CLS increased from lean (34.8%) to overweight (50%) to obese (100%).

1.4 Obesity-associated structural and compositional changes to breast adipose tissue

Breast tissue is a composite of fibroglandular tissue surrounded by abundant adipose tissue (Figure 1). Therefore, obesity-dependent structural changes to adipose tissue, including interstitial fibrosis and inflammation (Figure 1) alter the breast microenvironment and, thus, potentially tumorigenesis. For the purposes of the studies reported in Chapters 1-3, only the adipose tissue, and not the fibroglandular compartment of breast tissue, is being modeled.

Table 1: Demographic and clinicopathological features of a cohort of 50 women undergoing mastectomy for preventative or therapeutic reasons. BMI = body mass index, BRCA = breast cancer 1, early onset gene, ER = estrogen receptor, PR = progesterone receptor, HER2 = human epidermal growth factor receptor 2, HR = hormone receptor. Statistically significant p-values, as determined by either ANOVA for continuous variables or Fisher's exact test for categorical variables are bolded. Published in Springer NL, *et al*. *Am J Path* 2019;189(10);2019-2035

	All (n=50)	Lean (n=23)	Overweight (n=18)	Obese (n=9)	p-value
Age, mean +/- SD	47.1 +/- 8.6	45.0 +/- 8.7	49.5 +/- 8.2	47.6 +/- 8.8	0.243
Race, n (%)					
Asian	5 (10.2%)	2 (8.7%)	3 (17.7%)	0 (0%)	
Black	5 (10.2%)	1 (4.4%)	2 (11.8%)	2 (22.2%)	
White	39 (79.6%)	20 (86.9%)	12 (70.6%)	7 (77.8%)	0.379
missing	1 (2%)	0 (0%)	1 (5.6%)	0 (0%)	0.54
BMI, Mean +/- SD	26.3 +/- 5.5	22.1 +/- 1.8	27.5 +/- 1.6	34.6 +/- 6.1	**<0.001**
Menopausal, n (%)					
Pre	33 (66%)	19 (82.6%)	11 (61.1%)	3 (33.3%)	
Post	17 (34%)	4 (17.4%)	7 (38.9%)	6 (66.7%)	**0.024**
CLS, n (%)					
No	24 (48%)	15 (65.2%)	9 (50%)	0 (0%)	
Yes	26 (52%)	8 (34.8%)	9 (50%)	9 (100%)	**0.002**
BRCA mutation, n (%)					
BRCA1	4 (8%)	1 (4.4%)	2 (11.1%)	1 (11.1%)	
BRCA2	1 (2%)	0 (0%)	0 (0%)	1 (11.1%)	
Negative	45 (90%)	22 (95.7%)	16 (88.9%)	7 (77.8%)	0.248
Invasive, n (%)					
No	11 (22%)	5 (21.7%)	5 (27.8%)	1 (11.1%)	
Yes	39 (78%)	18 (78.3%)	13 (72.2%)	8 (88.9%)	0.674
ER, n (%)					
Neg	9 (22%)	4 (20%)	3 (23.1%)	2 (25%)	
Pos	32 (78.1%)	16 (80%)	10 (76.9%)	6 (75%)	1
missing	9 (18%)	3 (13.0%)	5 (27.8%)	1 (11.1%)	0.493
PR, n (%)					
Neg	12 (30.8%)	5 (27.8%)	4 (30.8%)	3 (37.5%)	
Pos	27 (69.2%)	13 (72.2%)	9 (69.2%)	5 (62.5%)	0.905
missing	11 (22%)	5 (21.7%)	5 (27.8%)	1 (11.1%)	0.674
HER2, n (%)					
Neg	32 (82.1%)	13 (72.2%)	11 (84.6%)	8 (100%)	
Pos	7 (18%)	5 (27.8%)	2 (15.4%)	0 (0%)	0.315
missing	11 (22%)	5 (21.7%)	5 (27.8%)	1 (11.1%)	0.674
Triple Negative, n (%)	8 (20.5%)	3 (16.7%)	3 (23.1%)	2 (25%)	0.639

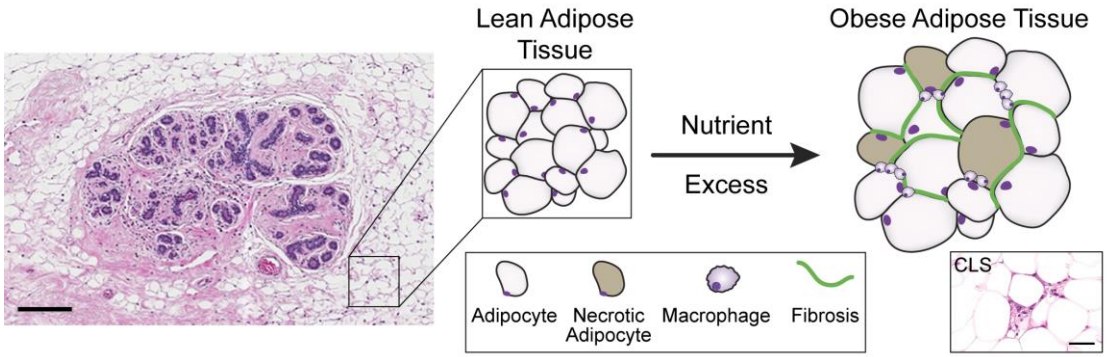

Figure 1: Fibroglandular breast tissue exists in close proximity to adipose tissue that undergoes structural alterations during obesity, including increased fibrosis secondary to hypoxia and infiltrates of macrophages responding to adipocytes undergoing necrosis, visualized as CLS. Hematoxylin and Eosin (H&E), Bar = 300 μm, CLS inset Bar = 100 μm. Published in Springer NL, *et al*. *Am J Path* 2019;189(10);2019-2035

1.5 Macrophage polarization

Macrophages derive from either circulating monocyte or yolk sac-derived tissue resident pools and can be broadly classified into two phenotypes, referred to as polarization: 1) M1/classically activated macrophages that are pro-inflammatory in response to triggers like interferon gamma (IFNγ) and lipopolysaccharide (LPS) and 2) M2/alternatively activated macrophages which are anti-inflammatory, stimulated by the cytokines interleukin-4 and 13 (IL-4 and IL-13) and involved in repair and remodeling of tissues[71]. Chemical stimuli inducing these phenotypes and markers of M1 versus M2 macrophage relevant to this body of work are summarized in Figure 2. Generally, M1 macrophages are considered tumoricidal whereas M2 macrophages are considered tumor promoting[72]. Hence, it is not surprising that tumor cells appear to educate the majority of TAMs to be biased toward an M2 phenotype[73]. Macrophages are phenotypically diverse and plastic and their phenotypes overlap on both an individual[74] and cell population[75,76] level. Nevertheless, the simplified classification

of macrophages as M1 and M2 that is used here provides a framework to gain valuable new insights.

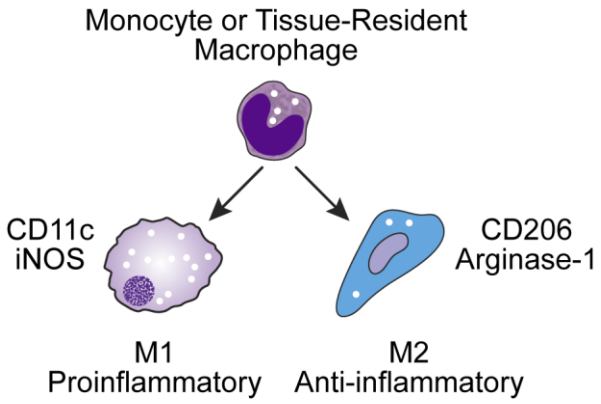

Figure 2: Macrophages can polarize into two broad categories based on effector function: M1 pro-inflammatory macrophages and M2-anti-inflammatory macrophages. CD11c and CD206 are membrane molecules and inducible nitric oxide synthase (iNOS) and arginase-1 are intracellular enzymes used in the studies reported herein to differentiate between these polarization states. Published in Springer NL, *et al*. *Am J Path* 2019;189(10);2019-203

1.6 Spatial organization of macrophages in human breast tissue

Recent discoveries from diabetes research showed that local proliferation of anti-inflammatory M2 macrophages within interstitial regions of subcutaneous and epididymal white adipose tissue contributes to the macrophage burden in mice[35]. Additionally, obesity in humans increases the number of CLS[67]. However, a direct comparison of macrophage phenotype in human breast adipose tissue CLS versus interstitial regions is missing.

By immunostaining for the M1 marker CD11c and the M2 marker CD206, we examined the density of pro- and anti-inflammatory macrophages in both interstitial regions and CLS of tumor-free regions of human breast tissue using a positive pixel count algorithm (Figure 3).

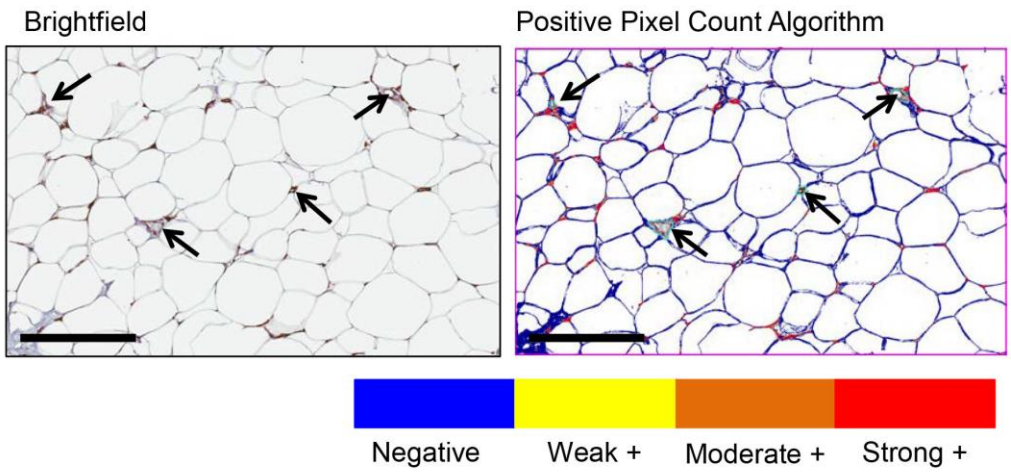

Figure 3: Methodology for the ImageScope positive pixel count algorithm. Five representative fields of breast adipose tissue were analyzed per section. The negative selection tool was used to exclude cross-reactive or non-specific staining (arrows, illustrating CD206 immunoreactive vasculature). Pixels were categorized as negative, weak, moderate or strong. For the purposes of this study, only strong positive pixels are included in analysis. Analysis was performed blinded to BMI for each section. Bar = 200µm. Published in Springer NL, *et al*. *Am J Path* 2019;189(10);2019-2035

Although both CD11c+ and CD206+ macrophages were present in CLS (Figure 4A, upper), quantitative image analysis revealed that CD206+ macrophages were the dominant phenotype in the adipose tissue interstitium in both lean and obese individuals (Figure 4B). While obesity increased the density of CD206+ macrophages, no difference was detected for CD11c+ macrophages in the interstitium (Figure 4B).

Importantly, the quantity of interstitial CD206+ macrophages was not affected by the specimens' CLS status (Figure 5). These findings suggest that CD206+ macrophages in the stromal vascular compartment develop through mechanisms independent of those commonly associated with the formation of CLS, such as cytokine-mediated recruitment of circulating monocytes, differentiation to macrophages, and M1 polarization in response to adipocyte-secreted factors[34,77,78].

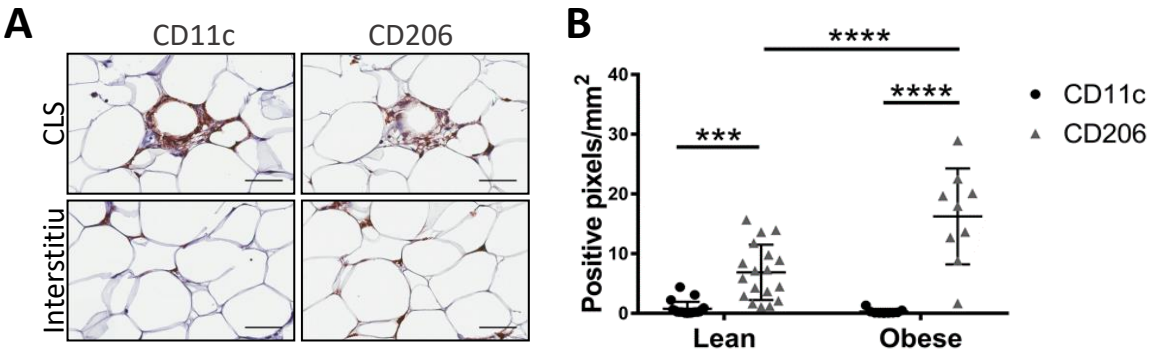

Figure 4: A) Representative photomicrographs from the breast adipose tissue of one woman with obesity illustrating two spatially distinct compartments of macrophages, CLS that are composed predominantly of CD11c+ M1-biased macrophages, and interstitial macrophages between adipocytes, composed predominantly of CD206+ M2-biased macrophages as determined by immunohistochemistry (IHC). Bar = 100µm. **B**) The interstitium of breast adipose tissue contains more CD206+ versus CD11c+ macrophages regardless of obesity; however, CD206+ macrophage density is increased in obese versus lean women. Analysis was performed blinded to BMI for each section n=26 sections, 5 representative images per section, each data point is the average value of those 5 images. Two-way ANOVA with Tukey's post-test, data are expressed as means ± SD *** = p <0.001, **** = p <0.0001. Published in Springer NL, *et al*. *Am J Path* 2019;189(10);2019-2035

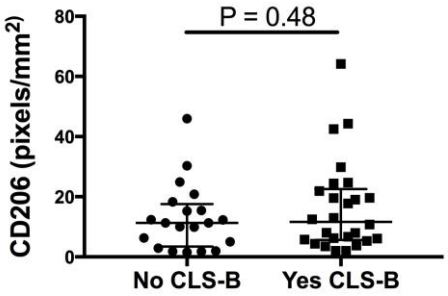

Figure 5: CD206 immunoreactivity of macrophages in the interstitial adipose tissue compartment is independent of the presence or absence of crown-like structures in breast (CLS-B) adipose tissue. CLS presence was determined by pathologist assessment of H&E-stained serial sections. Analysis was performed blinded to BMI for each section For CD206 quantification, 5 representative images per section were analyzed. Each data point is the average of the 5 images per section. Data represented as median and interquartile range, Mann-Whitney U analysis. Unpublished data.

1.7 Confirmation of macrophage phenotypes via computational biology methodology

To corroborate our IHC data with a more comprehensive molecular data set, we performed CIBERSORT analysis to estimate the proportions of M2-biased versus M1-biased macrophages in lean and obese human breast adipose tissue[70] from the same cohort of women used for IHC studies. CIBERSORT is a computational approach that allowed us to infer the representation of different macrophage phenotypes based on the transcriptome of bulk breast tissue.

Similar to IHC results, CIBERSORT analysis predicted more M2-biased macrophages in breast adipose tissue regardless of BMI (Figure 6) and that the burden of M2 macrophages was higher in obese versus lean adipose tissue whereas no difference was detected for RNA transcript patterns indicative of M1-biased macrophages (Figure 6).

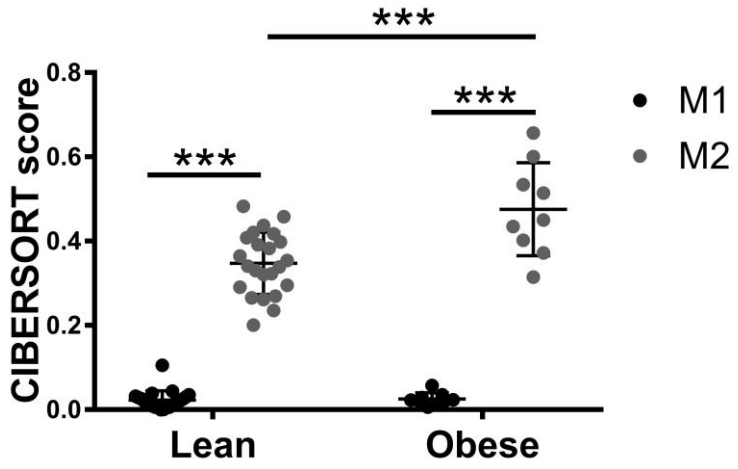

Figure 6: Computational analysis of macrophage phenotype via CIBERSORT analysis of RNA transcripts (n = 26) corroborates IHC data with significant enrichment of M2-biased macrophages in obese versus lean breast tissue. Two-way ANOVA, data represented as mean ± SD. *** = p <0.001, **** = p <0.0001. Published in Springer NL, *et al*. *Am J Path* 2019;189(10);2019-2035

Collectively, these results suggest that, although obesity is associated with a pro-inflammatory M1 macrophage phenotype both histologically and biochemically[34,37], M2-biased macrophages are the predominant macrophage population in breast adipose tissue interstitium and increase with obesity.

1.8 Interstitial fibrosis of human samples correlates to M2-biased macrophage polarization state

Prior work suggested that obesity causes interstitial fibrosis[29,79], increased fibrosis correlates to increased macrophage infiltration[11], and an anti-inflammatory macrophage phenotype can be induced by compositional, mechanical and topographical cues associated with fibrotic ECM remodeling[52,54,80,81]. Therefore, we next questioned whether interstitial fibrosis in obese breast adipose tissue might mediate the detected differences in macrophage populations.

First, we confirmed by image analysis of picrosirius red-stained cross-sections that obesity is associated with increased interstitial collagen, a hallmark of fibrosis, in our patient cohort[29,32]. Interstitial collagen deposition between adipocytes was significantly increased in samples from obese individuals (Figure 7A and B) and positively correlated with BMI (Figure 8A). Image analysis of consecutive cross-sections revealed that increased interstitial fibrosis correlated with greater numbers of CD206+ macrophages (Figure 7C). This finding was supported by analysis of paired histological and RNA samples, which suggested that interstitial fibrosis and CIBERSORT M2 score were similarly interrelated (Figure 7D). Importantly, the same trends were not evident for CD11c+ macrophages within the interstitium or CIBERSORT M1 score (Figure 7E and 7F, respectively). Similarly, no correlation existed between the density of interstitial CD11c+ macrophages and BMI (Figure 8B). These results suggest that obesity-associated interstitial fibrosis could have a direct

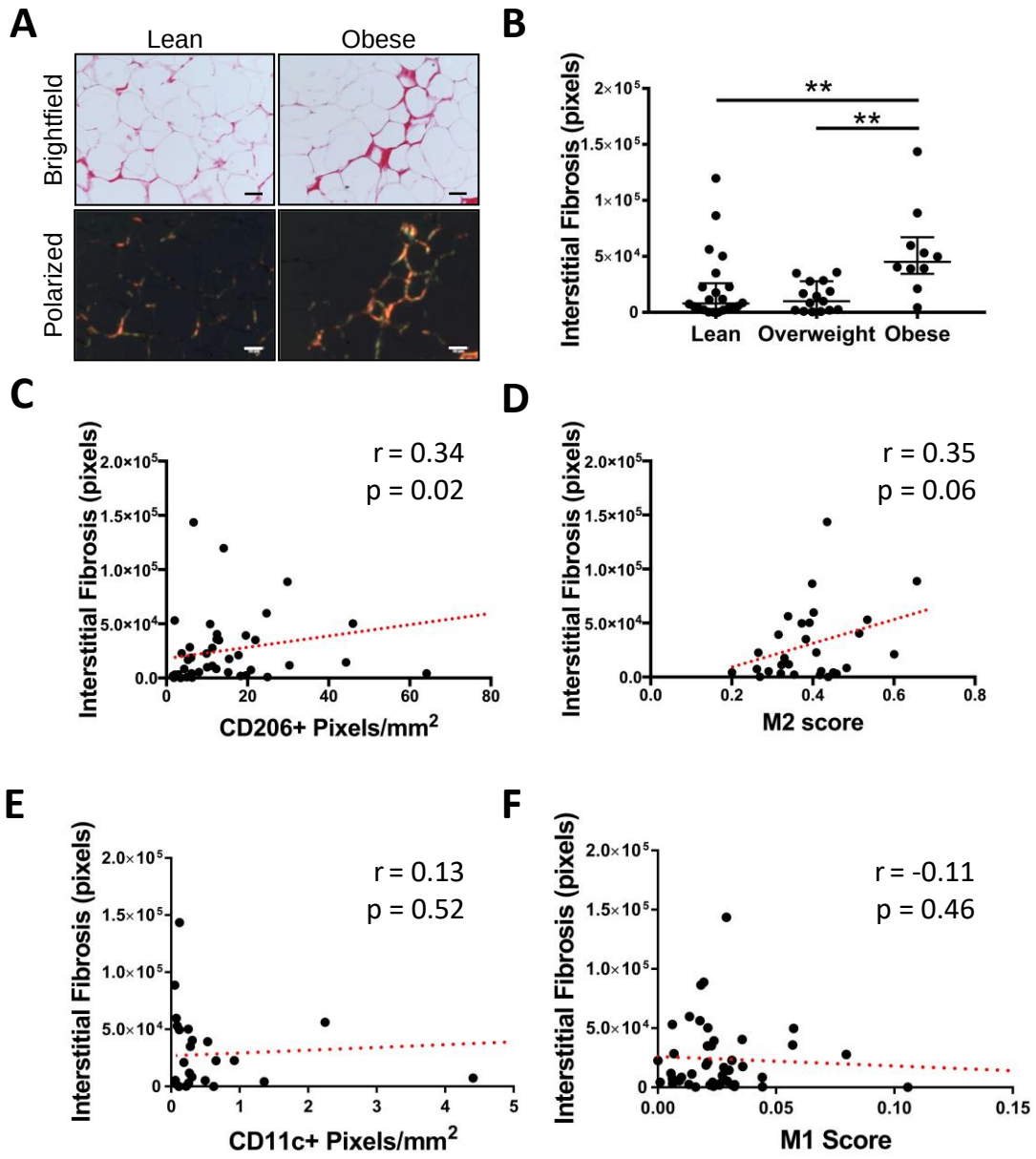

Figure 7: A and **B**) Interstitial extracellular matrix (ECM) is more fibrotic in obese versus lean or overweight breast adipose tissue as determined by image analysis and pixel quantification of picrosirius red stained sections under polarized light. Analysis was performed blinded to BMI for each section. Data represented as median and interquartile range, Kruskal-Wallis analysis n=37, 5 representative images per section, ** = p <0.01 Bar = 50µm. **C**, **D, E, and F**) Interstitial fibrosis positively correlates to CD206+ IHC and CIBERSORT M2 score (**C** and **D**, n=37) but not CD11c IHC (**E**, n=26) or CIBERSORT M1 score (**F**, n=37). (**C**-**F**) Red dashed line illustrates the best fit line as determined by linear regression. Published in Springer NL, *et al*. *Am J Path* 2019;189(10);2019-2035

effect on macrophage polarization towards a M2- but not M1-biased phenotype in breast adipose tissue.

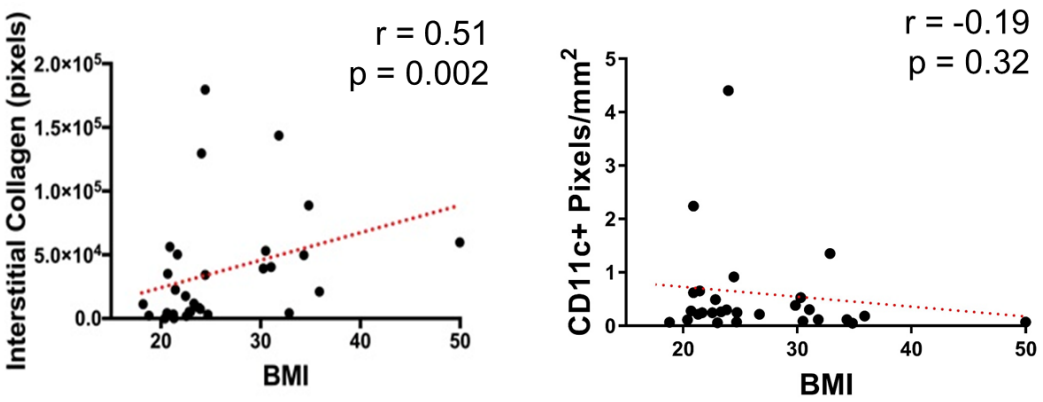

Figure 8: A) Spearman Rank correlation between BMI and interstitial fibrosis as determined by image analysis and positive pixel quantification of picrosirius red stained sections from lean and obese women imaged under polarized light (n=26).**B)** Spearman Rank correlation between BMI and CD11c labeling as determined by image analysis and positive pixel quantification of IHC sections from lean and obese women (n = 28). Red dashed line illustrates the best fit line as determined by linear regression. Published in Springer NL, *et al*. *Am J Path* 2019;189(10);2019-2035

These results suggest that obesity-associated interstitial fibrosis could have a direct effect on macrophage polarization towards a M2- but not M1-biased phenotype in breast adipose tissue.

1.9 Mammographic and histological breast density are not predictive of interstitial fibrosis or macrophage content

Given our observations that obesity causes an increase in interstitial fibrosis, but that obesity is typically associated with decreased breast tissue density due to accumulation of fatty tissue, which appears radiolucent on mammography[82], we next evaluated whether bulk breast fibrosis, i.e. the ratio of fibroglandular tissue to adipose tissue, would correlate to M2 macrophage phenotype.

As expected, histological density grade was inversely related to BMI (Figure 9A) and there was a significant difference in the proportions of mammographic patterns between, lean, overweight, and obese women (Figure 9B). The differences between mammographic density pattern and histopathological density score between lean, overweight, and obese women (Figure 9A and B) did not predict interstitial fibrosis (Figure 10A) or M2 macrophage burden as detected by CD206 IHC and CIBERSORT M2 data (Figure 10B and C).

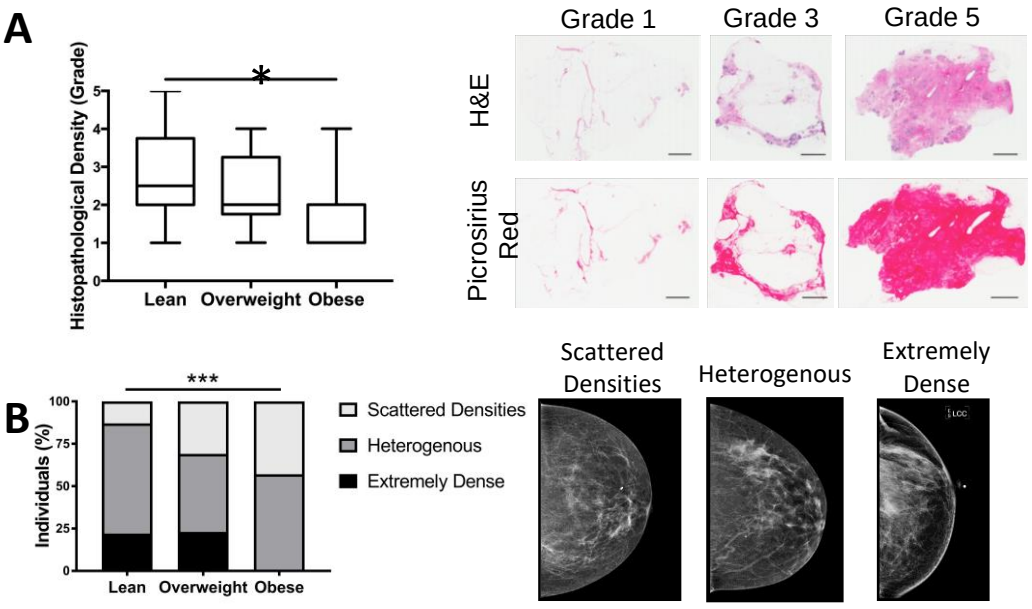

Figure 9: A) Histological breast density, assessed by the ratio of fibrous tissue to adipose tissue[15] (i.e. bulk fibrosis) is inversely correlated with BMI. Data represented as median, interquartile range, and min-max, Kruskal-Wallis analysis, $p < 0.05$ n=50 sections. **B)** The distribution of mammographic density patterns is significantly different between body condition, Chi-squared analysis, $p < 0.001$. Published in Springer NL, *et al*. *Am J Path* 2019;189(10);2019-2035

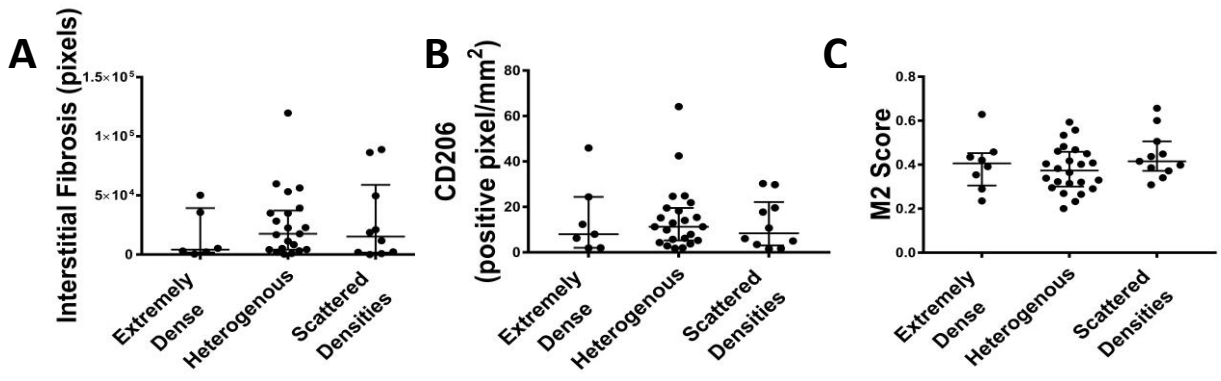

Figure 10: A) The distribution of mammographic density patterns is not predictive of interstitial fibrosis. Additionally, macrophage burden, as determined by both **B)** CD206 IHC and **C)** CIBERSORT analysis of RNA transcripts, cannot be predicted by mammographic density pattern, data represented as median and interquartile range, Kruskal-Wallis analysis, n=26, data represented as median and interquartile range.

Collectively, these results indicate that obesity-associated interstitial fibrosis might play a role in modulating macrophage phenotype and function in obese breast adipose tissue, but that these changes cannot be diagnosed with conventional clinical imaging techniques that focus on detection of gross breast tissue density.

1.10 Discussion

The link between chronic inflammation and cancer development is well-established[83–85]; however, in the case of obesity, much of the focus has been on WATi in the form of CLS. WATi has been associated with both an increased risk of breast cancer[48] and worse prognosis[46,47]. WATi has been shown to be reversible with weight loss in mouse models of obesity[49]. However, a recent secondary analysis of a large randomized clinical trial indicated that weight loss in postmenopausal women did not significantly reduce risk for invasive breast cancer development[86]. This suggests that, although WATi in the form of CLS appears to be reversible with weight loss, other

changes to adipose tissue during obesity, such as fibrosis or expanded M2 macrophage populations, may be playing a role.

The recognition of the relationship between anti-inflammatory macrophages and upregulated cancer-related pathways in obese adipose tissue macrophages spans the last decade[50,68]. Indeed, similar to our study, M2 macrophages have been previously identified to reside within the interstitium of obese adipose tissue[28,35]. However, our global hypothesis that the interactions between obesity-associated interstitial fibrosis and macrophages might promote M2 or tumor-associated macrophage (TAM)-like polarization is a unique inquiry brought about by the recent characterization of interstitial fibrosis within breast adipose tissue[42] and that macrophages are sensitive to both biochemical and biophysical changes of the ECM that occur with fibrosis[52,54]. Due to substantial plasticity of macrophage function, and overlapping phenotypes of macrophage subsets, therapeutically targeting tumor-promoting macrophages has yet to yield positive results in clinical trials[87]. Therefore, targeting the underlying interstitial fibrosis might be a novel approach to modulate the microenvironment and prevent TAM-like functions of adipose tissue macrophages in obesity.

Macrophages are a very heterogeneous population of cells in which the M1 and M2 nomenclature used here represent extremes. Indeed, recent studies have illustrated that adipose tissue macrophages have activation states that do not conform to the classical definitions of M1 or M2 macrophages[74,88,89]. We acknowledge that the characterization of macrophages as either M1- or M2-biased in our study is oversimplified; however, our findings have identified compelling trends, and is a starting point for additional inquiry in this underexplored field of the physical, rather than chemical, microenvironment participating in the process of macrophage polarization. A limitation of our study is the use of single markers to determine an M1

versus M2-bias of macrophages. However, approaches that afford detailed characterization of macrophage phenotype such as flow cytometry, gene expression profiling, and computational methodologies sacrifice the spatial organization and relationships that were essential findings in our study. We elected not to perform double-labeling experiments to assess dual-expression of CD11c and CD206 in our study cohort. There is conflicting information in the literature regarding the presence of CD11c, CD206 double-positive macrophages in adipose tissue. One study performed in a diet-induced mouse model of obesity found no overlap between CD11c+ and CD206+ macrophages via flow cytometry[90]. However, other studies using adipose tissue from both mice and people have identified a low percentage of CD11c, CD206, double-positive macrophages, ranging from 7-20% of adipose tissue macrophages[91,92]. We consider it unlikely that inclusion of a small proportion of double-positive cells in our dataset would significantly alter our conclusions, particularly given the robust corroboration of CIBERSORT analysis of macrophage RNA transcripts with our IHC data.

Unlike IHC which is binary or, at best, semiquantitative based on labeling intensity, CIBERSORT analysis provides a score on a continuous scale that is more likely to recapitulate the spectrum of macrophage activation states. Furthermore, as CIBERSORT uses a large dataset of 547 genes to predict macrophage activation, thus is potentially more comprehensive in determining macrophage polarization than any feasible number of IHC markers. Nevertheless, future studies could be performed utilizing additional IHC markers to increase characterization of macrophage populations localized within the breast adipose interstitium.

We identified a trend for breast adipose tissue from women with obesity to have a higher density of interstitial fibrosis and that this degree of interstitial fibrosis appears to associate with M2-biased, but not M1-biased macrophage populations.

Admittedly, there was significant overlap in the degree of interstitial fibrosis between the lean and obese women in our cohort. In retrospect, this overlap is likely due to a paucity of adipose tissue to evaluate in some of the sections from lean women and inclusion of some fibroglandular areas of breast. The five lean women with the highest interstitial fibrosis scores all had a bulk fibrosis score (derived from the ratio of fibroglandular tissue to fat) of 4 or 5 indicating very little adipose tissue present within these tissue sections. Digitally scanned sections, which would facilitate freehand exclusion of fibroglandular regions for analysis and calculation of total area analyzed for normalization purposes, could not be used in this case due to the need to view picrosirius red stained sections under crossed polarized light. Additional tissue sections from each women could be analyzed to increase the total area of adipose tissue to select from and minimize inadvertent inclusion of fibroglandular tissue in the analysis. The lack of adipose tissue in these sections has also likely affected the correlations between interstitial fibrosis and macrophage phenotype, which are, admittedly, weak. Additional women and multiple breast sections per woman, should be evaluated to confirm our initial findings.

Increased mammographic density has consistently been identified as an independent risk factor for breast cancer[8,82]. Recent evidence indicates that an increase in macrophage numbers within the breast fibroglandular region positively correlates with the amount of stromal collagen[93], cancer invasion, and aggression[11]. However, neither of these studies assessed BMI within their cohort, macrophage populations residing adjacent to the fibroglandular compartment within the adipose tissue, or distinct subsets of macrophage populations. Interestingly, our study found that mammography is insensitive to detect interstitial fibrosis within breast adipose tissue. This finding alters the paradigm of the definition of breast density suggesting that microscale fibrosis might be similarly important to gross/bulk fibrosis. Knowing that

the interstitial adipose tissue M2-biased macrophages are migratory[35], future studies are needed to evaluate whether this population is a source for recruitment of TAMs into the fibroglandular compartment during tumor development.

A limitation of the study is the use of breast tissue derived from tumor-bearing women undergoing mastectomy for therapeutic purposes. Within the tumor microenvironment there is extensive crosstalk between cancer and stromal cells. Regarding the cross-talk between cancer cells and adipocytes, the majority of research has been unidirectional evaluating paracrine effects of cancer-associated adipose tissue on breast cancer cells, which has been extensively analyzed and reviewed elsewhere[94–96]. The effect of the cancer secretome on adipose tissue associated with the tumor is less understood. One study, using a mouse melanoma cancer model, identified abundant inflammation and fibrosis in adipose tissue (similar to what we have observed in obesity) immediately adjacent to the implanted tumor relative to distant (contralateral) control adipose tissue[97]. Given this information, since all of the samples collected for our studies were derived from an unaffected quarter of breast, or the contralateral breast in cases of double mastectomy, breast cancer-mediated paracrine effects on distant adipose tissue are considered less likely. Yet, current evidence regarding primary tumor ability to prime distant sites for metastasis, the "pre-metastatic niche" also suggests that tumor-derived influence on distant adipose tissue cannot be completely excluded. However, this effect should be similar in both lean and obese women in our population as there was no difference in breast cancer subtypes between groups. Nevertheless, tumor-free breast adipose tissue could be requested from biospecimen repositories such as the National Disease Research Interchange to confirm our results.

CHAPTER 2

EXTRACELLULAR MATRIX-MACROPHAGE INTERACTIONS IN OBESITY REGULATE MACROPHAGE ACTIVATION AND FUNCTION

Chapter written using content modified from the following publication:
Nora L. Springer[1,2,3], Neil M. Iyengar[4,5], Rohan Bareja[6], Akanksha Verma[6], Maxine Jochelson[7], Dilip D. Giri[4], Xi Kathy Zhou[8], Olivier Elemento[6], Andrew J. Dannenberg[5], and Claudia Fischbach[2,9] Obesity-associated extracellular matrix remodeling promotes a macrophage phenotype similar to tumor-associated macrophages. *Am J Path* 2019;189(10);2019-2035. PMID: 31323189

[1]Biological and Biomedical Sciences, Cornell University, Ithaca, NY
[2]Meinig School of Biomedical Engineering, Cornell University, Ithaca, NY
[3]Department of Diagnostic Medicine/Pathobiology, Kansas State University, Manhattan, KS
[4]Department of Medicine, Memorial Sloan Kettering Cancer Center, New York, NY
[5]Department of Medicine, Weill Cornell Medicine, New York, NY
[6]Institute for Computational Biomedicine, Caryl and Israel Englander Institute for Precision Medicine, Weill Cornell Medicine, New York, NY
[7]Department of Radiology, Memorial Sloan Kettering Cancer Center, New York, NY
[8]Department of Healthcare Policy and Research, Weill Cornell Medicine, New York, NY
[9]Kavli Institute at Cornell for Nanoscale Science, Cornell University, Ithaca, NY

N.L.S performed all histological and in vitro experiments unless otherwise indicated. N.M.I and A.J.D provided clinical samples and demographic data, X.K.Z provided

biostatistical support, D.D.G performed initial CLS assessment, M.J. provided mammographic interpretation. R.B., A.V, and O.E. performed transcriptomic and computational analysis. N.L.S, and C.F. designed the project and wrote the paper. All authors provided input on the manuscript.

2.1 Introduction

Macrophages are hematopoietic cells that have wide physiologic roles in the body ranging from innate immunity to trophic roles during development and disease[21]. During health, fibrosis and macrophagic inflammation are well-coordinated and self-limiting; for example, resolution of mechanical[98] and biochemical stimuli upon completion of wound healing[99]. Tumors, on the other hand, behave like 'wounds that never heal' and thus are characterized by continued and unchecked pro-fibrotic and pro-inflammatory signaling[100]. Indeed, increased stroma stiffness in clinical breast cancer samples positively correlates with the number of infiltrated macrophages, called tumor-associated macrophages, and this correlation is stronger in more aggressive tumor subtypes[11].

While most previous work studying the functional link between inflammation and the ECM has focused on how macrophages mediate fibrotic ECM remodeling[101–103], the opposite may be equally relevant; i.e., how the ECM influences macrophages. Within adipose tissue, macrophages also interact with ECM as they exist within the interstitial space between adipocytes[35] in which fibrotic remodeling is abundant. Nevertheless, it remains unknown whether or not obesity-associated differences in interstitial ECM remodeling modulate macrophage polarization towards an anti-inflammatory and possibly pro-tumorigenic phenotype. Yet this possibility is conceivable as macrophages can transition to an M2 phenotype when interacting with

substrates mimicking biochemical and biophysical changes representative of fibrotic ECM remodeling[52,54,104].

Here, we explore the hypothesis that obesity-associated ECM remodeling modulates macrophage polarization. To assess whether the *in vivo* correlation between interstitial fibrosis and anti-inflammatory M2 macrophage phenotype has a causal relationship, we utilized an *in vitro* model system utilizing decellularized ECM derived from lean and obese adipose stromal cells from mouse inguinal fat pads and murine bone marrow-derived macrophages that allowed us to directly interrogate macrophage phenotypic changes in response to obesity-specific ECM remodeling.

2.2 Materials and Methods

Animal Usage

The Cornell University and Kansas State University Institutional Animal Care and Use Committees approved mouse usage for both adipose stromal cell (ASC) and bone marrow-derived macrophage (BMDM) isolation under protocol number 2009-0117 and 4094, respectively.

Preparation of the decellularized ECM model system

Decellularized ECMs were created by in vitro culture of ASCs isolated from lean and obese mice. ASC were harvested using aseptic technique from the inguinal fat pad of age-matched 10-week-old female wildtype (WT) C57Bl6/J mice and genetically obese B6.Cg-Lepob/J (*ob/ob*) mice (both strains from The Jackson Laboratory, Bar Harbor, ME) after CO_2 euthanasia. The fat pad was maintained under sterile conditions, minced, and digested in collagenase at 37 ^{o}C for 1hr. After digestion, the stromal-vascular fraction of fat was separated from adipocytes by density centrifugation and subsequent filtration and then expanded in 1:1 Dulbecco's

Modified Eagle Medium and Ham's F12 Nutrient Mixture (DMEM/F12) (both obtained from Gibco, Waltham, MA) enriched with 10% fetal bovine serum (FBS, Atlanta Biologicals, Flowery Branch, GA) and 1% Penicillin/Streptomycin (Gibco) to select for ASC. Expanded ASCs were cultured on plastic coverslips (Nunc Thermanox, Rochester, NY) for 10 days prior to detergent-based decellularization. Decellularization was achieved as previously described[42,105]. Briefly, ASC cultures were washed with PBS and subsequently incubated in 0.5% Triton-X + 200 mM NH_4OH[42,106,107] followed by incubation in 1U/mL DNase (VWR Amresco, Radnor, PA) at 37 ^oC to remove cellular membranes, organelles, and nucleic acids. Following decellularization, maintenance of native matrix structure and key compositional components was confirmed by immunofluorescence (IF) analysis of fibronectin (Millipore-Sigma, St. Louis, MO, F7387) and collagen type I (Abcam ab34710) via confocal microscopy (ZEISS 710, Pleasonton, CA) and image analysis.

Bone marrow-derived macrophage (BMDM) isolation

Bone marrow was isolated from the femurs and tibiae of 10-16-week-old WT C57Bl6/J mice. Briefly, after bone extraction, remaining musculature was stripped and the bones were cut via sterile scissors at the proximal and distal physis. Using a syringe and 25g needle, the bone marrow was flushed from the metaphyseal regions and diaphysis with DMEM cell culture media into a sterile tissue culture plate. Bone marrow was suspended and plated in 9 cm dishes and cultured at 37 °C. Progenitor cells were differentiated into BMDM in DMEM + 10% FBS + 1% Penicillin/Streptomycin + 10 ng/mL recombinant mouse macrophage colony stimulating factor (M-CSF, R&D Systems, Minneapolis, MN) and were used for experiments between day 7 and 10 post-collection.

Assessment of macrophage morphology and activation

Prior to experiments assessing ECM-mediated regulation of macrophage polarization, we assessed our capability to polarize BMDM to M1 versus M2 macrophages in 2D culture using standard protocol[76]. BMDM were seeded on 20ug/mL Fn-coated glass coverslips at 10,000 cells per coverslip and allowed to adhere overnight. After adherence, BMDM were cultured either in complete DMEM to maintain a non-polarized phenotype (M0), or complete DMEM + 100ng/mL LPS or 20ng/mL IL-4 and 20ng/mL IL-13, to induce M1 and M2 polarization, respectively. After 24 hours culture, BMDM were labeled with 4'6-diamidino-2-phenylindole (DAPI), phalloidin (Molecular Probes AlexaFluor®568), and goat polyclonal anti-arginase-1 (Santa Cruz Biotechnology sc-18351) followed by a secondary anti-goat AlexaFluor®488. Labeled BMDM were evaluated under both phase contrast and epifluorescence microscopy for morphological features characteristic of M1 and M2 macrophages *in vitro*[23] and arginase-1expression.

BMDM were seeded on lean and obese decellularized ECM at a concentration of 10,000 cells/coverslip and cultured in DMEM + 10% FBS + 1% Penicillin/Streptomycin and 10ng/mL recombinant mouse M-CSF. After 72 hours of culture, BMDM and ECM were fixed with 4% paraformaldehyde (PFA). Cells were labeled with 4'6-diamidino-2-phenylindole (DAPI) and phalloidin (Molecular Probes AlexaFluor, Waltham, MA), while decellularized ECM was visualized by immunostaining with rabbit anti-fibronectin (Fn) antibody (Millipore-Sigma F3648). Macrophage polarization state was evaluated by quantifying the murine M1 marker iNOS (Abcam, ab3523) and M2 marker arginase-1[76] protein levels (Santa Cruz Biotechnology, Dallas, TX, sc-18351) via IF image analysis. Macrophage proliferation was assessed via bromodeoxyuridine (BrdU, Invitrogen, Waltham, MA) incorporation and immunostaining with anti-BrdU antibody (Invitrogen) after 10 hours of culture.

Preliminary studies demonstrated that BMDM cultured on decellularized ECM will not polarize without appropriate stimulation; therefore, BMDM were stimulated to undergo M1 polarization with 100ng/mL lipopolysaccharide (LPS) (Millipore-Sigma) or M2 polarization with 20 ng/mL interleukin (IL)-4 and -13 (R&D Systems) for decellularized ECM experiments, unless otherwise noted.

Statistical Analysis

All statistical analysis was performed using Prism v7.0 (GraphPad Software, La Jolla, CA). Normality assumption of the parametric method was assessed by the Shapiro-Wilk test. Continuous data are represented as the mean ± SD or the median and interquartile range. Specific statistical tests used and number of independent samples and replicates per experiment are listed in the figure legends. A Tukey's post-hoc test was used when needed to account for multiple comparisons. Significance was set at $P < 0.05$.

2.3 Decellularized extracellular matrix model to study macrophage-ECM interactions in obesity

Macrophages have typically been studied in monolayer culture on tissue-culture plastic or by *in vivo* models. While traditional tissue culture methods have led to important new insights, they cannot recapitulate the ECM compositional, structural, and mechanical changes that regulate macrophages during fibrosis. *In vivo* mouse models, on the other hand, may not fully mimic human disease due to structural differences in the mouse mammary gland[108] and difficulty in controlling isolated or select parameters. Natural biomaterials, such as decellularized ECM, offer a unique and controlled opportunity to study macrophage-ECM interactions, given their intrinsic biochemical and physical similarity to the native ECM[107]. They can be

prepared from cells or tissues prone to increased fibrotic remodeling[42], such as adipose stromal cells, and are suitable to study macrophage responses to ECM-structure, biochemical composition, or mechanics.

Obesity-associated, fibrotic ECM remodeling in people is characterized by increased concentrations of fibrillar ECM components including fibronectin and collagen type I that can be visualized by IHC and Second Harmonic Generation (SHG) imaging, respectively (Figure 11A). Importantly, detergent-based decellularization of ECMs deposited by lean and obese ASCs isolated from wildtype (WT) and genetically obese (*ob/ob*) mice (Figure 11B) can be used to generate cell culture substrates with similar compositional and structural properties as the interstitial ECM identified in lean versus obese breast adipose tissue from people (Figure 11A and C)[42].

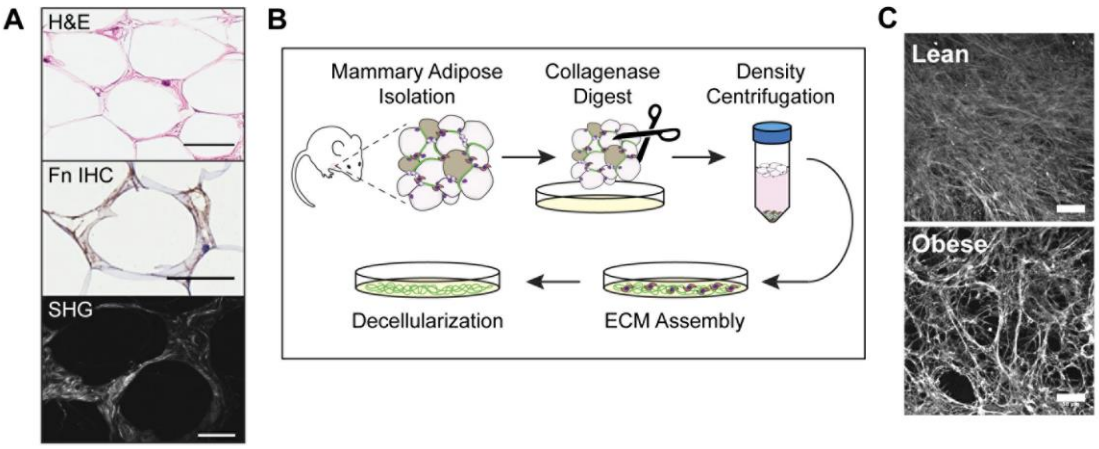

Figure 11: A) Representative photomicrographs illustrating the distribution of human adipose tissue interstitial ECM in between adipocytes via H&E (top) and visualizing fibronectin (Fn) and collagen, two key components of interstitial fibrosis, by IHC (middle) and second harmonic generation (SHG) imaging (bottom), respectively. Bar = 50 µm. **B**) Schematic illustrating protocol for adipose stromal cell isolation (ASC) from the inguinal fat pad of lean wild-type and obese (*ob/ob*) age-matched mice and their use for preparation of decellularized ECMs. **C**) Representative confocal microscopy images of decellularized ECM assembled by lean and obese ASCs after immunostaining for Fn, illustrating a similar fibrillar composition as seen in human adipose interstitial ECM. Bar = 50 µm. Published in Springer NL, *et al*. *Am J Path* 2019;189(10);2019-2035

Following decellularization, maintenance of native matrix structure and key compositional components was confirmed by immunofluorescence analysis of fibronectin (Sigma F7387) and collagen type I (Abcam ab34710) via confocal microscopy (Zeiss 710) and image analysis (Figure 12).

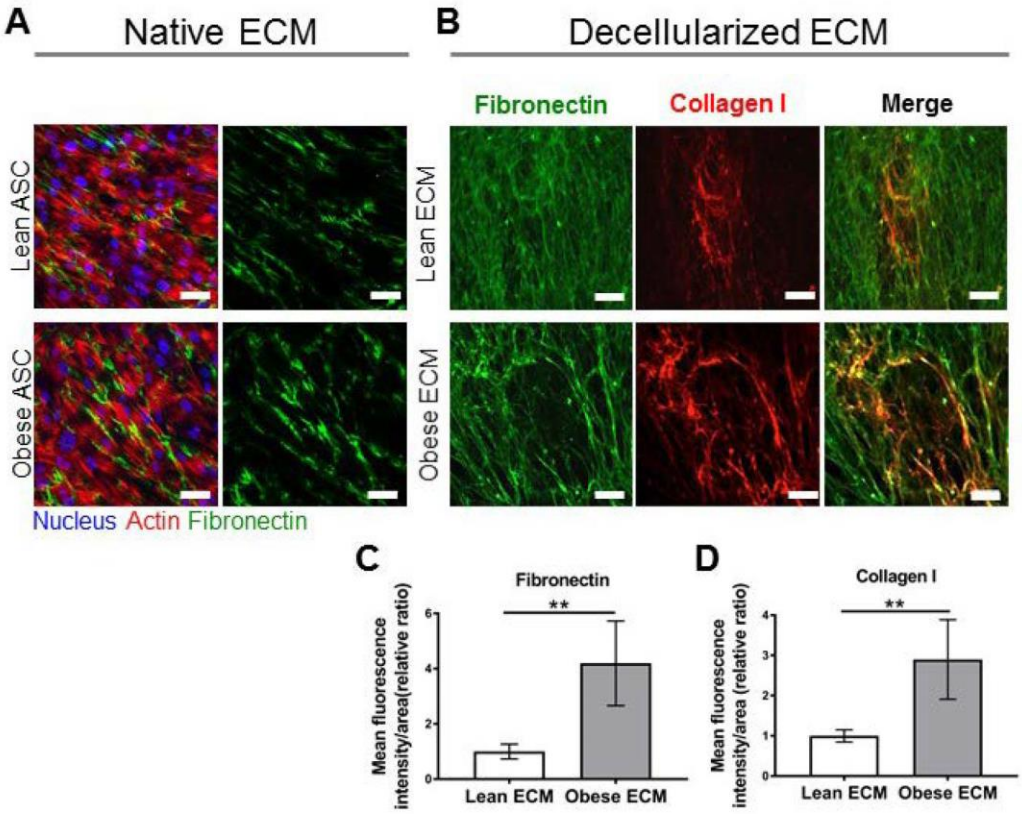

Figure 12: The *in vitro* decellularized extracellular matrix model mimics *in vivo* interstitial fibrosis. **A)** Composite and single-channel confocal microscopy image of ECM assembled by lean and obese adipose stromal cells (ASC). **B)** After decellularization, matrices retain a similar fibrillar structure with increased ECM component (Fibronectin [Sigma F7387], Collagen I [Abcam ab34710]) deposition in matrices assembled by obese ASC (**C, D**) as determined by immunofluorescence image analysis of 3 coverslips per condition and 10 images per coverslip. Data are mean ± SD from one representative experiment, Student's t-test analysis. ** = $p < 0.01$ Published in Springer NL, *et al*. *Am J Path* 2019;189(10);2019-2035

2.4 Preparation and validation of bone marrow-derived macrophages (BMDM)

Syngeneic, primary BMDMs were used to assess ECM-mediated regulation of macrophage polarization. In our hands, we were able to recapitulate characteristic morphological changes of *in vitro* M1 versus M2 polarization identified by others[23,52], including a circular and spread morphology for M1-polarized macrophages and elongated morphology for M2-polarized macrophages (Figure 13).

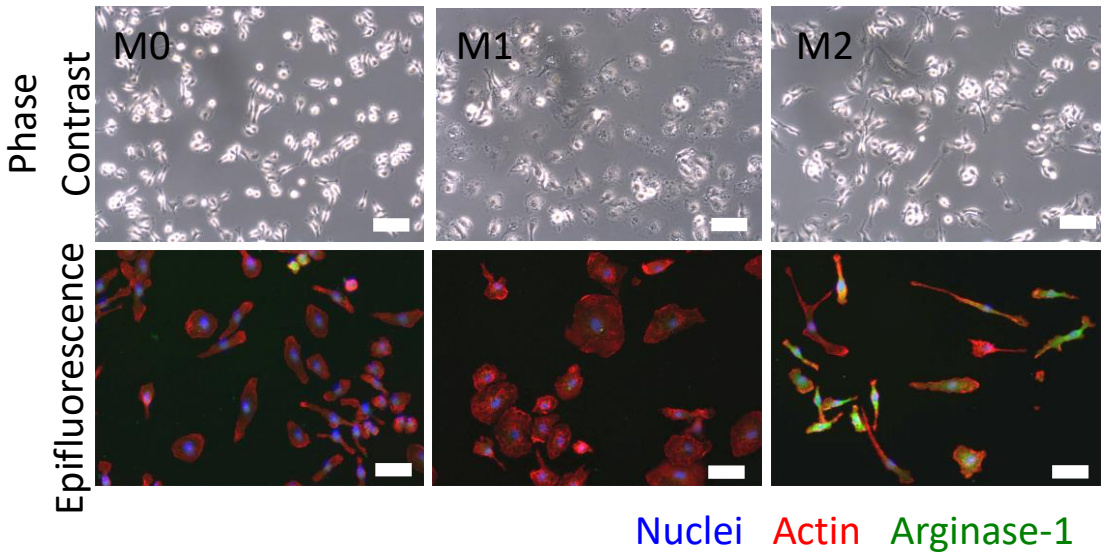

Figure 13: Representative phase contrast and epifluorescence microscopy images of bone marrow-derived macrophages (BMDM) cultured without stimulation (M0), with 100ng/mL LPS (M1) and with 20ng/mL IL-4 and 20ng/mL IL-13 (M2). Note that macrophages stimulated to polarize to an M1 phenotype display a characteristic rounded and flattened shape and lack Arginase-1 expression on epifluorescence microscopy. Macrophages that are stimulated to polarize to an M2 phenotype are elongated with arginase-1 expression. Unstimulated BMDM (M0) have an intermediate morphology and mostly lack arginase-1 expression. Phase contrast scale bar = 50um, epifluorescence scale bar = 25um. Unpublished data.

2.5 Assessment of ECM-mediated macrophage morphology

Because macrophage morphology correlates with polarization state, we first assessed whether macrophage morphology can be directly regulated by contact with

lean versus ECM. To do this, we assessed BMDM alignment with ECM fibers and BMDM aspect ratio when cultured on decellularized ECMs assembled by lean versus obese ASCs. Interestingly, BMDMs cultured on obese ECM exhibited more significant alignment in the direction of ECM fibers than their counterparts cultured on lean ECMs (Figure 14). Additionally, analysis of the cells' aspect ratio revealed that macrophages were more elongated when they were cultured on obese versus lean ECM (Figure 15). This data supports our hypothesis that contact with obesity-associated ECM promotes an anti-inflammatory M2-biased phenotype as interactions with ECM resulting in increased alignment and elongation have been shown to upregulate phenotypic markers of anti-inflammatory M2 macrophages[52,109].

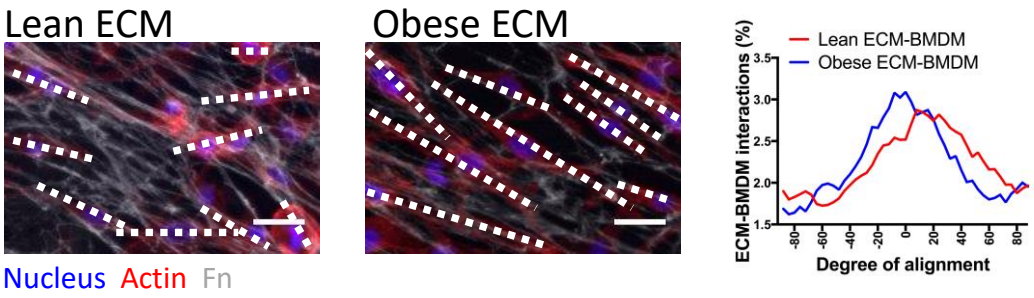

Figure 14: Representative confocal microscopy images of decellularized ECM assembled by lean and obese ASCs after immunostaining for Fn. Bar = 50 µm. BMDM and ECM alignment were both quantified using the directionality plugin in Image J. Directional alignment was normalized to 0° per condition in order to control for differences in sample orientation during imaging; angle distribution was binned into 20° increments, as previously described[110]. For each condition, 3 randomly selected sections were analyzed per sample for a total of 3 samples per condition. BMDM cultured on lean and obese decellularized matrices (dashed lines highlight the long axis of the macrophages) are more aligned with the matrix (0 on X-axis represents perfect alignment). Published in Springer NL, *et al*. *Am J Path* 2019;189(10);2019-2035

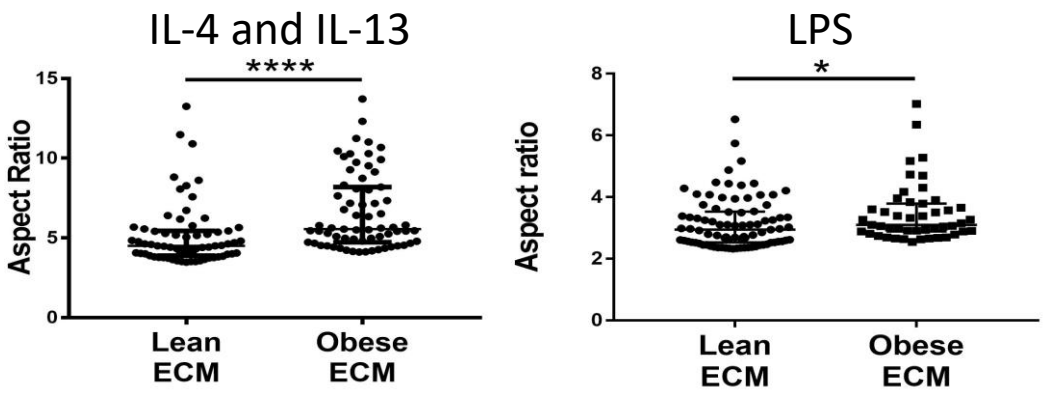

Figure 15: Bone marrow derived-macrophages (BMDM) exhibit increased elongation, regardless of polarization stimulation,when cultured on obese versus lean decellularized ECM as determined by confocal microscopy and image analysis using the fit elipse algorithm in Image J. Data are represented as median and interquartile range of top 25% of cells plotted, Mann Whitney U analysis, * = $p < 0.05$ **** = $p < 0.0001$. Published in Springer NL, *et al*. *Am J Path* 2019;189(10);2019-2035

2.6 Assessment of ECM-mediated macrophage proliferation

Furthermore, previous reports indicated that proliferation of adipose tissue macrophages occurs exclusively in CD206+ M2 macrophages in obesity[35]. Accordingly, macrophage proliferation was assessed via bromodeoxyuridine (BrdU) incorporation and immunostaining with anti-BrdU antibody (BrdU staining kit, Invitrogen 93-3943) after 10 hours of culture. BMDM cultured on obese versus lean ECMs were also more proliferative as detected by BrdU staining (Figure 16).

2.7 ECM-mediated macrophage polarization

To test whether the different ECMs also affected macrophage polarization under the influence of appropriate cytokine stimulation, we assessed BMDM arginase-1 and CD206 (Abcam ab64693) as markers of M2-bias, and iNOS expression as a marker of M1-bais via IF.

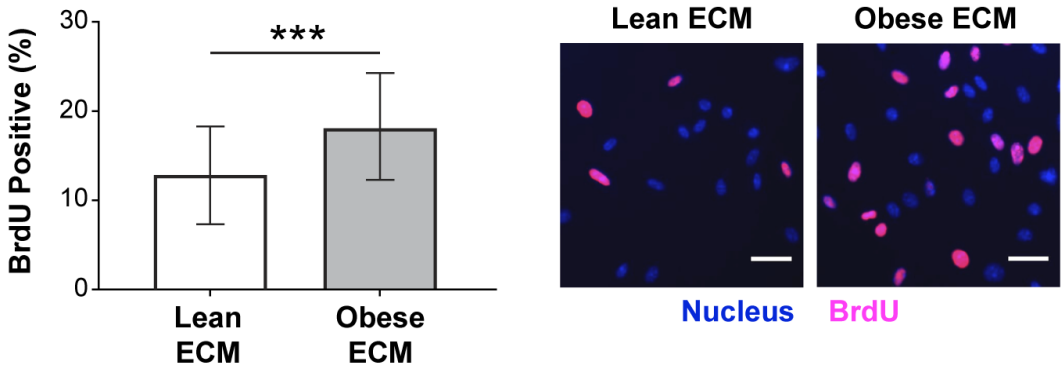

Figure 16: BMDM cultured on obese decellularized ECM are more proliferative as determined by BrdU incorporation with IF image analysis, 3 independent experiments, 30 representative images per condition per experiment, Bar = 25µm. Data are represented as mean ± SD, Student's t-test analysis. *** = $p < 0.001$ Published in Springer NL, *et al*. *Am J Path* 2019;189(10);2019-2035

Immunofluorescence image analysis indicated consistently increased numbers of arginase-1- and CD206-positive BMDMs cultured on obese ECM versus lean ECM (Figure 17). There was no difference in iNOS expression in the face of LPS stimulation with BMDM cultured on lean versus obese ECM (Figure 18). Taken together, these results suggest that macrophage interactions with obese ECM enhance an anti-inflammatory M2 macrophage phenotype when exposed to IL-4 and IL-13 whereas interactions with lean ECM do not influence M1 polarization when exposed to LPS stimulation.

2.8 Discussion

Given their intrinsic biochemical and physical similarity to the native ECM, decellularized ECMs prepared by detergent-based extraction offer promise to study macrophage activation[107]. They can be prepared from cells or tissues prone to increased fibrotic remodeling[42] and are suitable to study macrophage responses to

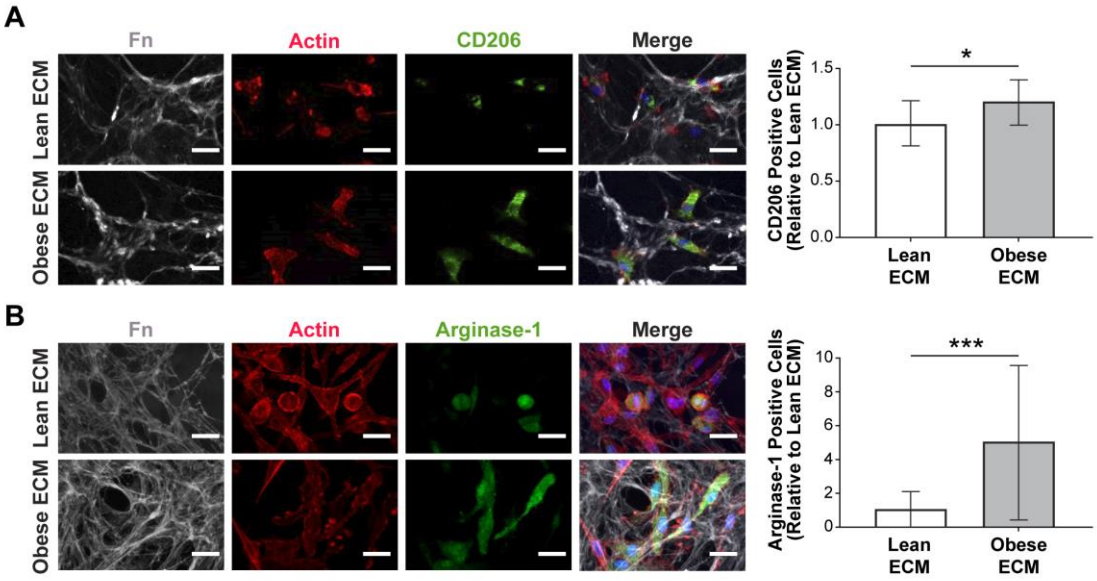

Figure 17: A greater proportion of BMDM cultured on obese decellularized matrix express the M2-macrophage marker arginase-1, when exposed to interleukin (IL) -4 and IL-13, as determined by number of positive cells identified by IF confocal image analysis, 3 independent experiments, 15 images per condition per experiment. Bar = 25µm. Data are represented as mean ± SD, Student's t-test analysis. * = $p < 0.05$ and *** = $p < 0.001$ Published in Springer NL, *et al*. *Am J Path* 2019;189(10);2019-2035

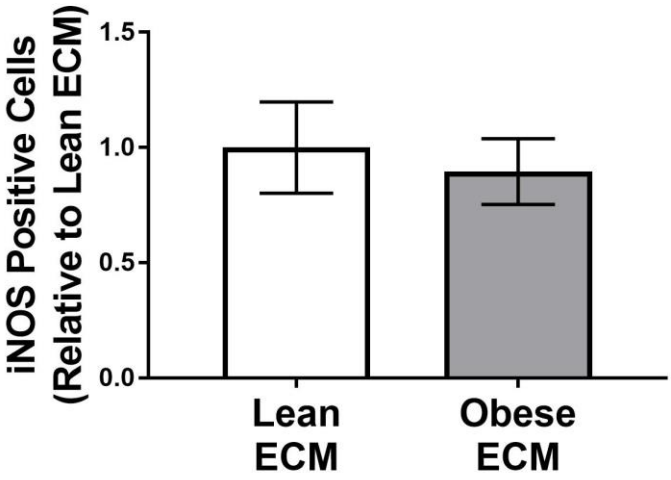

Figure 18: There is a no significant difference in iNOS expression in LPS-treated BMDM cultured on obese versus lean decellularized matrices as determined by epifluorescence microscopy and image analysis. Data are represented as mean ± SD, Student's t-test analysis. Published in Springer NL, *et al*. *Am J Path* 2019;189(10);2019-2035

ECM-dependent changes in mechanosignaling or mechanoactivation activation of growth factors, such as transforming growth factor (TGF) β. However, decellularized ECMs do have limitations such as variation between batches, difficulty in scaling up for higher throughput applications, and are mostly prepared from cells derived in 2D cultures, which may alter parent-cell functions from natural physiology. Controlling functional properties of these ECMs selectively and across multiple time and length scales is still difficult and, due to the limited thickness of such substrates, re-seeded cells may respond to the underlying culture plate rather than the ECM itself[111].

However, culture of BMDM on decellularized ECM did identify differences in macrophage phenotype between ECMs assembled by lean versus obese ASCs. There are several physical factors that might play a role in this observed difference. First, substrate stiffness is one of the best-studied physical factors that modulates macrophage function. Substrate stiffness has been identified to reduce pro-inflammatory responses[54,104] and obesity-associated ECM remodeling has been identified to have increased stiffness over the lean counterpart both *in vivo* and in the decellularized ECM model system used here[42]. Thus ECM stiffness is a compelling avenue for further investigation of obesity-associated ECM enhancing M2-bias to macrophage polarization.

Yet, stiffness alone might not explain the observed differences as the structure of ECM incorporate several other physical factors known to modulate macrophage functions. For example, cellular elongation has been shown to promote an M2-biased macrophage phenotype in the absence of cytokine stimulation[52]. The increased aspect ratio and linearity observed in macrophages cultured on the obese ECM suggests that the properties of macrophage adhesion to obese ECM facilitate cellular elongation and thus may additionally either promote an anti-inflammatory phenotype or inhibit a pro-inflammatory phenotype during macrophage polarization.

Topography is also known to play a role in macrophage polarization states. Differences in substrate roughness[112,113], fiber diameter[25,114,115], porosity[109,114], or spatial confinement[109] have all impacted macrophage activation states. Prior work in our laboratory detected thicker and more linearized ECM fibers in obese versus lean ECM[42] This finding is a captivating target for further evaluation as thicker or stretched ECM fibrils are typically stiffer than thinner or unstretched fibers[116,117], which may impact macrophage activation simultaneously through mechanical and topographical mechanisms. A deeper characterization of the structural and topographical differences between the lean and obese decellularized ECM is necessary to identify potential physical contributors to macrophage polarization. Interestingly, studies in other laboratories have found that M2 activation is quite sensitive to spatial/topographical manipulation, whereas the M1 activation state appears to be insensitive to these cues[52,109], similar to what we have reported herein in both our *in vivo* IHC and CIBERSORT data as well as the *in vitro* immunofluorescence studies. Future studies need to be performed to assess whether physical influences, such as ECM composition and structure, are sufficient to overcome pro-inflammatory stimuli.

One limitation of this study is the use of a single modality, immunofluorescence, to identify macrophage polarization state. Immunofluorescence is semi-quantitative regarding enzyme and protein expression and IF results could be corroborated by more quantitative methods such as ELISA of cytokine profiles on cell culture supernatants or reverse transcriptase (RT) quantitative (q) PCR for proteins of interest. We attempted both of these latter modalities. However, because the decellularized ECM can only be generated in small quantities using 13mm coverslips, and because seeding a high density of macrophages leads to proteolytic degradation of the ECM, standard assays such as ELISA and RT-qPCR are challenging. We attempted ELISA on supernatants for the M2 markers IL-10 and TGFbeta and the M1

markers TNFalpha and IL1beta. Unfortunately, the signal was below the detection limit, which we attribute to the low necessary cell numbers described above. We also attempted RT-qPCR but the decellularized matrix from the in vitro platform contaminates the cellular RNA during the extraction process resulting in a low concentration of poor quality RNA for analysis.

Another limitation of the study is the use of a single *in vitro* model system utilizing hematogenously-derived macrophages. Many tissue macrophages are not hematogenously-derived but rather are a self-renewing population originating from the embryonic yolk-sac[118,119]. One could argue that bone marrow-derived macrophages are not an ideal choice to model adipose tissue macrophages; however, M-CSF-1-cultured macrophages from murine bone marrow are recognized as a reproducible *in vitro* experimental standard[76], and thus are considered an appropriate choice for these experiments. Additionally, experimental evidence from breast cancer research indicates increased recruitment of hematogenously-derived macrophages into adipose tissue during the process of obesity[120], further supporting the relevance of the BMDM model system within this context. However, future experiments utilizing alternative *in vitro* and *ex vivo* macrophage model systems would be worthwhile.

CHAPTER 3

OBESE EXTRACELLULAR MATRIX-MACROPHAGE SIGNALING PROMOTES A PHENOTYPE SIMILAR TO PRO-ANGIOGENIC TUMOR-ASSOCIATED MACROPHAGES

Chapter written using content modified from the following publication:

Nora L. Springer[1,2,3], Neil M. Iyengar[4,5], Rohan Bareja[6], Akanksha Verma[6], Maxine Jochelson[7], Dilip D. Giri[4], Xi Kathy Zhou[8], Olivier Elemento[6], Andrew J. Dannenberg[5], and Claudia Fischbach[2,9] Obesity-associated extracellular matrix remodeling promotes a macrophage phenotype similar to tumor-associated macrophages. *Am J Path* 2019;189(10);2019-2035. PMID: 31323189

[1]Biological and Biomedical Sciences, Cornell University, Ithaca, NY

[2]Meinig School of Biomedical Engineering, Cornell University, Ithaca, NY

[3]Department of Diagnostic Medicine/Pathobiology, Kansas State University, Manhattan, KS

[4]Department of Medicine, Memorial Sloan Kettering Cancer Center, New York, NY

[5]Department of Medicine, Weill Cornell Medicine, New York, NY

[6]Institute for Computational Biomedicine, Caryl and Israel Englander Institute for Precision Medicine, Weill Cornell Medicine, New York, NY

[7]Department of Radiology, Memorial Sloan Kettering Cancer Center, New York, NY

[8]Department of Healthcare Policy and Research, Weill Cornell Medicine, New York, NY

[9]Kavli Institute at Cornell for Nanoscale Science, Cornell University, Ithaca, NY

N.L.S performed all histological and in vitro experiments unless otherwise indicated. N.M.I and A.J.D provided clinical samples and demographic data, X.K.Z provided

biostatistical support, D.D.G performed initial CLS assessment, M.J. provided mammographic interpretation. R.B., A.V, and O.E. performed transcriptomic and computational analysis. N.L.S, and C.F. designed the project and wrote the paper. All authors provided input on the manuscript.

3.1 Introduction:

All solid tumors recruit macrophages into their microenvironment and these macrophages are termed tumor-associated macrophages, also known as TAM. In most cases, TAM promote the growth and metastasis of tumors and the density of TAM correlates with poor prognosis in many types of cancers. TAM phenotypically resemble M2 or anti-inflammatory macrophages[121]. TAM's pro-tumorigenic functions overlap with and appear to be dysregulated normal physiological functions of M2 macrophages, such as dampening of the pro-inflammatory immune response[122], which would potentially be tumoricidal, facilitating fibrosis, which aids in cancer cell invasion and metastasis, and angiogenesis, which facilitates tumor growth and metastasis[20].

Spatially, TAMs often reside along the tumor-stroma border, an area that is characterized by increased fibrotic ECM remodeling[12,121], suggesting that peritumoral fibrosis and TAM are functionally coupled. While TAMs have been shown to enhance collagenous deposition within tumors[123], experimental evidence suggests that the converse, tumor-associated ECM remodeling directly modulating macrophage functions[124], may also be true. In obesity, M2 macrophages residing in the interstitial space between adipocytes also interact with remodeled and fibrotic ECM[35], similar to TAMs in tumors, leading to the hypothesis that macrophages residing in obese adipose tissue are phenotypically and functionally similar to TAM and therefore might contribute to the tumor-permissive microenvironment of obesity.

Gaining an improved understanding of how obesity modulates M1 and M2 macrophage density and function in the human breast is critical since M2 macrophages share similarities with tumor-associated macrophages (TAMs)[125] and thus, could play an important role in tumorigenesis[20] by suppressing anti-tumor immune responses[73], promoting angiogenesis[126], and assisting with cancer cell intravasation and metastasis[22].

Here, we explore the hypothesis that macrophages residing within obese adipose tissue resemble TAM using genomics, immunological, and molecular biological techniques.

3.2 Materials and Methods

Breast tissue transcriptomic and computational analysis

At the time of collection, fresh breast tissue specimens were snap-frozen, stored in RNAlater (Ambion, Foster City, CA) and total RNA was extracted for RNA-seq using the RNeasy Mini Kit (Qiagen, Valencia, CA). Polyadenylated RNA-seq was performed using the standard Illumina (San Diego, CA) Truseq kits and samples were sequenced using the HiSeq2000 platform. All reads were independently aligned with STAR_2.4.0f1 for sequence alignment against the human genome build hg19, downloaded via the UCSC genome browser, and SAMTOOLS v0.1.19 for sorting and indexing reads. Cufflinks (2.0.2) was used to get the expression values (FPKMS), and Gencode v19 GTF file for annotation. The gene counts from htseq-count[127] and DESeq2 Bioconductor package[128] were used to identify differentially expressed genes. The hypergeometric test and Gene Set Enrichment Analysis (GSEA)[129] was used to identify enriched signatures using the *different* pathways collection in the MSigDB database[130]. Gene-name based enrichment analysis was also performed using the webtool ENRICHR[131,132].

Assessing vascular and macrophage density in white adipose tissue.

Vascular density in breast white adipose tissue was evaluated via IHC on archived FFPE breast tissue. Five-micrometer sections were probed with rabbit polyclonal anti-CD31 (Abcam ab28364). The signal was amplified using Vectastain ABC universal kit (Vector Laboratories, Burlingame, CA) and detected with peroxidase substrate and DAB chromogen (ThermoFisher, Waltham, MA) with hematoxylin counter stain. Samples with repeatable severe sectioning artifact were excluded from analysis. Stained slides were digitally archived with an Aperio CS2 microscope (Leica Biosystems, Buffalo Grove, IL) and were analyzed with the ImageScope software positive pixel count algorithm v9.

Assessment of macrophage-secreted factors on endothelial cell behavior

A transwell assay was used to assess the effect of macrophage-secreted factors on endothelial cell migration. BMDM were seeded on lean and obese ECM at a density of 50,000 cells/coverslip in the presence of 10% serum and 10ng/mL recombinant mouse M-CSF. After overnight adhesion, BMDM coverslips were transferred to a new 24 well plate and media was changed to DMEM + 5% FBS + 20ng/mL IL-4 and 20ng/mL IL-13. An 8.0 μm pore polycarbonate membrane tissue culture insert (Corning Falcon, Corning, NY) that had been previously coated with 70 μg/mL rat-tail collagen type I was placed over each coverslip. After 6 hours culture time, Human Umbilical Vein Endothelial Cells (HUVEC, passage 2-3, Lonza, Allendale, NJ) cultured in M199 medium (BioWhittaker, Walkersville, MD) + 20% FBS + 1% Penicillin/Streptomycin + 30 μg/mL endothelial cell growth supplement (Millipore-Sigma), 2 mM glutamax (Gibco), and 2,500 U heparin salt (Millipore-Sigma) were seeded on top of the transwell insert at 50,000 cells/insert. After a subsequent 12 hours of culture at 37^{o}C and 5% CO_2, the transwell inserts were fixed

with 4% PFA (Electron Microscopy Sciences, Hatfield PA) and the distal side of the membrane was stained with DAPI. Nuclei of cells that had migrated through the membrane were manually counted (Image J) on four 10x objective fluorescent microscopy images (12, 3, 6, and 9 o'clock positions) per membrane with 3 membranes per condition per experiment.

Endothelial cell tubulogenesis was assessed via a Matrigel (Corning) tube-formation assay. BMDM were cultured on lean or obese ECM in medium containing 5% serum and no M-CSF. After 24 hours of culture, conditioned medium was collected, concentrated 10X in a 3kDa molecular weight centrifugation filter unit (Millipore-Sigma), and diluted back to a 1X concentration using EBM2 without growth factors. Using the reconstituted conditioned media, HUVECs were seeded on growth factor-reduced Matrigel-coated 96 well plates at a density of 10,000 cells/well and cultured for 12 hours. Subsequently, the media was carefully removed from the wells and HUVECs were incubated in Calcein AM (Invitrogen) to stain viable cells. After 15 minutes incubation at 37 °C, the wells were rinsed with PBS. A single 2x objective representative fluorescent image (covering the entire monolayer of each well) was captured and analyzed for HUVEC tube branch points, indicating increased network formation in response to chemical mediators in the conditioned medium, via manual counting in ImageJ. Three wells were analyzed per condition per experiment.

Angiogenesis multiplex protein array

BMDM were cultured on lean or obese ECM in medium containing 5% serum and no M-CSF. After 24 hours of culture, conditioned medium was collected, concentrated 10X in a 3kDa molecular weight centrifugation filter unit (MilliporeSigma), and diluted back to a 5X concentration using EBM2 without growth factors. Conditioned medium (BMDM-CM) was applied to membranes from a

multiplex sandwich ELISA angiogenesis protein array (R&D Systems ARY015) following kit instructions. Analysis was performed by pixel analysis of the raw integrated density (the sum of all pixel densities in the region of interest) in Image J.

Statistical Analysis

All statistical analysis was performed using Prism v7.0 (GraphPad Software, La Jolla, CA). Normality assumption of the parametric method was assessed by the Shapiro-Wilk test. Continuous data are represented as the mean ± SD or the median and interquartile range. Specific statistical tests used and number of independent samples and replicates per experiment are listed in the figure legends. A Tukey's post-hoc test was used when needed to account for multiple comparisons. Significance was set at $P < 0.05$.

3.3 Transcriptional identification of TAM

Given that M2 macrophage functions, such as promoting fibrosis and angiogenesis, and immune suppression, are commonly associated with increased tumorigenesis, we questioned whether the transcriptomic signature of obesity-associated M2-like macrophages in cancer-free breast tissue resembles that of TAMs. Accordingly, we compared a published gene expression signature of TAMs[133] to the RNA transcripts of obesity-associated M2 macrophages via Gene Set Enrichment Analysis (GSEA).

This analysis revealed 96 genes that are significantly upregulated in both the TAM gene signature and tumor-free breast tissue in obese versus lean women (Figure 19). As the TAM dataset was derived from the MMTV-PyMT mouse model of breast tumorigenesis, we evaluated whether the identified gene set would have human

relevance by querying the 96 upregulated TAM genes against the ARCHS4 human gene database (*https://amp.pharm.mssm.edu/archs4/data.html*).

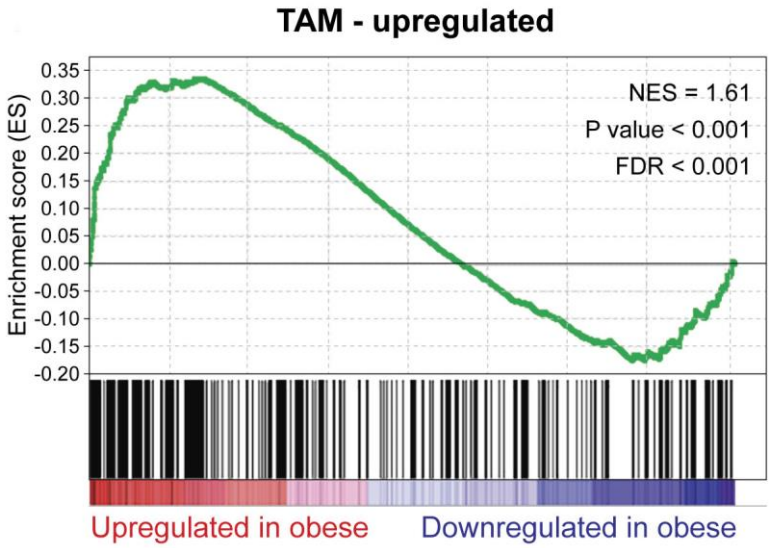

Figure 19: Gene set enrichment analysis[129] illustrates that M2 macrophage-related genes in obese breast tissue samples are concordant to a published gene profile of TAM[133], n=26. Published in Springer NL, *et al*. *Am J Path* 2019;189(10);2019-2035

We observed that the human macrophage signature was significantly enriched (52/96 genes, $p < 2.2 \times 10^{-6}$), indicating the human relevance of macrophage enrichment in mouse-derived TAMs (Figure 20).

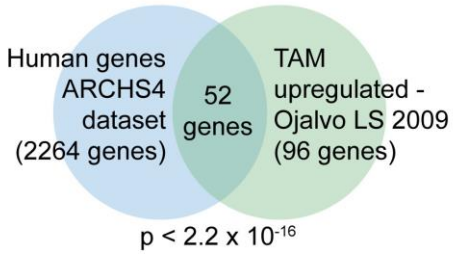

Figure 20: Comparison of TAM gene profile[133] to ARCHS4 human tissue dataset (*https://amp.pharm.mssm.edu/archs4/data.html)* indicates significant overlap (n=52) between the MMTV-PyMT-derived TAM genes and human macrophage genes via ENRICHR[131,132] analysis tool. Published in Springer NL, *et al*. *Am J Path* 2019;189(10);2019-2035

Importantly, these 52 human-relevant macrophage genes were capable of differentiating the majority of obese versus lean individuals based on differential expression levels in breast tissue (Figure 21). Interestingly, two lean women clustered with the obese rather than lean individuals, but histological analysis revealed that their breast adipose tissue had comparable levels of breast inflammation as the obese samples as determined by quantification of CLS number. Both women also had CIBERSORT M2 scores in the top 50% of our cohort. These findings could be compatible with recent evidence suggesting that a subset of women with normal BMI but histological evidence of breast inflammation[4] or increased adiposity when measured via dual-energy x-ray absorbitometry (DXA)[3] are at increased risk for breast cancer development, similar to obese individuals.

When the 52 genes were divided into categories based on cellular function (Table 2), differences in immune response- and angiogenesis-related genes were the most enriched subsets (Figure 22), compatible with known functional properties of TAMs[17,126,134,135].

Collectively, these results suggest that obesity is associated with macrophage phenotypic changes that resemble those of TAM, based on computational analysis of macrophage gene transcripts from tumor-free breast adipose tissue.

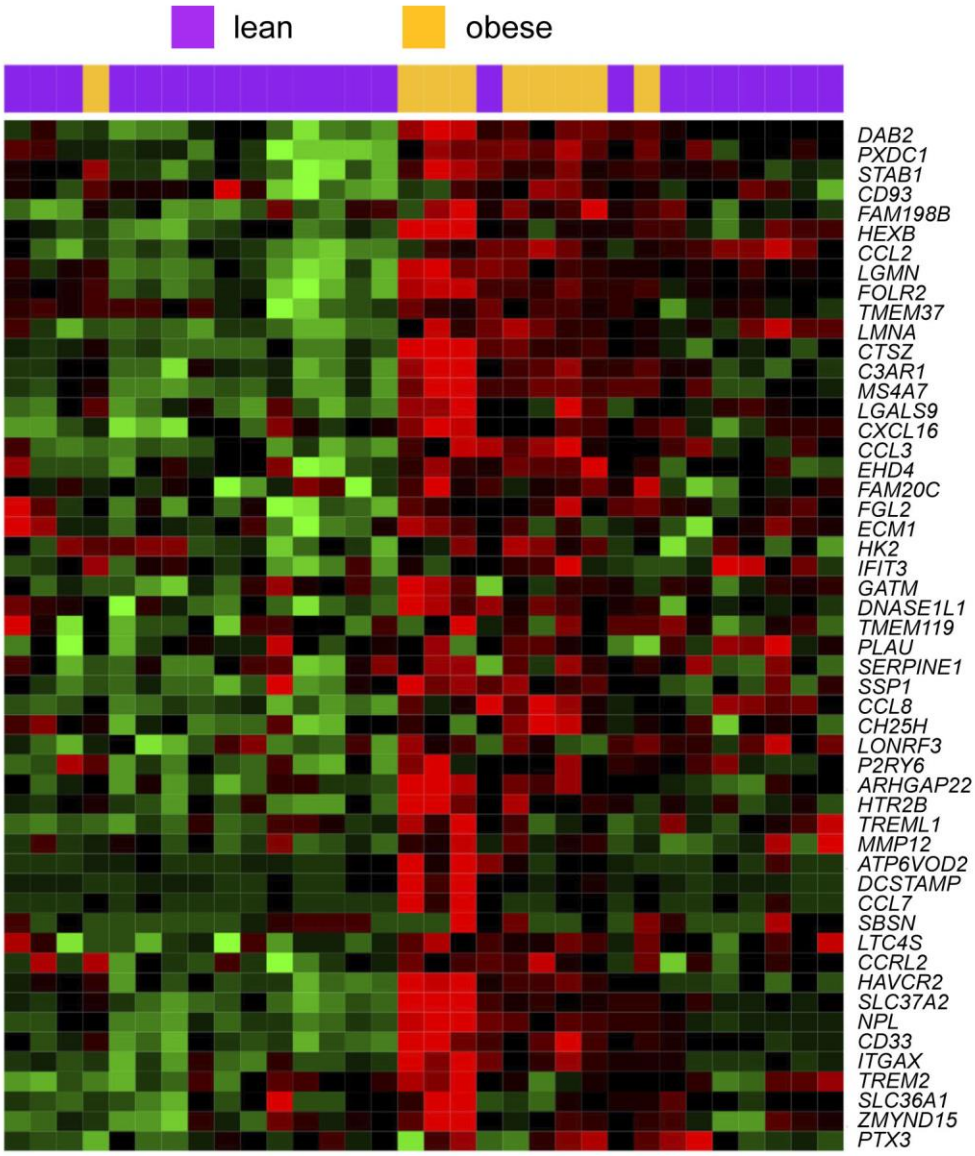

Figure 21: The 52 genes identified via GSEA and ENRICHR analysis is capable of delineating the majority of lean versus obese women based on differential gene expression. Published in Springer NL, *et al*. *Am J Path* 2019;189(10);2019-2035

Table 2: Known genes upregulated in tumor-associated macrophages that are also upregulated in macrophages from obese versus lean breast tissue. Genes are grouped by function. Published in Springer NL, *et al*. *Am J Path* 2019;189(10);2019-2035

TAM gene function	TAM genes
Immune Response	*C3AR1, CCL2, CCL3, CCL7, CCL8, CCRL2, CD33, CXCL16, DCSTAMP, FGL2, IFIT3, LGALS9, LGMN, LTC4S, PTX3, TREM2*
Angiogenesis	*CTSZ, ECM1, HK2, MMP12, PLAU, SERPINE1, SBSN, SPP1, STAB1*
Signal Transduction	*EHD4, FAM20C, HTR2B, MS4A7, P2RY6, TREML1*
Metabolism	*CH25H, DNASE1L1, GATM, HAVCR2, LMNA, LONRF3*
Transport	*ATP6V0D2, FOLR2, SLC36A1, SLC37A2, TMEM37*
Development	*DAB2, HEXB, ZMYND15*
Adhesion/Motility	*CD93, ITGAX*
Unknown	*ARHGAP22, FAM198B, NPL, PXDC1, TMEM119*

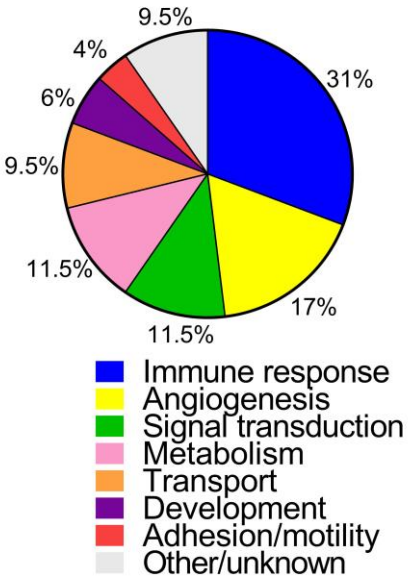

Figure 22: Differential gene expression analysis of macrophage-associated genes suggests varied physiological functions of macrophages in obese breast tissue. n=52. Published in Springer NL, *et al*. *Am J Path* 2019;189(10);2019-2035

3.4 Obesity-primed macrophages promote angiogenesis

Obesity is associated with increased vascular density in adipose tissue[136], a finding that is typically attributed to an adipocyte hypertrophy-mediated increase in hypoxia and consequential upregulation of pro-angiogenic factor secretion[25]. However, it remains unclear whether or not obesity-associated, fibrotic ECM remodeling may independently activate angiogenesis by stimulating macrophage transition into a pro-angiogenic M2 phenotype. As increased angiogenesis is a necessary checkpoint for tumor growth and metastasis[137,138] and because we found that macrophages in obese adipose tissue upregulate angiogenesis-related genes (Table 2, Figure 22), we evaluated whether vascular density and presence of M2-biased macrophages correlated in histological samples from our patient cohort.

The density of CD206+ macrophages in the adipose tissue interstitium correlated with positive pixel counts for the endothelial cell marker CD31+ (Figure

23) suggesting a potential functional relationship between macrophage phenotype and density and vascularity in obese adipose tissue.

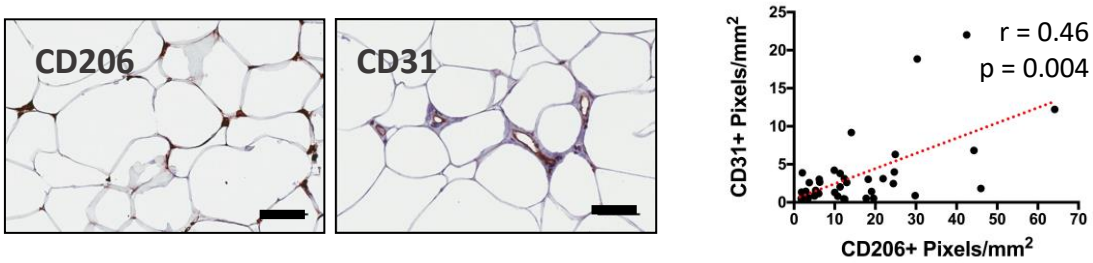

Figure 23: CD206+ macrophages and CD31+ vascular profiles are positively correlated based on IHC image analysis of clinical samples N=43. 5 images of adipose tissue per section analyzed. Analysis was performed blinded to BMI for each section. Bar = 100µm. Red dashed line illustrates the best fit line as determined by linear regression. Published in Springer NL, *et al*. *Am J Path* 2019;189(10);2019-2035

Assessment of macrophage-secreted factors on endothelial cell behavior

Given that many other mechanisms are active *in vivo* and could be responsible for these observations, we next questioned whether BMDM cultured on obese ECM would possess increased pro-angiogenic capability as compared to BMDM cultured on lean ECM. Endothelial cell migration and endothelial cell tubulogenesis in response to macrophage-secreted factors were assessed via a transwell assay and a Matrigel tube-formation assay, respectively.

We found that BMDM cultured on obese ECM increased HUVEC migration relative to BMDM cultured on either lean ECM or Fn-coated coverslips (Figure 24A). Additionally, conditioned medium collected from BMDM cultures on obese matrices stimulated increased tubulogenesis of HUVECs on growth factor reduced Matrigel relative to BMDM-conditioned medium from lean ECM or Fn-coated coverslips (Figure 24B). These results suggest that macrophages in contact with obesity-associated ECM could promote vascular remodeling by releasing pro-angiogenic

factors, possibly playing a role in the recognized link between obesity and tumor development and progression.

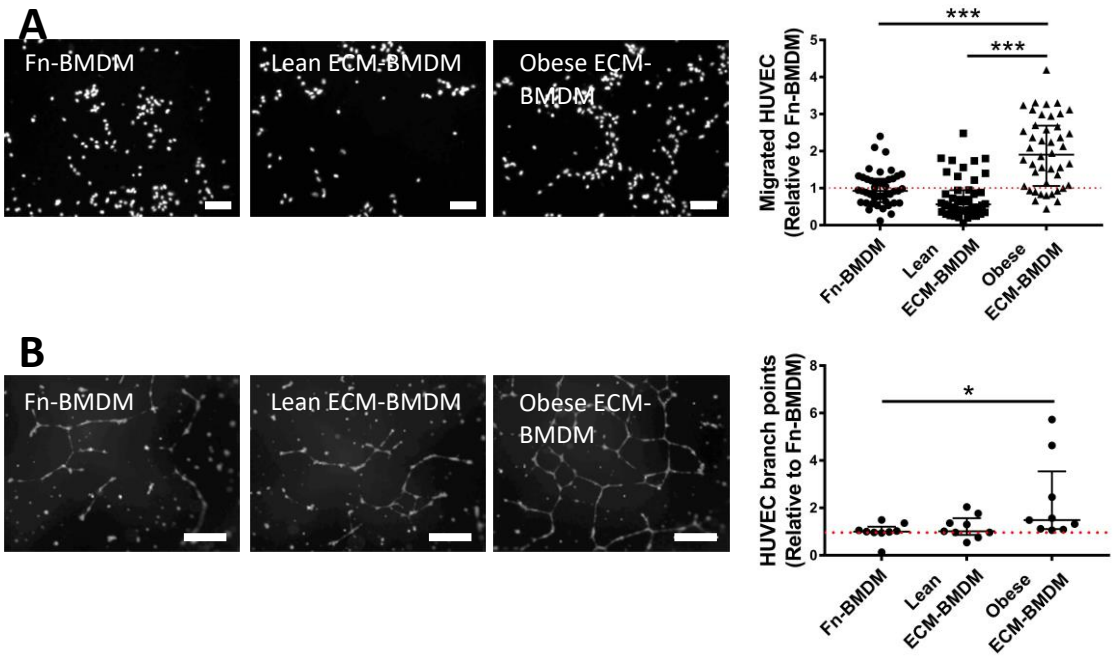

Figure 24: A) Endothelial cell transwell migration towards BMDM is significantly increased when IL-4 and IL-13 stimulated BMDM are in contact with obese versus lean or fibronectin (Fn) control ECMs; data represented as median and interquartile range, Kruskal-Wallis analysis, 3 independent experiments, 3 transwells per condition per experiment, 4 images per transwell. Bar = 50µm **B**) Endothelial cell tubulogenesis is increased in the presence of conditioned medium collected from unstimulated BMDM cultured on obese versus lean ECM or Fn control substrates. Data represented as median and interquartile range, Kruskal-Wallis analysis, 3 independent experiments, 3 wells per condition, one representative image per well. Bar = 100µm. Published in Springer NL, *et al*. *Am J Path* 2019;189(10);2019-2035

3.5 Osteopontin (SPP1) and TIMP-1 are potential mediators of obese ECM-proangiogenic stimulus of macrophages

We next attempted to identify candidate pro-angiogenic factors that were increased in conditioned medium from BMDM cultured on obese versus lean decellularized ECM. Two angiogenesis-associated proteins of interest, osteopontin (OPN) and tissue inhibitor of matrix metalloproteinase (TIMP)-1 were significantly

increased in BMDM-CM. Interestingly, osteopontin (also known as secreted phosphoprotein (SPP)-1) was one of the angiogenesis transcripts identified as being upregulated in obese versus lean women (Figure 21, Table 2) via differential gene expression analysis of TAM-associated transcripts.

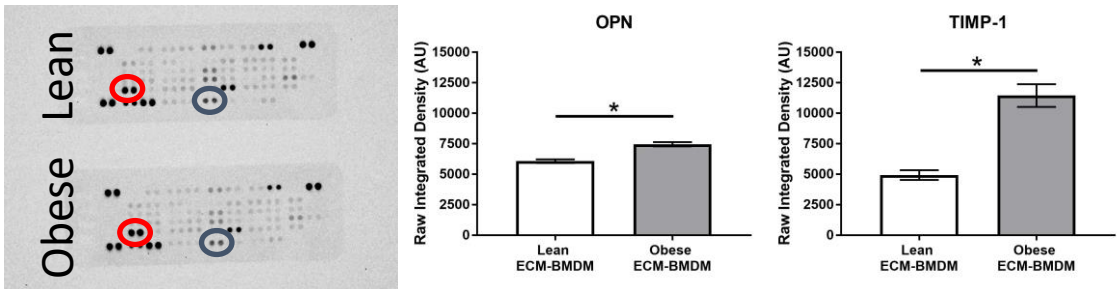

Figure 25: Conditioned media from BMDM cultured on lean and obese decellularized ECM were used for an angiogenesis protein multiplex array. Osteopontin (red ovals) and TIMP-1 (blue ovals) expression levels were increased BMDM-CM from obese decellularized matrix. Student's t-test, * = $p < 0.05$. Unpublished data.

3.6 Discussion

The tumor promoting functions of macrophages are manifold and – in addition to modulating angiogenesis - include direct effects on tumor growth, invasion, metastasis, and stroma remodeling[20,123,139,140]. We focused on the effect of obesity-associated ECM on transition to M2-like macrophages and possible functional implications on endothelial cells to demonstrate the broad significance of obesity-associated ECM in regulating stromal cell functions contributing to tumorigenesis. While future studies will be necessary to further validate the molecular mechanisms underlying our results, our findings are complementary to previous work. For example, others have shown that peri-tumoral adipose tissue not only contains increased collagen content, but also represents a rich depot of pro-angiogenic macrophages[97]. Additionally, obese (and therefore inflamed) adipose tissue has been

shown to promote stromal vascularization and angiogenesis prior to tumor development with implications for tumorigenesis[120]. Based on our data, it is plausible that interstitial fibrosis in adipose tissue can contribute to increased angiogenesis via modulation of macrophage phenotype. Indeed, the field of regenerative medicine and biomaterials has been utilizing alterations in matrix composition to modulate macrophage response and guide proper wound healing for surgical implant devices for some time[80,141–144]. Future studies utilizing engineered co-culture models that integrate ASCs, macrophages, endothelial cells as well as varying ECM composition and mechanics to recapitulate the complex obese adipose tissue microenvironment are necessary to identify the impact of obese adipose tissue on macrophages, angiogenesis, and ultimately tumor cell behavior[145–147].

Several angiogenesis-related genes were upregulated in the obese macrophage gene signature including secreted phosphoprotein 1 (*SPP1*, also known as and referred to herein as osteopontin or *OPN*), serpin E1 and stabilin 1. Of these three, OPN is the best characterized in obesity and with regard to TAMs. Thus, OPN an enticing target for future studies. OPN is a multifunctional cytokine expressed by many cell types with both paracrine and autocrine activities that plays a role in multiple hallmarks of cancer[148]. OPN is highly secreted by macrophages in adipose tissue[149]. During the process of obesity, OPN expression is upregulated resulting in recruitment of macrophages into the fat pad and stimulation of local macrophage proliferation resulting in a positive feedback loop contributing to obesity-associated inflammation[149–151]. Within the tumor microenvironment, cancer cells are a large source of OPN in the tumor microenvironment. However, TAMs are capable of supplying sufficient OPN to rescue cancer cell motility and invasion in OPN knockdown models[152], suggesting that a source of OPN within the obese breast adipose tissue microenvironment might accelerate tumorigenesis, through paracrine

interactions, during the initiating stages of neoplastic transformation. TAM expression of OPN stimulates COX-2 production and subsequent PGE_2 production, both known players in tumor growth and angiogenesis[153]. Interestingly, COX-2-expressing TAM numbers have recently been correlated to collagen deposition and density within tumor stroma but not epithelial nests[154] suggesting that ECM-remodeling might play a regulatory role in the OPN-COX-2 signaling axis contributing to breast cancer.

Although less is known about its physiological role in obesity or breast cancer, TIMP-1 is another enticing target for further evaluation. TIMP-1 is upregulated in adipose tissue during obesity although there is conflicting data as to whether TIMP-1 is secreted by adipocytes or cells within the stromal vascular fraction, such as macrophages[155,156]. In a high fat diet but obesity-resistant BALBc mouse model, TIMP-1 was found to be upregulated and contribute to syngeneic mammary carcinoma cell migration[157]. The high fat diet in this mouse model was sufficient to induce marked adipose tissue inflammation based on histology images, but adipose tissue interstitial fibrosis was not assessed in this study. In another study that assessed adipose tissue inflammation independently of obesity, TIMP-1 was found to be upregulated in inflamed peritumoral adipose tissue relative to non-inflamed distant adipose tissue[97]. Intriguingly, this peritumoral adipose tissue was characterized by extensive fibrosis, increased M2-biased macrophage density, and increased blood vessel density relative to distant adipose tissue depots[97], similar to characteristics described for obese versus lean adipose tissue. Additional studies are necessary to identify whether adipose tissue macrophages are the source for TIMP-1 secretion and whether this secretion has functional consequences for tumor angiogenesis.

CHAPTER 4

DISCUSSION AND FUTURE DIRECTIONS

4.1 Biomaterials approaches to modeling ECM-macrophage interactions

Macrophages play critical roles in homeostasis through roles in immunity and tissue regeneration and repair. However, when macrophages become dysregulated, they are potent contributors to pathological conditions such as chronic inflammation and cancer. Because of these conflicting roles, a thorough understanding of macrophage polarization, differentiation, and functional plasticity under conditions of health and disease is critical. In Chapter 2, I presented data showing that obesity-associated ECM remodeling modulates macrophage polarization. Although the mechanisms via which this observation occurs are not fully elucidated, changes in mechanotransduction may play a role. How physical factors affect macrophage functions has garnered some attention in the past several years, but still remains poorly understood. Members of the physical sciences and engineering research community have an opportunity to advance this field through the use of engineered model systems to study macrophage activation.

Macrophages and their precursors are fully capable to adapt their behavior to a variety of compressive and shear stresses, strains, and tissue elasticities during tissue invasion (Figure 26)[158]. Yet, our knowledge of the cellular and molecular signals that may underlie differential macrophage responses to their mechanical environment is still somewhat limited and currently mostly derived from extrapolating results obtained with other cell types (Figure 26B).

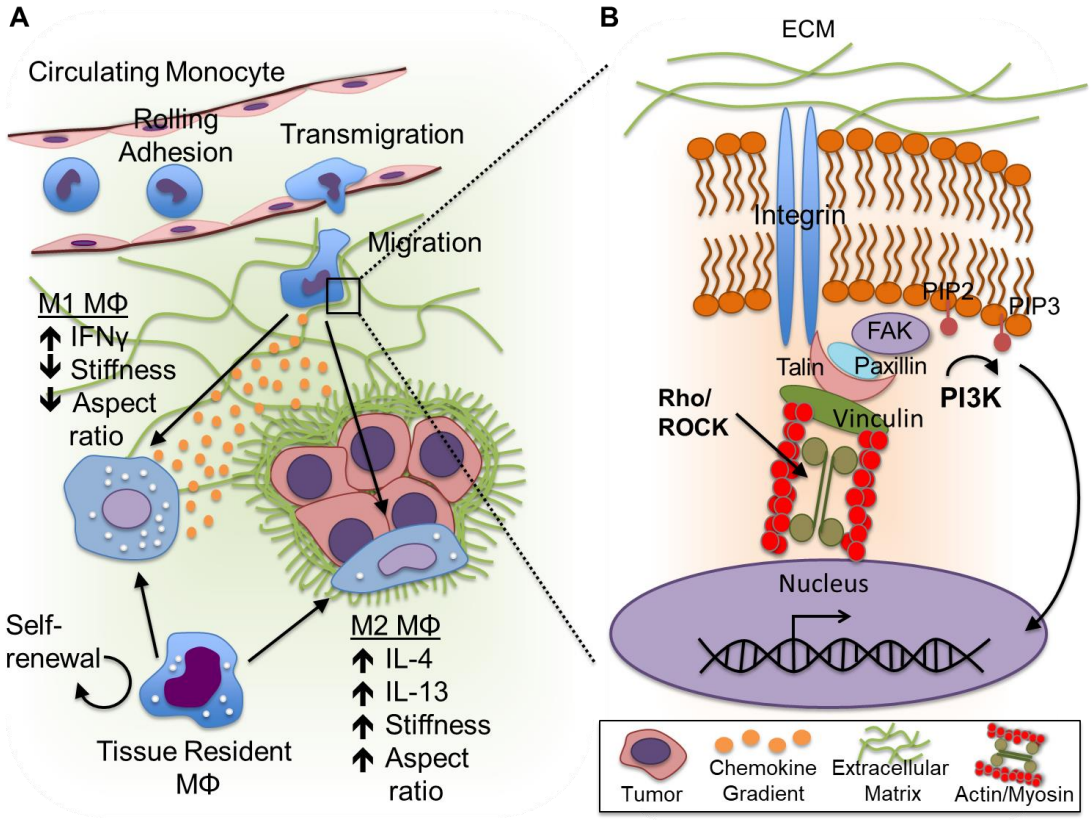

Figure 26: Mechanosignaling regulation of macrophage phenotype. **A**) Macrophages (MΦ) derived from either the circulating monocyte pool or the tissue resident macrophage pool must adapt and respond to a variety of stresses and strains during their lifespan. Differentiation into either classically (M1) or alternatively activated (M2) macrophages is directed by chemokine and cytokine input, but possibly also by varied mechanosignaling caused by changes in ECM stiffness and/or cell morphology. **B**) Close-up view of cell-ECM interactions and mechanotransduction. Integrin attachment to ECM activates signal transduction via Rho GTPase-mediated actin-myosin contractility and stimulation of downstream targets of the phosphoinositide-3 kinase (PI3K) pathway that regulate cell functions. FAK = focal adhesion kinase, ROCK=Rho-associated protein kinase, PIP2 = phosphatidylinositol (4,5)-bisphosphate, PIP3 = phosphatidylinositol (3,4,5)-trisphosphate. Published in Springer, NL and Fischbach C. *Curr Opin Biotech*, 2016;40:16-23

Studies with mesenchymal stem and tumor cells, for example, have revealed that ECM mechanical alterations mediate phenotypic changes by regulating integrin

clustering, focal adhesion formation, and cell contractility in a manner that depends on Rho GTPase and Rho-associated protein kinase (ROCK) signaling[9,159]. Stiffness-dependent increases in cell contractility, in turn, cross-talk with growth factor receptor signaling and can up-regulate down-stream events such as phosphatidylinositol 3-kinase (PI3K) signaling, an important participant in oncogenic transformation[160–162] as well as the resolution of the acute inflammatory response and bias toward an anti-inflammatory (M2) macrophage phenotype[163].

Recent evidence indicates that the phenotype of macrophages is dependent on substrate stiffness. In fact, increased substrate rigidity decreases macrophage pro-inflammatory responses directly[54,104,164] but may also indirectly affect macrophages by modulating cell shape[164]. Forcing macrophages into an elongated shape with micropatterned arrays of fibronectin upregulates M2 markers and decreases response to pro-inflammatory stimuli[164]. These findings are further supported by the finding that ROCK and PI3K both appear to play a role in macrophage polarization and phenotypic switching[165,166]. Finally, ECM stiffness-dependent changes in cell contractility can stimulate paracrine signaling of macrophage-modulating morphogens; e.g., by enhancing mechanoactivation of transforming growth factor β1 (TGFβ1)[167], a potent immunosuppressive cytokine that modulates macrophages to a more M2 phenotype and reduces pro-inflammatory cytokine secretion[168].

Obesity-associated adipose tissue ECM has been found to be stiffer than its lean counterpart[42]. Therefore, alterations in mechanotransduction between lean versus obese ECM may play a role in the observed difference in macrophage polarization presented in Chapter 2. Polyacrylamide (PA) hydrogels, a synthetic biomaterial platform are often used in *in vitro* experiments to allow for more controlled modulation of ECM physicochemical parameters. While PA hydrogels are inherently non-adhesive, they can be functionalized to enable cell binding by coupling purified

ECM components, decellularized ECM, or peptide sequences thereof [169]. For example, PA hydrogels modified with fibronectin or arginylglycylaspartic acid (RGD) adhesion peptides and adjusted in their cross-linking density through altering the ratio of acrylamide to bisacrylamide are routinely used to analyze stiffness-dependent cell responses[170].

However, the polyacrylamide hydrogel platform has limitations including the inability to be remodeled or for cells to be encapsulated into these gels due to monomer toxicity. Thus, these studies are limited to 2D formats. Polyethylene glycol (PEG)-based hydrogels circumvent the dimensionality and toxicity shortcomings, but cannot be remodeled by cells either. Introducing and/or removing functionalities (e.g. integrin adhesion sites and matrix metalloproteinase [MMP]-cleavable sequences) through light-dependent mechanisms (e.g. photo-initiated addition, photo-crosslinking, or photo-degradation[171–175]) or via modular bioclick and bioclip reactions can help to address this shortcoming. Selectively adding or removing functionality at a desired timepoint[176,177] or in a specific location[172,173] additionally provides the opportunity to introduce temporal and spatial control over both chemical and mechanical properties of the respective hydrogel. Despite their advantages, these model systems are often amorphous and lack ECM structural entities that drive macrophage behavior.

To mimic the combination of fibrillar components and porosity in the native ECM, fibers prepared through electrospinning or polymerization of native ECM components could be integrated into composite hydrogels[178]. Integrating varyingly stiff and thick fibers[117] into hydrogels of altered bulk mechanical properties will permit decoupling of the effects of individual fiber versus bulk stiffness properties on macrophages. Differentiating between these properties will be critical as most current research focuses on bulk mechanical properties, but disregards that fiber mechanics are similarly important and may, in fact, lead to differential cell responses[179]. Finally,

being able to modulate the orientation of such fibers, for example, by unidirectional compression of the fiber-containing hydrogels[180] will enable new insights. This manipulation will allow assessing whether changes in collagen fiber orientation[12] in lean versus obese adipose tissue impacts macrophage polarization.

While the above described biomaterials strategies could allow for multicomponent analysis of macrophage function in response to obesity-associated ECM remodeling, these systems are coupled to ever evolving complexity and thus future opportunities. For example, computational strategies are likely necessary to analyze the large multifaceted data sets and distinguish individual influences on cell behavior in a dynamic network of exponentially increasing interactions. Studying macrophage behavior in 3D tissue-engineered models furthermore requires high resolution imaging modalities for real-time tracking of cells and subcellular-components, which may not be routinely accessible by many labs. Moreover, incorporation of macrophages into these bioengineered model systems will alter the physicochemical properties of the ECM mimics over time. Assessing the spatiotemporal feedback of macrophage phenotype and ECM compositional, structural, and mechanical properties will be necessary to advance our knowledge of the underlying mechanisms. In addition to evaluating the influence of ECM-mediated stress and strain on immune cells, as well as immune-cell sensed deformation of the substrate[181], biomaterials models should reflect the multicellular composition of fibrosis-associated microenvironment. For example, fibrosis is characterized by altered vasculature and thus altered convective and diffusive transport properties. Recently, interstitial flow has been shown to regulate macrophage polarization state[182]. Microfluidic co-culture devices with integrated vascular networks should be used to further evaluate the role of transport properties as well as shear and interstitial pressure on processes essential to macrophage function[182–184]. Ultimately, all of the above

mentioned model systems should be extended to investigate the physical control of other immune cells that play important regulatory roles in fibrosis and/or tumor-associated microenvironments. In summary, the rapid development of new biomaterials and tissue engineering strategies provides an opportunity to further our understanding of macrophage interactions with fibrotic ECM microenvironments and their relevance to tumorigenesis.

4.2 Comprehensive characterization of obesity-associated ECM and macrophage populations

We identified that obesity is associated with an increased density of anti-inflammatory macrophages that functionally resemble tumor-associated macrophages and that extracellular matrix remodeling in obese adipose tissue contributes to this phenomenon. However, the mechanisms underlying this observation are still unknown. Additional experiments characterizing compositional and structural differences in lean versus obese adipose tissue extracellular matrix, assessment of real-time matrix-macrophage interactions, and a comprehensive characterization of macrophage subsets in obese adipose tissue are necessary to further our understanding in this field. Below, I discuss some potential avenues for further investigation.

ECM composition

Decellularized ECM is being increasingly used for both clinical/regenerative and experimental purposes. Yet, a thorough understanding of the bioactive properties of these matrices is sorely lacking. Prior work in our laboratory as well as some of the data presented herein have identified that obesity-associated ECM contains a greater density of fibronectin and collagen I relative to its lean counterpart. However, this is an admittedly narrow assessment of the decellularized ECM platform and depends

primarily on immunostaining which can be confounded by antibody cross-reactivity as well as having limited quantitative ability.

Proteomics is a more robust and unbiased method to assess ECM composition. The matrixome of ECM assembled by adipose stromal cells has been described[185], but to my knowledge, differences in bioactive matrix proteins between lean and obese decellularized ECM and between native and decellularized adipose tissue ECM have not been assessed. Nevertheless, identifying the unique characteristics of our decellularized ECM platform, rather than relying on published datasets, would be worthwhile as the yield of proteomic data from decellularized ECM is highly dependent on the method of detergent extraction as well as the sensitivity of the proteomic method to detect cross-linked or insoluble matrix components[186]. Due to the high collagen content of ECM, additional proteomic analysis after collagenase digestion might increase yield for low abundance proteins[187] that may be important bioactive mediators of macrophage function. Although not a hypothesis-driven approach, proteomic differential expression analysis or abundance analysis should identify differences in obese matrix composition and identify or prioritize targets for future mechanistic studies.

ECM structure and macrophage interactions

A broad knowledge of the composition of lean versus obese adipose tissue ECM will be most valuable when coupled with structural and spatial knowledge of ECM-macrophage interactions. The mainstay techniques to assess ECM structure and topography are confocal microscopy, second harmonic generation imaging, and scanning electron microscopy and all techniques could play a role in future directions of this project. Once candidate ECM components with disproportionate proteomic expression are identified, immunostaining of decellularized ECM for these

components with and without adherent macrophages would provide valuable information as to distribution and relevance to macrophage adhesion. As thicker sections would facilitate 3D reconstruction for spatial organization, seeding macrophages into tissue-derived decellularized matrices[188] could be attempted. To enhance the mimicry of native tissues, tissue-derived decellularized ECM can be reconstituted with inclusion of carbohydrates in medium to create spaces of exclusion due to macromolecular crowding. This process of macromolecular crowding enhances fibril nucleation and more closely mimics the native ECM[189]. Scanning electron microscopy (SEM) could be performed for qualitative assessment of fiber diameter, linearity, roughness, and porosity, all physical factors that have been indicated to guide macrophage polarization on any of the above mentioned model systems. SEM performed on samples with seeded macrophages would allow for high-resolution assessment of macrophage morphology concurrent with localized ECM topography.

The above-mentioned modalities are static, whereas knowledge of macrophage interaction with ECM components in real time might add valuable insights to ECM-mediated regulation of macrophage polarization. Fluorescence imaging of fresh post-mortem adipose tissue explants has been used to track macrophage proliferation and migration previously[35]; however this technique requires fluorescence tagging of macrophages, either through immunological methods or using transgenic fluorescent proteins. Intravital microscopy is a powerful tool for live tissue imaging or serial imaging of lesions over time in murine models. Intravital second or third harmonic generation microscopy does not require fluorescence labeling. Leukocytes can be recognized via their internal granularity and morphology[190,191] amongst a visible background of collagen structures to track migration and function *in vivo*. Harmonic generation microscopy has the added benefit of identifying and quantifying collagen remodeling or fibrosis within tumor microenvironments[123,192], and thus is likely to

have the same capability within the lean versus obese adipose tissue microenvironment. Assessing structural changes in ECM remodeling, and macrophage recruitment, polarization, and association with ECM within an individual (i.e. laboratory mouse) over time during obesity induction and maintenance could be paradigm-shifting in our understanding of adipose tissue biology during obesity.

Further characterizing macrophage subsets and their spatial distribution

Beyond a detailed accounting of adipose tissue ECM in lean and obese individuals, additional work needs to be done to precisely qualify macrophage subsets. As noted previously, macrophages are extremely heterogenous in cellular phenotype and functions. To date, five subsets of macrophages have been identified, M1 and M2a, b, c, and d[193] and are best differentiated by large panels of cell surface markers, often measured by flow cytometry, or gene expression profiling[76,194]. Adipose tissue-macrophage that do not fit within the above defined subsets are also being identified[195]. Tumor-associated macrophages are also divided into subsets, similar to M2 macrophages, based on functionality[121].

Our study was a jumping-off point using the broad categories of M1 (pro-inflammatory) and M2 (anti-inflammatory) macrophages using single IHC markers for each subset and corroboration of IHC findings with computational methods. The LM22 CIBERSORT algorithm does not subdivide M2 macrophages into subsets based on gene expression profile nor can this method provide spatial information that was critical to our study objective. Flow cytometry on cell suspensions derived from adipose tissue has been performed previously[196,197] and would provide more detailed characterization about macrophage subsets in lean and obese breast adipose tissue, but also would lose the spatial component desired in this study. Immunohistochemical staining for multiple macrophage markers on serial sections of breast adipose tissue

could be performed. This approach is labor-intensive, time consuming, and does not precisely co-localize expression at the single cell level.

Newer modalities like multiplex immunofluorescence IHC would accommodate for the limitations of all the above mentioned methodologies. Multiplex IHC has the advantage of evaluating up to 30 markers simultaneously[198]. The multispectral microscopic analysis improves signal separation allowing for more precise analysis of colocalization and spatial distribution. Modifications to the protocol using cleared tissues and transparent tissue tomography for 3D reconstructions[199] or systems biology approaches to manage large data sets acquired by whole slide imaging[200] will only enhance the applicability and power of this platform for research purposes. Although multiplex IHC is most frequently used to evaluate the immune microenvironment in solid tumors for immuno-oncology purposes, the technology should be readily transferred to adipose tissue.

Further genomic characterization of adipose tissue macrophage populations is necessary. The CIBERSORT data presented herein was derived from the transcriptome of bulk tissue biopsies. Although the majority of our samples contained a high proportion of adipose tissue, genomic data from fibroglandular macrophages would also be included in our dataset. To overcome this limitation, future studies could be peformed on adipose tissue that has been dissected away from the fibroglandular tissue. Single-cell RNA sequencing followed by principal component analysis would be an unbiased way to identify functionally distinct adipose tissue macrophage populations. After macrophage populations are identified via unbiased genomic analysis, specific spatially segregated macrophages can be selected for comparison via laser capture microdissection. Due to the heterogeneity of breast tissue and breast cancers, laser capture microdissection has been used abundantly in this field to isolate relative pure cell populations for evaluation. However, a literature search

failed to identify whether this modality has been previously used to interrogate macrophage subsets between lean or obese breast adipose tissue, between fibroglandular and adipose compartments of breast tissue, or between TAM and adipose macrophages in breast tissue. These studies could be attempted on archived tissues, but would be best performed prospectively on frozen tissue sections as tissue processing, handling, and archiving of FFPE tissues can all negatively affect RNA integrity[201].

4.3 Obese adipose tissue as a depot for tumor-promoting immune cells

In addition to comprehensive characterization of macrophage populations in obese adipose tissue, additional experiments need to be performed to determine whether these cells have a functional consequence on cancer development or progression. We identified OPN as a differentially expressed gene in macrophages between lean and obese women. Indeed, OPN has been documented to be expressed at high levels in obese adipose tissue and the primary source of OPN in adipose tissue is from macrophages[149]. This process results in a positive feedback loop of macrophage accumulation as OPN is a potent inducer macrophage proliferation[151]. Interestingly, we also identified a trend for higher OPN secretion by macrophages when they were in contact with obesity-derived ECMs. OPN is an enticing target for further evaluation as OPN is a ubiquitous bioactive molecule in the tumor microenvironment where it is secreted by stromal cells, breast cancer cells, and TAM to enhances breast cancer growth and metastasis[152,202,203]. Whether OPN secreted by M2 macrophages in obese adipose tissue contribute to breast cancer initiation and whether obesity-associated ECM remodeling modulates macrophage OPN secretion is currently unknown.

Earlier, we posited a theory that macrophages residing in the interstitium of obese breast adipose tissue could be a depot for recruitment of TAM into the tumor bulk. Studies have assessed methods of cancer cell recruitment of TAM or metastasis-associated macrophages (MAM) from hematogenously-derived monocytes[204,205], but I was unable to locate studies that assessed TAM recruitment from macrophages residing in adjacent noncancerous tissues. Prior work has illustrated that obese adipose tissue recruits increased numbers of macrophages relative to lean adipose tissue through CCL2 signaling. This macrophage recruitment enhances early tumor development through increased angiogenesis in a humanized mammary model system[120]. Increased numbers of macrophages were present in xenografts from mice modeling obesity, but neither the phenotype nor the tissue provenance of these macrophages was identified in this study. Determining whether adipose tissue macrophages are recruited to become TAM will require carefully choreographed *in vivo* experiments with tools that can either track macrophages over time, such as serial intravital microscopy experiments or produce a trackable macrophage population arising from the mammary fat pad, for example, via adoptive transfer techniques.

4.4 The cumulative effect and reversibility of obesity-associated ECM remodeling on cancer risk

Although the focus of this work was on the effect of obesity-associated remodeling on immune cell, specifically macrophage, phenotype, there are interesting and valuable areas of further inquiry on the extracellular matrix remodeling itself. Recently, it has been discovered that pro-tumorigenic properties of obesity, specifically epigenetic modifications, can persist and enhance tumorigenesis even after return to normal body weight in a mouse model of diet-induced obesity[206]. Although

some reversal is seen in ECM remodeling after caloric restriction[42], whether this reversal imparts a biological impact has yet to be determined.

This question is critical at a population level. Lifestyle modifications such as diet and physical activity are first-line interventions to reduce cancer risk associated with obesity. However, inherent qualities such as genetics[207], epigenetics[208], and early-life factors[209] dramatically influence the effectiveness of these interventions. Adipose tissue stromal remodeling during obesity may be similarly important in the effectiveness of lifestyle interventions to reduce cancer risk at the population level. Therefore, an increased understanding of adipose tissue biology during obesity is necessary to supplement or refine lifestyle interventions to prevent cancer.

Evaluating which aspects of obesity-associated ECM remodeling are reversible, whether there are retained effects that are pro-tumorigenic after weight loss, and at what timepoint interventions are effective, will require careful experimental design to assure translatability. The mouse model of obesity (diet-induced versus genetic), diet composition, mouse sex and reproductive status (i.e. ovary intact versus ovariectomized), housing conditions, and interventions (ex: low fat, caloric restriction, exercise, or intermittent fasting, amongst others) all have substantial impact on study results. Age-matched controls will be necessary to uncouple the effect of aging versus obesity as similar tissue-level structural changes and morbidities occur in both processes, an observation termed adipaging[210] Thoughtful collaborations with population scientists to model and identify mechanisms underlying observed clinical effects is likely the most efficient way to gather meaningful and translatable results.

4.5 Broader Impacts and Concluding Remarks

Obesity is a recognized preventable risk factor for 12 cancers, including breast cancer discussed in this work. Our observations that obesity-associated ECM remodeling modulates macrophage phenotype in a manner that may contribute to a tumor-permissive microenvironment is broadly applicable to other obesity-associated cancers. In particular, the proposed future directions would be beneficial for study of obesity-associated cancer types that, similar to breast, are in association with a fat pad, such as sublingual squamous cell carcinoma, and ovarian and prostatic carcinomas. Our work might also have applicability to obesity-associated tumors that arise in mucosal lumens, such as uterine, gastric, and colorectal mucosa, but become in contact with abdominal fat in later stages of disease when the tumor extends through the organ wall. The role of the physical properties of the obese microenvironment in metastasis to the omentum, a common metastatic site for ovarian, gastric, and colorectal cancers, has yet to be explored and could offer new insights into theories of metastasis such as seed and soil[211] or pre-metastatic niche[212] development.

The observation that ECM remodeling contributes to macrophage phenotype also has implications for the immune microenvironment of solid tumors. With the advent of immune therapy, the field of immuno-oncology has exploded with major focus on understanding the role of immune cell subsets in anti- and pro-tumorigenic processes. The tumor microenvironment can be divided into three main compartments: tumor parenchymal cells, stromal-vascular cells, and immune cells. The reciprocal interactions between tumor cells and stroma[213,214] or tumor cells and immune cells[215] have been studied and reviewed. A focus on stroma/ECM and immune cell interactions has been slowly increasing over the past several years[18,216]. Current challenges in immunotherapy include efficacy of checkpoint inhibitors and accessibility of chimeric antigen receptor (CAR)-T cells to solid tumors. Targeting

the stromal microenvironment of solid tumors might be a novel way to improve the efficacy of current immunotherapeutics or identify targets for new therapeutics.

Physical sciences approaches to cancer research are increasing in use and becoming widely accepted in the oncology community. Over the past fifteen years, since the seminal publication highlighting the responsiveness of cancer cells to the mechanical environment[9], there has been growing interest in this field. Investigating the physical regulation of immune cells has lagged behind, but is slowly gaining momentum and has profound implications for oncology as well as many other inflammatory and degenerative diseases. Transdisciplinary, team-based science, incorporating physical scientists and engineers, immunologists, clinicians, and population-based scientists is necessary to increase our knowledge regarding the physical microenvironment contributing to cancer initiation, growth, and metastasis with the goal to improve preventative modalities or identify new or repurposed therapeutics.

APPENDIX

COLLABORATIVE *IN VIVO* STUDIES INVESTIGATING THE STROMAL MICROENVIRONMENT IN GASTRIC AND BREAST CANCER PATHOGENESIS

Select contents of this appendix reproduced from:

Lourenço B[1,2,3,4,5], Springer NL[1,8], Ferreira D[2,3,4,7], Oliveira C[2,4,6], Granja PL[2,3,5,7], and Fischbach C[1,9]. CD44v6 increases gastric cancer malignant phenotype by modulating adipose stromal cell-mediated ECM remodeling. *Int Biol (Camb)* 2018;10(3):145-158. PMID: 29450424 PMCID: PMC5988203

[1]Nancy E. and Peter C. Meinig School of Biomedical Engineering, Cornell University, Ithaca, NY, United States

[2]i3S - Instituto de Investigação e Inovação em Saúde, Universidade do Porto, Portugal

[3]INEB - Instituto de Engenharia Biomédica, Universidade do Porto, Portugal

[4]IPATIMUP - Instituto de Patologia e Imunologia Molecular da Universidade do Porto, Portugal

[5]Faculdade de Engenharia, Universidade do Porto, Portugal

[6]Faculdade de Medicina, Universidade do Porto, Portugal

[7]ICBAS - Instituto de Ciências Biomédica Abel Salazar, Universidade do Porto, Portugal

[8]Biological and Biomedical Sciences, Cornell University, Ithaca, NY, United States

[9]Kavli Institute at Cornell for Nanoscale Science, Cornell University, Ithaca, NY, United States

BNL, PLG, and CF conceptualized the project. BNL, NLS, and DF performed experiments and formal analysis. BNL wrote the original draft. NLS, DF, CO, PLG, and CF reviewed and edited the manuscript. PLG, CO, and CF acquired funding and supervised the project.

He F[1], Springer NL[1,2], Whitman MA[1], Pathi SP[1], Lee Y[1], Mohanan S[3], Marcott S[1], Chiou AE[1], Blank BS[4], Iyengar NM[5], Morris PG[5], Jochelson MS[6], Hudis CA[5], Shah P[1,7], Kunitake J[8], Estroff LA[8,9], Lammerding J[1,7], Fischbach C[1,9]. Hydroxyapatite mineral enhances malignant potential in a tissue-engineered model of ductal carcinoma in situ (DCIS). *Biomaterials* 2019:224;119489. PMID: 31546097

[1]Nancy E. and Peter C. Meinig School of Biomedical Engineering, Cornell University, Ithaca, NY, 14853, USA
[2]Department of Diagnostic Medicine/Pathobiology, Kansas State University College of Veterinary Medicine, Manhattan, KS, 66506, USA
[3]Department of Biomedical Sciences, Baker Institute for Animal Health, Cornell University, Ithaca, NY, 14853, USA
[4]Cornell Center for Animal Resources and Education, College of Veterinary Medicine, Cornell University, Ithaca, NY, 14853, USA
[5]Breast Medicine Service, Department of Medicine, Memorial Sloan Kettering Cancer Center/Evelyn H. Lauder Breast and Imaging Center, New York, NY, 10065, USA
[6]Department of Radiology, Memorial Sloan Kettering Cancer Center/Evelyn H. Lauder Breast and Imaging Center, New York, NY, 10065, USA
[7]Weill Institute for Cell and Molecular Biology, Cornell University, Ithaca, NY, 14853, USA

[8]Department of Materials Science and Engineering, Cornell University, Ithaca, NY, 14853, USA
[9]Kavli Institute at Cornell for Nanoscale Science, Cornell University, Ithaca, NY, 14853, USA

F.H. performed all experiments unless otherwise indicated. S.P.P., Y.L., S.M., and P.S. performed or assisted *in vitro* experiments. M.W., A.E.C., B.B., assisted *in vivo* experiments. N.S. and S.M. performed pathological diagnoses. N.I., P.G.M., M.J., and C.A.H. provided clinical samples. J.A.M.R.K. and L.A.E. analyzed the patient sample data. J.L. provided key reagents and tools. F.H. and C.F. designed the project and wrote the paper with input from S.P.P. All authors have approved the final article.

A.1 Introduction

Tumors are a composite of both malignant and non-malignant cells (such as immune cells, vasculature, fibroblasts and extracellular matrix). The role of the tumor microenvironment in cancer initiation, progression, and metastasis is evolving. Extracellular matrix remodeling and mineralization are common features in both malignancy and in pathological conditions associated with increased risk of cancer development and metastasis. Because of my expertise in pathology and familiarity with laboratory animal models, I contributed several *in vivo* studies evaluating the role of ASC-mediated ECM remodeling or tissue microcalcifications in tumorigenesis to the projects of other graduate students and postdoctoral scholars in the Fischbach laboratory.

A.2 CD44v6 increases gastric cancer malignant phenotype by modulating adipose stromal cell-mediated ECM remodeling

CD44v6 expression has been associated with poor prognosis in several human cancers, particularly those originating in the gastrointestinal tract. Nevertheless, the relationship between CD44v6 overexpression and the clinicopathological features of gastric carcinoma (GC) remains unknown. To unravel whether CD44v6 expression by tumor cells affects the desmoplastic reaction and tumor growth of GC, we used an isogenic human GC cell line overexpressing the CD44v6 isoform (CD44v6 cells), previously established by our collaborators[217]. This model was generated using the CD44-negative MKN74 cell line transfected to overexpress the CD44v6 isoform utilizing the variant CD44-04– ENST00000415148 (OriGene) cloned into a pIRES-EGFP2 expression vector[217].

MKN74 cells, CD44v6 cells, and 3T3-L1 preadipocytes (ATCC) were routinely cultured in Dulbecco's Modified Eagle Medium (DMEM, Gibco) containing 10% fetal bovine serum (FBS, Atlanta Biologicals) and 1% penicillin/streptomycin (Pen/Strep, Gibco), and supplemented with 1% geneticin (Gibco) to select for transfected cells in the case of CD44v6 cells. Human ASCs (Lonza) were cultured in their corresponding growth media (ADSC-GM, Lonza). Cell cultures were maintained at 37 °C + 5% CO_2.

Animal studies were performed in accordance with protocol 2009-0117 as approved by Cornell's University Institutional Animal Care and Use Committee (IACUC). MKN74 and CD44v6 cells were injected individually or in combination with ASCs (maximum number of cells = 9.5 x 10^5 in 100 µL of DMEM, 10% FBS, 1% Pen/Strep) into the subcutaneous space of five-week-old, female NOD.CB17-Prkdcscid/J (SCID) mice (4 mice, 2 tumors per mouse) per condition. Tumors were measured and volume calculated weekly. Explants were harvested eight weeks after

implantation, imaged, and formalin fixed for subsequent paraffin-embedding and histological analysis.

Five-mm tissue sections were stained with Hematoxylin and Eosin (H&E) or Masson's Trichrome. To assess the degree of desmoplasia, H&E sections were scored by a pathologist (NLS) in a blinded manner using the following rubric:

Grade 1: delicate indistinct fibrovascular stroma diffusely throughout sheets of neoplastic cells

Grade 2: thin distinct bands of fibrovascular stroma throughout sheets of neoplastic cells

Grade 3: thin distinct fibrovascular bands separating neoplastic cells into packeted arrangements

Grade 4: streaming thick fibrovascular bands separating neoplastic cells into packeted arrangements.

Desmoplasia scoring was confirmed with Masson's Trichrome sections using digitally scanned images and Aperio ImageScope software. Tumor cell proliferation was assessed via manual counting of Ki67 (Dako, clone MIB-1) immunoreactive nuclei in 5 representative fields of view at 200-fold magnification per tumor using ImageJ software.

Parental MKN74 and CD44v6-expressing cells were injected individually into SCID mice (Fig. 27A) to evaluate tumor formation and malignancy *in vivo*. After eight weeks of tumor growth, tumors resulting from CD44v6 subcutaneous xenografts trended toward more rapid growth and increased tumor size when compared to MKN74 subcutaneous xenografts (Fig. 27D). Increased tumor growth correlated with increased desmoplastic (fibrotic) response as CD44v6 tumors contained more fibrous stroma intersecting packets of malignant epithelial cells relative to MKN74 tumors (Fig. 27E) based on histological analysis. Furthermore, Masson's Trichrome staining

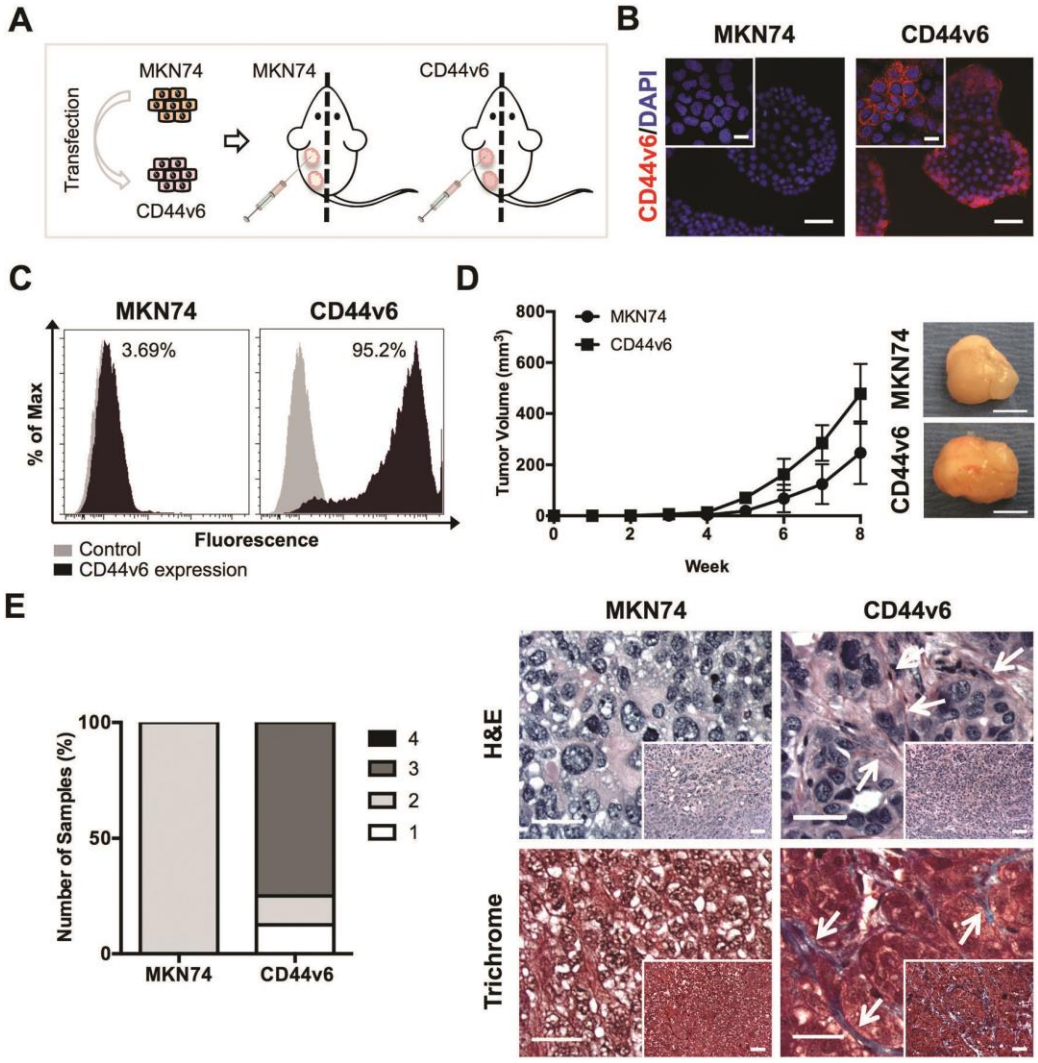

Figure 27: CD44v6 alters tumor growth and architecture in vivo. (A) Schematic showing the establishment of a gastric cancer (GC) cell line stably expressing CD44v6 and study design for subcutaneous xenograft injections of GC cells individually in SCID mice. (B) Immunofluorescence images showing CD44v6 isoform expression and nuclei (DAPI) on MKN74 and CD44v6 cells. Scale bars = 50 mm. Inset bars = 20 mm. (C) Representative histograms of MKN74 and CD44v6 analysis by flow cytometry quantifying CD44v6 expression. (D) Tumor volume from MKN74 (n = 3) and CD44v6 (n = 8) subcutaneous xenografts over eight weeks of growth and representative gross images of explanted tumors at week 8. Scale bars = 5 mm. (E) Histological grading and representative photomicrographs of the desmoplastic response of MKN74 and CD44v6 subcutaneous xenografts on Hematoxylin and Eosin (H&E) stained sections with confirmation of collagen deposition (blue) via Masson's Trichrome-stained sections after 8 weeks of subcutaneous injection. Arrows indicate fibrotic tissue. Scale bars = 25 mm, inset bars = 50 mm. Published in Lourenco B, *et al*. *Int Biol* 2018;10(3):145-158

confirmed overexpresson of CD44v6 promotes tumor desmoplasia as there was greater collagen content(blue) in tumors formed by CD44v6 cells as compared to tumors formed by MKN74 cells (Fig. 27E).

CD44v6 soluble factors were found to promote ASC differentiation to myofibroblasts *in vitro*[105]. We assessed the biological relevance of this finding by comparing CD44v6 xeongrafts alone with CD44v6 + ASCs xenografts. Based on histopathological evaluation, co-implantation of ASCs with CD44v6 cells resulted in increased heterogeneity of the desmoplastic response and a higher proportion of grade 4 desmoplasia versus CD44v6 cells implanted alone (Fig. 28). Masson's Trichrome

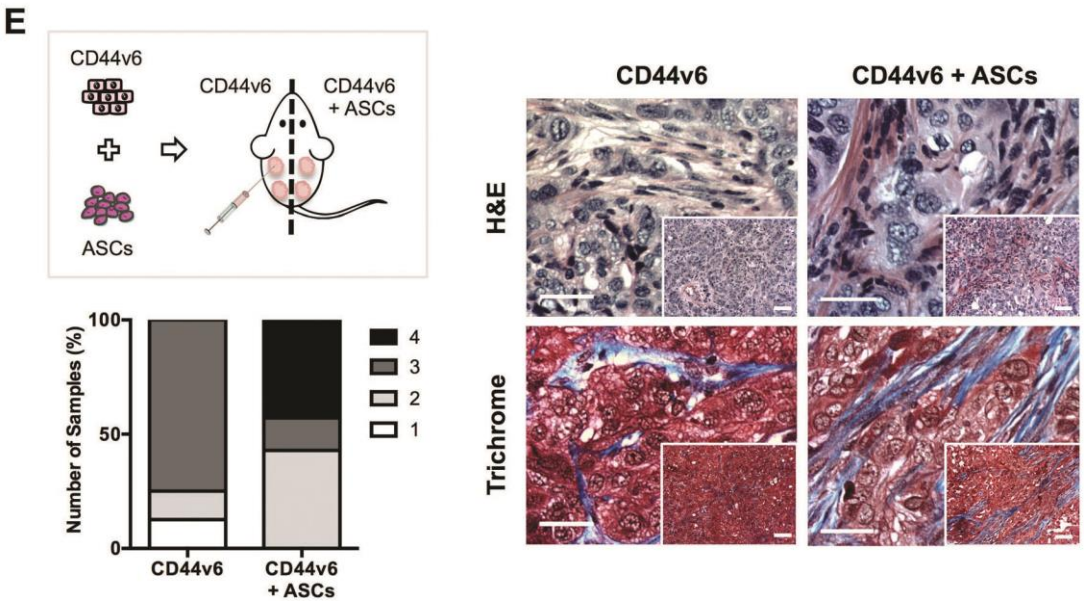

Figure 28: Schematic of xenografting conditions. CD44v6 cells were injected into SCID mice either alone (n = 8) or in combination with ASCs (n = 7) and tumors were harvested after 8 weeks. Representative photomicrographs of H&E-stained cross-sections and confirmation of collagen deposition (blue) via Masson's Trichrome stained sections. Corresponding histological scoring of desmoplasia based on H&E sections. Tumors were harvested 8 weeks after injection. Scale bars = 25 mm, Inset bars = 50 mm. * $p < 0.05$. Published in Lourenco B, *et al*. *Int Biol* 2018;10(3):145-158

staining confirmed this finding with greater collagen deposition (blue) in co-implanted tumors (Fig. 28), suggesting that CD44v6 overexpression enhances myofibroblast differentiation with subsequent collagen deposition, contributing to a desmoplastic tumor microenvironment in GC.

Furthermore, CD44v6 + ASCs tumors had increased fibrous stroma (Fig. 29D), in contrast to tumors derived from MKN74 + ASCs on histopathological evaluation. Increased cell proliferation, as determined by Ki67 immunoreactivity, accompanied this desmoplastic response in CD44v6 + ASCs tumors relative to MKN74 + ASCs tumors, (Fig. 29D). Additionally, larger and more pleomorphic nuclei were found in CD44v6 + ASCs tumors than in MKN74 + ASCs tumors suggesting increased malignancy when CD44v6 is expressed (Fig. 29D). Overall, these findings indicate that CD44v6 expression modulates GC malignant behavior *in vivo* by enhancing ASC-mediated contributions to tumor stroma formation

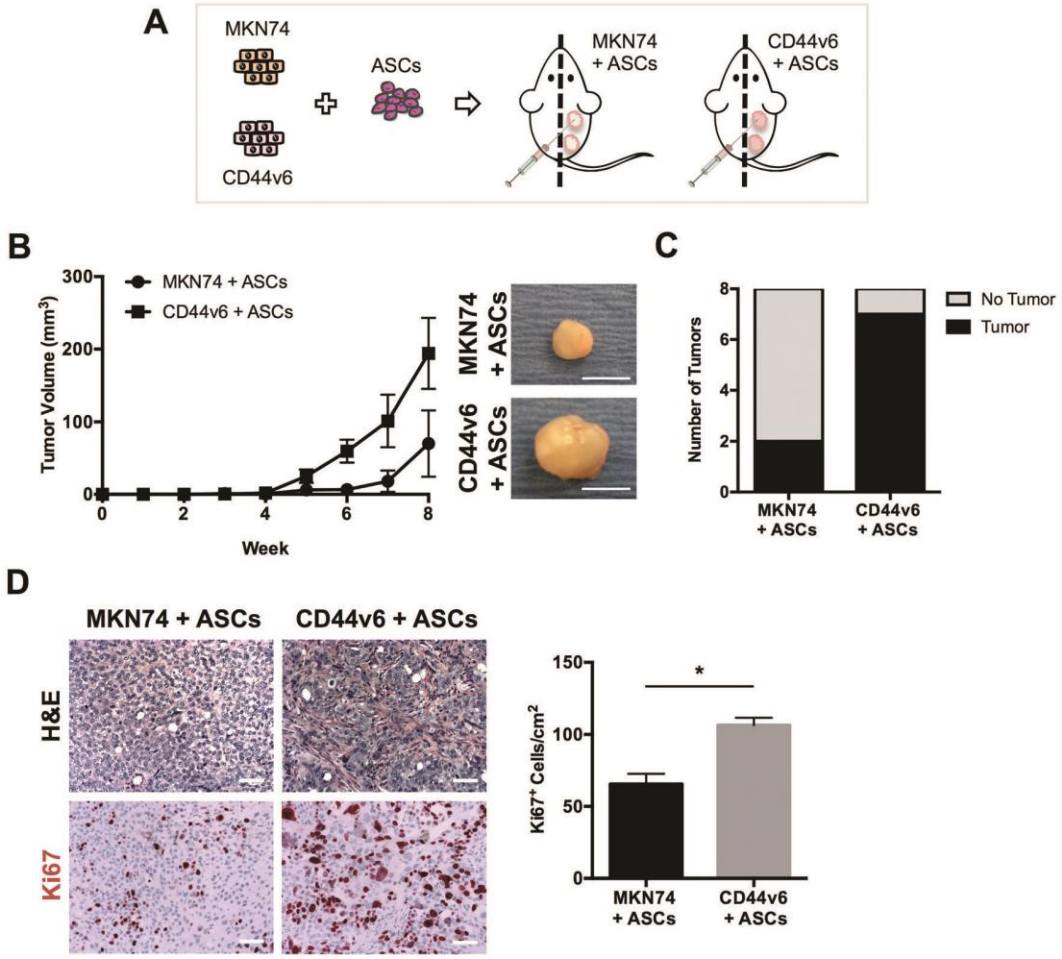

Figure 29: Upon co-injection with ASCs CD44v6 tumors are more proliferative and desmoplastic than MKN74 tumors. (A) Schematic showing the study design for subcutaneous xenograft co-injections of MKN74 and CD44v6 cells with ASCs in SCID mice. (B) Measurement of tumor volume from MKN74 with ASCs (n = 3) and CD44v6 with ASCs (n = 8) subcutaneous xenografts over eight weeks of tumor growth with representative gross images of tumors explanted at the end of the experiment. Scale bars = 5 mm. (C) Comparison of the number of tumors formed per total number of subcutaneous implantations between experimental conditions. Analysis was performed 8 weeks after subcutaneous injection. (D) Representative photomicrographs of H&E stained sections of tumors collected 8 weeks after subcutaneous implantation of MKN74 cells + ASCs and CD44v6 cells + ASCs. Comparison of GC cell proliferation between conditions as quantified by immunohistochemical analysis of Ki67 positive cells (n = 7). Scale bars = 50 mm. * $p < 0.05$. Published in Lourenco B, *et al*. *Int Biol* 2018;10(3):145-158

A.3 Hydroxyapatite mineral enhances malignant potential in a tissue-engineered model of ductal carcinoma in situ (DCIS)

Ductal carcinoma *in situ* (DCIS) can be a precursor lesion to invasive breast carcinomas; however, the mechanisms underlying this transition and determining which DCIS lesions will progress to invasive carcinoma are poorly understood. Mammographic detection of microcalcifications (MC) is a common method for diagnosing DCIS. The composition of the MC is important as non-stoichiometric hydroxyapatite (HA) mineral is frequently associated with malignant disease, yet it is unclear whether HA can actively promote malignancy. To investigate this question, we compared phenotypic outcomes of breast cancer cells cultured in control or HA-containing poly(lactide-*co*-glycolide) (PLG) scaffolds.

Human mammary epithelial cell line MCF10DCIS.com was cultured in 1:1 DMEM/F12 (Gibco) supplemented with 5% horse serum (Invitrogen), 1% penicillin/streptomycin (Gibco), 10 μg/ml insulin (Sigma), 0.5 μg/ml hydrocortisone (Sigma), 100 ng/ml cholera toxin (Sigma), and 20 ng/ml EGF (Millipore).

Porous, polymeric scaffolds were fabricated using a gas-foaming, particulate leaching method [218]. For hydroxyapatite-containing (HA) scaffolds, poly(lactide-*co*-glycolide) (PLG) microparticles (ground and sieved, ~250 μm diameter; Lakeshore Biomaterials) and PLG microspheres (formed by double emulsion, ~5–50 μm diameter; Lakeshore Biomaterials) were dry-mixed with nanocrystalline hydroxyapatite (Sigma #677418; phase-pure; stoichiometric; length 20–600 nm) and sodium chloride (sieved, ~250–400 μm diameter; J.T. Baker). The mixture was then pressed to form matrices (8.5mm diameter, 1mm thick) at room temperature in a dye press (Fred. S. Carver) and then pressurized in carbon dioxide (800 psi) with a non-stirred vessel (Parr Instruments). After a quick de-pressurization, scaffolds were

soaked for 24 h in de-ionized water to leach out the sodium chloride. Non-mineral-containing (PLG) scaffolds were fabricated similarly, excluding the hydroxyapatite in the starting mixture.

Animal studies were conducted in accordance with Cornell University guidelines and were approved by Cornell University's Institutional Animal Care and Use Committee (IACUC). 6- to 7-week-old female Hsd:Athymic Nude-Foxn1nu mice (n=5 or 6) from Envigo were used for MCF10DCIS.com scaffold-xenograft studies. Scaffolds were seeded with 5×10^5 cells, maintained in dynamic culture conditions for 24 h, and then kept on ice until implantation. Mice were anesthetized, and incisions were made to the dorsal interscapular skin. Contralateral subcutaneous pockets in the infrascapular regions containing the third pair of mammary glands were then gently enlarged using a sterile forceps, and then irrigated with sterile PBS. Cell-seeded scaffolds were then inserted into subcutaneous pockets, one on each side.

After explantation, the scaffold-tumors were fixed in 4%PFA and embedded in paraffin. The fixed and embedded scaffold-tumors were stained with hematoxylin and eosin (H&E) and Masson's Trichrome. Scanned images were then transferred to a board-certified pathologist for specific evaluation and diagnosis. Epithelial morphology, an assessment of ductal organization, was scored on a 1-to-4 scale, with 1 representing <25% fields containing organized tubules and acinar arrangements with central comedo and with 2, 3, and 4 representing 25–50%, 50–75%, and >75% fields with the aforementioned qualities, respectively. Fibrosis was scored on a 1-to-3 scale, with 1 representing thin distinct bands of fibrovascular stroma throughout sheets of neoplastic cells, and with 2 and 3 representing streaming thick fibrovascular bands separating neoplastic cells in <50% and >50% of fields, respectively. Cells with visible chromosomes were assessed as Mitotic Figures (ten 200x fields counted per sample). This analysis was performed blind.

Scaffold-xenografts were harvested after 4 weeks and subjected to histopathological analyses (Fig. 30A). As expected, both HA and PLG scaffolds were largely degraded by the experimental endpoint (data not shown) [219]. On H&E stained cross-sections, the PLG control scaffold tumors were typically composed of comedo-type lesions with relatively organized ductal structures (Fig. 30B and C), which is comparable to previous non-scaffold-based xenograft studies with the same MCF10DCIS.com cell line at this timepoint[220]. In contrast, the HA condition had significantly disorganized epithelial morphologies (Fig. 30B and C). Furthermore, increased levels of fibrosis within HA scaffold xenografts (Fig. 30D and E) was evident on Masson's Trichrome stained sections. DCIS xenografts implanted in HA scaffolds also had greater mitotic activity versus DCIS xenografts implanted in PLG scaffolds (Fig. 30F). Interestingly, greater mitotic activity was associated with greater fibrosis (Fig. 30G). These data suggest that HA mineral may regulate tumor malignancy *in vivo*, as evidenced by decreased epithelial organization and increased desmoplasia with associated higher mitotic index.

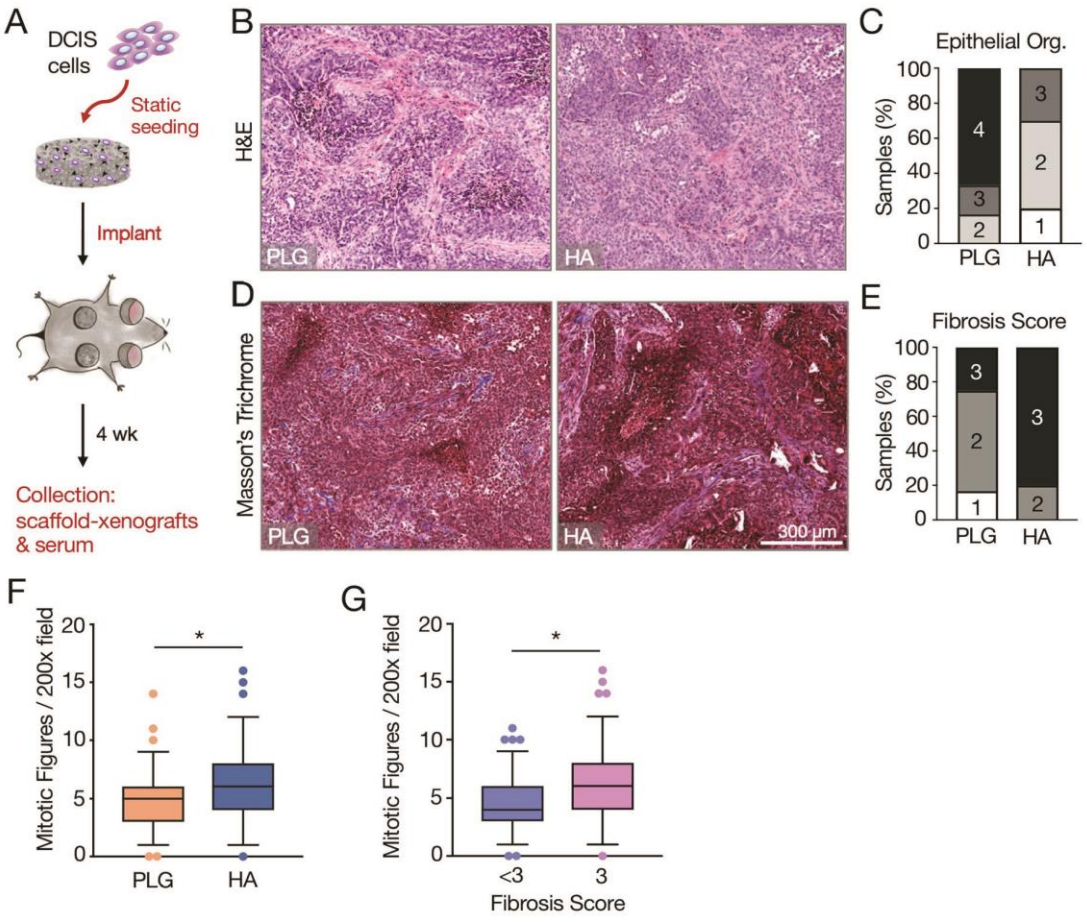

Figure 30: (**A**) Experimental setup for scaffold xenograft studies: Mineral-containing or control scaffolds seeded with 0.5e6 MCF10DCIS.com cells were implanted subcutaneously near the third mammary fat pad. Two scaffolds were implanted per animal. After 4 weeks, scaffold-xenograft tumors and serum were collected for histopathological and biochemical analyses. (**B**) Representative hematoxylin and eosin stained cross sections showing epithelial organization. (**C**) Histopathological scoring of the epithelial organization as seen in (B). Rubric: 1-to-4, least-to-most organized, details in methods. PLG *vs*. HA: $p < 0.05$. (**D**) Representative Masson's trichrome stained cross sections showing the presence of collagen fibers. (**E**) Histopathological scoring of the fibrosis as seen in (D). Rubric: 1-to-3, least-to-most fibrosis, details in methods. PLG *vs*. HA: $p < 0.05$. (**F**) Box-and-whisker plots showing Mitotic Figures (chromosomes in a given 200x field). Whiskers represent the 5th and 95th percentile. Outlier data points are depicted as dots. (**G**) Box-and-whisker plots showing Mitotic Figures as a function of Fibrosis Score. Whiskers represent the 5th and 95th percentile. Outlier data points are depicted as dots. For all plots, *$p < 0.05$. Published in He F, *et al*. *Biomaterials* 2019:224;119489

A.4 Obesity-associated extracellular matrix promotes malignancy by increasing stem-like properties in breast cancer cells

Obesity is associated with a worse clinical prognosis and increased mortality in breast cancer patients independent of subtype or menopausal status[1,2]. Although the underlying mechanisms remain poorly understood, increasing experimental evidence suggests that cancer stem cells (CSC), also known as tumor-initiating cells, may be associated with obesity-related metastatic disease and therapy resistance[221,222]. CSCs are functionally defined by their tumor-initiating capacity, expression of stem cell-associated molecular markers such as OCT-4, SOX-2, NANOG, and CD44,[223,224] limited responsiveness to anti-cancer therapies, and high metastatic potential,[225,226]. Therefore, CSC could play a key role in the positive correlation between obesity and increased malignancy and metastasis-related mortality. Recent experimental evidence suggests that abnormal extracellular matrix (ECM) remodeling and integrin-dependent mechanotransduction may independently promote CSC-like properties in tumor cells[227,228]. Whether or not similar mechanisms play a role in obesity and breast cancer tumorigenesis and progression remain unclear.

To determine whether NANOG expression correlates with increased ECM remodeling by obese vs. lean ASCs *in vivo,* we utilized a mouse xenograft model that allowed testing co-localization of desmoplasia and NANOG as a function of ASC co-implantation.

Animal protocols were approved by the Institutional Animal Care and Use Committees at Cornell University. Cell lines used in the xenograft study included MDA-MB-231 breast cancer cells transfected with a NANOG promoter GFP reporter construct (referred to as MDA-MB-231:NANOG-GFP)[229] and primary murine adipose stromal cells. ASCs were isolated from inguinal fat of age-matched 6-8 week-old female *ob/ob* (B6.Cg-Lep^{ob}/J) or lean wild type (C57BL/6J) control mice (Jackson

Laboratories). To obtain the stromal vascular fraction (SVF), excised fat was minced and digested with collagenase type I (1.5 mg/mL in Krebs-Ringer-HEPES buffer, Worthington Biochemical Corporation) followed by density centrifugation as previously described[42,230]. The digested tissue was passed through serial 100 μm and 70 μm cell strainers (Pierce) and centrifuged to separate the SVF from the top fat layer. The SVF was culture in 1:1 Dulbecco's Modified Eagle Medium (DMEM)/F12 (Gibco) supplemented with 10% FBS (Tissue Culture Biologicals) and 1% penicillin/streptomycin (Gibco) (referred to as complete medium) in standard tissue culture-treated flasks to select for plastic-adherent ASCs. For experiments, ASCs were expanded up to passage 3 in complete medium.

Tumor xenografts were generated by co-injection of equal numbers of MDA-MB-231:NANOG-GFP with lean or obese ASCs (0.45×10^6 of each cell type in PBS, 50 μL injection volume) into the subcutaneous space of three 6-weeks-old female NOD.CB17-Prkdcsscid/J mice (Jackson Laboratories).Four tumors per mouse (n=6 tumors per condition) were implanted, tumor size and animal weight were monitored each week. All procedures were conducted in accordance with Cornell University animal care guidelines.

Tumor xenografts were harvested six weeks after implantation and formalin fixed for subsequent paraffin-embedding and histological analysis. Five μm sections were stained with hematoxylin and eosin (H&E) or Masson's Trichrome stain to assess ECM deposition. NANOG immunohistochemistry was performed using a rabbit anti-NANOG antibody (Cell Signaling Technology, 4903S) after a peroxidase quench and heat-mediated antigen retrieval in EDTA buffer (pH 8.0). NANOG immunoreactivity was identified with Vector Laboratories ImmPress horseradish peroxidase secondary antibody and DAB chromogen. Tumor ECM distribution and NANOG immunoreactivity were assessed by a pathologist (NS) in a blinded manner

using digitally scanned images and Aperio ImageScope software. For desmoplasia analysis the following score was applied:

Grade 1 = indistinct delicate fibrovascular stroma diffusely through sheets of neoplastic cells

Grade 2 = thin distinct bands of fibrovascular stroma diffusely through sheets of neoplastic cells

Grade 3 = thin distinct fibrovascular strands separating neoplastic cells into packeted arrangements

Grade 4 = streaming thick fibrovascular strands separating neoplastic cells into small distinct packeted arrangements.

Histological evaluation of tumor explants revealed that co-implantation with obese ASCs had no effect on tumor size and mitotic index relative to co-implantation with lean ASCs (Fig. 31A and 31B). However, pathological scoring of H&E-stained cross-sections suggested a higher degree of desmoplasia in tumors resulting from co-implantation with obese rather than lean ASCs (Fig. 31C). Furthermore, the spatial distribution of fibrosis, as determined by Masson's Trichrome staining of collagen, varied between both conditions. Tumors co-implanted with lean ASCs primarily featured central and diffuse fibrosis, while tumors co-implanted with obese ASCs exhibited significant peripheral fibrosis (Fig. 31D and 31E). Importantly, analysis of consecutive cross-sections revealed that spatial differences in fibrosis correlated with localization of NANOG expression. In tumors resulting from co-implantation with obese ASCs, NANOG-expressing cells were almost exclusively localized to the tumor periphery, whereas tumors with lean ASCs exhibited more heterogeneous NANOG distribution (Fig. 31D and 31F). These data indicate that differences in ECM remodeling due to co-implanted ASCs may promote the sorting of stem-like cells to

the fibrotic periphery of breast tumor xenografts with potential functional implications for tumor invasion.

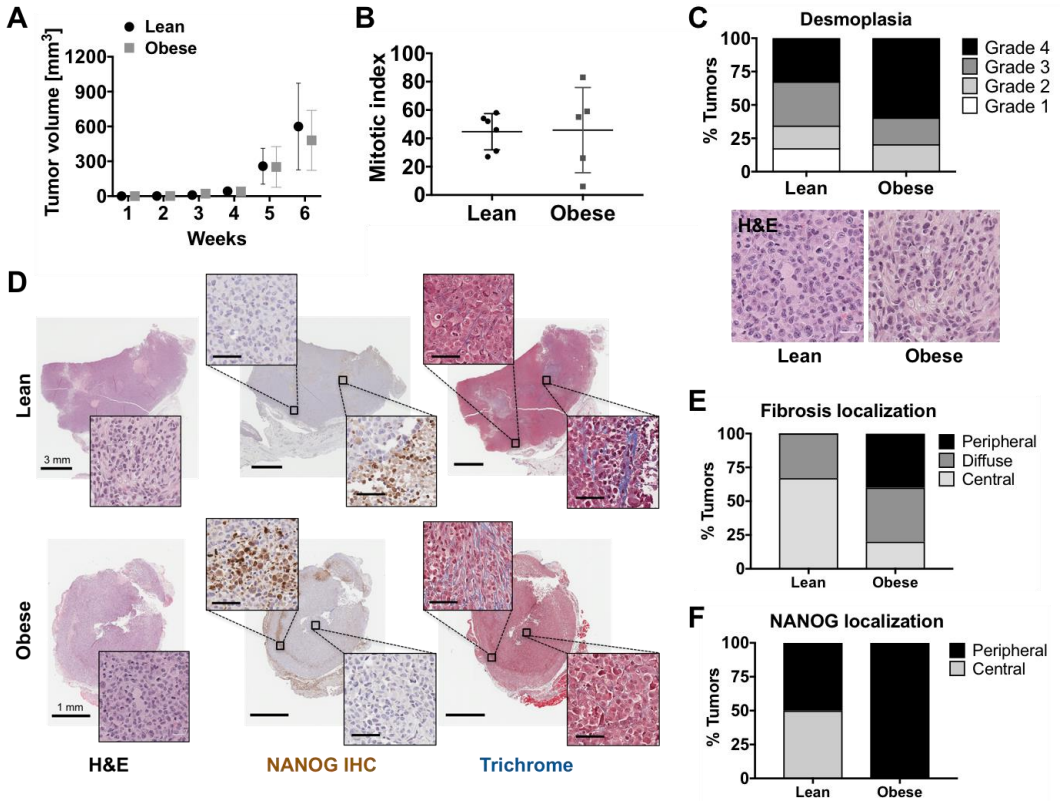

Figure 31: (A) Volumes of tumor xenografts generated by co-injecting MDA-MB-231:NANOG-GFP cells with either lean or obese ASCs into immunocompromised mice (n=6 for tumors with lean ASCs, n=5 for tumors with obese ASCs). **(B)** Histopathological scoring of mitotic index (p=0.9347). **(C)** Analysis of fibrosis in tumors with lean or obese ASCs (p<0.0001). Scale bar = 25 µm. **(D)** Histological images of tumors. Left panel shows representative H&E staining. Scale bars = 3 mm and 1 mm. NANOG expression (middle panel, NANOG IHC) and fibrosis (right panel, Masson's Trichrome) were assessed in consecutive tumor sections. Scale bars insets = 50 µm. **(E)** Histopathological scoring of the spatial distribution of fibrosis (p<0.0001) and **(F)** NANOG in tumors (p<0.0001). Reproduced from Wittmann K, Springer NL, Seo BR, McGregor A, Fleischmann D, Colville M, Paszek M, Reizes O, Lammerding J, and Fischbach C. Obesity-associated extracellular matrix promotes malignancy by increasing stem-like properties in breast cancer cells. *Cell Reports*, in revision

REFERENCES

1. Khandekar MJ, Cohen P, Spiegelman BM: Molecular mechanisms of cancer development in obesity. Nat Rev Cancer 2011, 11:886–895.

2. Chan DSM, Vieira AR, Aune D, Bandera E V., Greenwood DC, McTiernan A, Navarro Rosenblatt D, Thune I, Vieira R, Norat T: Body mass index and survival in women with breast cancer-systematic literature review and meta-analysis of 82 follow-up studies. Ann Oncol 2014, 25:1901–1914.

3. Iyengar NM, Arthur R, Manson JE, Chlebowski RT, Kroenke CH, Peterson L, Cheng T-YD, Feliciano EC, Lane D, Luo J, Nassir R, Pan K, Wassertheil-Smoller S, Kamensky V, Rohan TE, Dannenberg AJ: Association of Body Fat and Risk of Breast Cancer in Postmenopausal Women With Normal Body Mass Index. JAMA Oncol 2018, 10065:1–9.

4. Iyengar NM, Brown KA, Zhou XK, Gucalp A, Subbaramaiah K, Giri DD, Zahid H, Bhardwaj P, Wendel NK, Falcone DJ, Wang H, Williams S, Pollak M, Morrow M, Hudis CA, Dannenberg AJ: Metabolic obesity, adipose inflammation and elevated breast aromatase in women with normal body mass index. Cancer Prev Res 2017, 10:235–243.

5. Iyengar NM, Hudis CA, Dannenberg AJ: Obesity and Cancer: Local and Systemic Mechanisms. Annu Rev Med 2015, 66:297–309.

6. Howe LR, Subbaramaiah K, Hudis CA, Dannenberg AJ: Molecular pathways: Adipose inflammation as a mediator of obesity-associated cancer. Clin Cancer Res 2013, 19:6074–6083.

7. Park J, Morley TS, Kim M, Clegg DJ, Scherer PE: Obesity and cancer-mechanisms underlying tumour progression and recurrence. Nat Rev Endocrinol 2014, 10:455–465.

8. NF B, Guo H, LJ M, Sun L, Stone J, Fishell E, RA J, Hislop G, Chiarelli A, Minkin S, MJ Y: Mammographic density and the risk and detection of breast cancer. N Engl J Med 2007, 356:227–236.

9. Paszek MJ, Zahir N, Johnson KR, Lakins JN, Rozenberg GI, Gefen A, Reinhart-King C a., Margulies SS, Dembo M, Boettiger D, Hammer DA, Weaver VM: Tensional homeostasis and the malignant phenotype. Cancer Cell 2005, 8:241–254.

10. Qiao A, Gu F, Guo X, Zhang X, Fu L: Breast cancer-associated fibroblasts: their roles in tumor initiation, progression and clinical applications. Front Med 2016, 10:33–40.

11. Acerbi I, Cassereau L, Dean I, Shi Q, Au A, Park C, Chen YY, Liphardt J, Hwang ES, Weaver VM: Human breast cancer invasion and aggression correlates with ECM stiffening and immune cell infiltration. Integr Biol 2015, 7:1120–1134.

12. Provenzano PP, Eliceiri KW, Campbell JM, Inman DR, White JG, Keely PJ: Collagen reorganization at the tumor-stromal interface facilitates local invasion. BMC Med 2006, 4:38.

13. Conklin MW, Gangnon RE, Sprague BL, Van Gemert L, Hampton JM, Eliceiri KW, Bredfeldt JS, Liu Y, Surachaicharn N, Newcomb PA, Friedl A, Keely PJ, Trentham-Dietz A: Collagen alignment as a predictor of recurrence after ductal carcinoma in situ. Cancer Epidemiol Biomarkers Prev 2018, 27:138–145.

14. Provenzano PP, Inman DR, Eliceiri KW, Trier SM, Keely PJ: Contact guidance mediated three-dimensional cell migration is regulated by Rho/ROCK-dependent matrix reorganization. Biophys J 2008, 95:5374–5384.

15. Huo CW, Chew G, Hill P, Huang D, Ingman W, Hodson L, Brown KA, Magenau A, Allam AH, McGhee E, Timpson P, Henderson MA, Thompson EW, Britt K: High mammographic density is associated with an increase in stromal collagen and immune cells within the mammary epithelium. Breast Cancer Res 2015, 17:1–20.

16. DeNardo DG, Brennan DJ, Rexhepaj E, Ruffell B, Shiao SL, Madden SF, Gallagher WM, Wadhwani N, Keil SD, Junaid SA, Rugo HS, Shelley Hwang E, Jirström K, West BL, Coussens LM: Leukocyte complexity predicts breast cancer survival and functionally regulates response to chemotherapy. Cancer Discov 2011,1:54–67.

17. Koru-Sengul T, Santander AM, Miao F, Sanchez LG, Jorda M, Glück S, Ince TA, Nadji M, Chen Z, Penichet ML, Cleary MP, Torroella-Kouri M: Breast cancers from black women exhibit higher numbers of immunosuppressive macrophages with proliferative activity and of crown-like structures associated with lower survival compared to non-black Latinas and Caucasians. Breast Cancer Res Treat 2016, 158:113–126.

18. Afik R, Zigmond E, Vugman M, Klepfish M, Shimshoni E, Pasmanik-Chor M, Shenoy A, Bassat E, Halpern Z, Geiger T, Sagi I, Varol C: Tumor macrophages are pivotal constructors of tumor collagenous matrix. J Exp Med 2016, 213:2315–2331.

19. Franklin R a, Liao W, Sarkar A, Kim M V, Bivona MR, Liu K, Pamer EG, Li MO: The cellular and molecular origin of tumor-associated macrophages. Science 2014 344:921–925.

20. Qian B-Z, Pollard JW: Macrophage diversity enhances tumor progression and metastasis. Cell 2010, 141:39–51.

21. Pollard JW: Trophic macrophages in development and disease. Nat Rev Immunol 2009, 9:259–270.

22. Wyckoff JB, Wang Y, Lin EY, Li JF, Goswami S, Stanley ER, Segall JE, Pollard JW, Condeelis J: Direct visualization of macrophage-assisted tumor cell intravasation in mammary tumors. Cancer Res 2007, 67:2649–2656.

23. Jain N, Moeller J, Vogel V: Mechanobiology of Macrophages: How Physical

Factors Coregulate Macrophage Plasticity and Phagocytosis. Annu Rev Biomed Eng 2019, 21:267–297.

24. Sun K, Tordjman J, Clément K, Scherer PE: Fibrosis and Adipose Tissue Dysfunction. Cell Metab 2013, 18:470–477.

25. Halberg N, Khan T, Trujillo ME, Wernstedt-Asterholm I, Attie AD, Sherwani S, Wang Z V, Landskroner-Eiger S, Dineen S, Magalang UJ, Brekken R a, Scherer PE: Hypoxia-inducible factor 1alpha induces fibrosis and insulin resistance in white adipose tissue. Mol Cell Biol 2009, 29:4467–4483.

26. Kanneganti T-D, Dixit VD: Immunological complications of obesity. Nat Immunol 2012, 13:707–712.

27. Sun K, Tordjman J, Clément K, Scherer PE: Fibrosis and adipose tissue dysfunction. Cell Metab 2013, 18:470–477.

28. Lumeng CN, Delproposto JB, Westcott DJ, Saltiel AR: Phenotypic switching of adipose tissue macrophages with obesity is generated by spatiotemporal differences in macrophage subtypes. Diabetes 2008, 57:3239–3246.

29. Divoux A, Tordjman J, Lacasa D, Veyrie N, Hugol D, Aissat A, Basdevant A, Guerre-Millo M, Poitou C, Zucker J-D, Bedossa P, Clément K, Aissat A, Basdevant A, Zucker J-D, Bedossa P, Cle K: Fibrosis in Human Adipose Tissue : Composition , Distribution , and Link With Lipid Metabolism and Fat. Diabetes 2010, 59:2817–2825.

30. Khan T, Muise ES, Iyengar P, Wang Z V, Chandalia M, Abate N, Zhang BB, Bonaldo P, Chua S, Scherer PE: Metabolic dysregulation and adipose tissue fibrosis: role of collagen VI. Mol Cell Biol 2009, 29:1575–1591.

31. Pasarica M, Gowronska-Kozak B, Burk D, Remedios I, Hymel D, Gimble J, Ravussin E, Bray GA, Smith SR: Adipose tissue collagen VI in obesity. J Clin Endocrinol Metab 2009, 94:5155–5162.

32. Chun T-H: Peri-adipocyte ECM remodeling in obesity and adipose tissue fibrosis. Adipocyte 2012, 1:89–95.

33. Cinti S, Mitchell G, Barbatelli G, Murano I, Ceresi E, Faloia E, Wang S, Fortier M, Greenberg AS, Obin MS: Adipocyte death defines macrophage localization and function in adipose tissue of obese mice and humans. J Lipid Res 2005, 46:2347–2355.

34. Weisberg SP, McCann D, Desai M, Rosenbaum M, Leibel RL, Ferrante AW: Obesity is associated with macrophage accumulation in adipose tissue. J Clin Invest 2003, 112:1796–1808.

35. Haase J, Weyer U, Immig K, Klöting N, Blüher M, Eilers J, Bechmann I, Gericke M: Local proliferation of macrophages in adipose tissue during obesity-induced inflammation. Diabetologia 2014, 57:562–571.

36. Amano SU, Cohen JL, Vangala P, Tencerova M, Nicoloro SM, Yawe JC, Shen

Y, Czech MP, Aouadi M: Local proliferation of macrophages contributes to obesity-associated adipose tissue inflammation. Cell Metab 2014, 19:162–171.

37. Xu H, Barnes GT, Yang Q, Tan G, Yang D, Chou CJ, Sole J, Nichols A, Ross JS, Tartaglia LA: Chronic inflammation in fat plays a crucial role in the development of obesity-related insulin resistance. J Clin Invest 2003, 112:1821–1830.

38. Vandanmagsar B, Youm YH, Ravussin A, Galgani JE, Stadler K, Mynatt RL, Ravussin E, Stephens JM, Dixit VD: The NLRP3 inflammasome instigates obesity-induced inflammation and insulin resistance. Nat Med 2011, 17:179–189.

39. Kolb R, Phan L, Borcherding N, Liu Y, Yuan F, Janowski AM, Xie Q, Markan KR, Li W, Potthoff MJ, Fuentes-Mattei E, Ellies LG, Knudson CM, Lee MH, Yeung SCJ, Cassel SL, Sutterwala FS, Zhang W: Obesity-associated NLRC4 inflammasome activation drives breast cancer progression. Nat Commun 2016, 7:1–12.

40. Feng B, Jiao P, Nie Y, Kim T, Jun D, van Rooijen N, Yang Z, Xu H: Clodronate liposomes improve metabolic profile and reduce visceral adipose macrophage content in diet-induced obese mice. PLoS One 2011, 6:1–11.

41. Chandler EM, Seo BR, Califano JP, Andresen Eguiluz RC, Lee JS, Yoon CJ, Tims DT, Wang JX, Cheng L, Mohanan S, Buckley MR, Cohen I, Nikitin AY, Williams RM, Gourdon D, Reinhart-King CA, Fischbach C: Implanted adipose progenitor cells as physicochemical regulators of breast cancer. Proc Natl Acad Sci USA 2012, 109:9786–9791.

42. Seo BR, Bhardwaj P, Choi S, Gonzalez J, Eguiluz RCA, Wang K, Mohanan S, Morris PG, Du B, Zhou XK, Vahdat LT, Verma A, Elemento O, Hudis CA, Williams RM, Gourdon D, Dannenberg AJ, Fischbach C: Obesity-dependent changes in interstitial ECM mechanics promote breast tumorigenesis. Sci Transl Med 2015, 7:1–12.

43. Hillers LE, D'Amato J V., Chamberlin T, Paderta G, Arendt LM: Obesity-Activated Adipose-Derived Stromal Cells Promote Breast Cancer Growth and Invasion. Neoplasia 2018, 20:1161–1174.

44. Iyengar P: Adipocyte-derived collagen VI affects early mammary tumor progression in vivo, demonstrating a critical interaction in the tumor/stroma microenvironment. J Clin Invest 2005, 115:1163–1176.

45. Gucalp A, Iyengar NM, Zhou XK, Giri DD, Falcone DJ, Wang H, Williams S, Krasne MD, Yaghnam I, Kunzel B, Morris PG, Jones LW, Pollak M, Laudone VP, Hudis CA, Scher HI, Scardino PT, Eastham JA, Dannenberg AJ: Periprostatic adipose inflammation is associated with high-grade prostate cancer. Prostate Cancer Prostatic Dis 2017, 20:418–423.

46. Morris PG, Hudis CA, Giri D, Morrow M, Falcone DJ, Zhou XK, Du B, Brogi E, Crawford CB, Kopelovich L, Subbaramaiah K, Dannenberg AJ: Inflammation and increased aromatase expression occur in the breast tissue of

obese women with breast cancer. Cancer Prev Res 2011, 4:1021–1029.

47. Iyengar NM, Zhou XK, Gucalp A, Morris PG, Howe LR, Giri DD, Morrow M, Wang H, Pollak M, Jones LW, Hudis CA, Dannenberg AJ: Systemic Correlates of White Adipose Tissue Inflammation in Early-Stage Breast Cancer. Clin Cancer Res 2016, 22:2283–2289.

48. Carter JM, Hoskin TL, Pena MA, Brahmbhatt R, Winham SJ, Frost MH, Stallings-Mann M, Radisky DC, Knutson KL, Visscher DW, Degnim AC: Macrophagic "crown-like structures" are associated with an increased risk of breast cancer in benign breast disease. Cancer Prev Res 2018, 11:113-119.

49. Bhardwaj P, Du B, Zhou XK, Sue E, Harbus MD, Falcone DJ, Giri D, Hudis CA, Kopelovich L, Subbaramaiah K, Dannenberg AJ: Caloric restriction reverses obesity-induced mammary gland inflammation in mice. Cancer Prev Res 2013, 6:282–289.

50. Mayi TH, Daoudi M, Derudas B, Gross B, Bories G, Wouters K, Brozek J, Caiazzo R, Raverdi V, Pigeyre M, Allavena P, Mantovani A, Pattou F, Staels B, Chinetti-Gbaguidi G: Human adipose tissue macrophages display activation of cancer-related pathways. J Biol Chem 2012, 287:21904–21913.

51. Arendt LM, McCready J, Keller PJ, Baker DD, Naber SP, Seewaldt V, Kuperwasser C: Obesity promotes breast cancer by CCL2-mediated macrophage recruitment and angiogenesis. Cancer Res 2013, 73:6080–6093.

52. McWhorter FY, Wang T, Nguyen P, Chung T, Liu WF: Modulation of macrophage phenotype by cell shape. Proc Natl Acad Sci USA 2013, 110:17253–17258.

53. McWhorter FY, Davis CT, Liu WF: Physical and mechanical regulation of macrophage phenotype and function. Cell Mol Life Sci 2015, 72:1303–1316.

54. Patel NR, Bole M, Chen C, Hardin CC, Kho AT, Mih J, Deng L, Butler J, Tschumperlin D, Fredberg JJ, Krishnan R, Koziel H: Cell Elasticity Determines Macrophage Function. PLoS One 2012, 7:e41024.

55. Arnold M, Pandeya N, Byrnes G, Renehan AG, Stevens GA, Ezzati M, Ferlay J, Miranda JJ, Romieu I, Dikshit R, Forman D, Soerjomataram I: Global burden of cancer attributable to high body-mass index in 2012: a population-based study. Lancet Oncol 2015, 16:36–46.

56. van den Brandt PA, Spiegelman D, Yaun SS, Adami HO, Beeson L, Folsom AR, Fraser G, Goldbohm RA, Graham S, Kushi L, Marshall JR, Miller AB, Rohan T, Smith-Warner SA, Speizer FE, Willett WC, Wolk A, Hunter DJ: Pooled analysis of prospective cohort studies on height, weight, and breast cancer risk. Am J Epidemiol 2000, 152:514–527.

57. Trentham-Dietz a, Newcomb P a, Storer BE, Longnecker MP, Baron J, Greenberg ER, Willett WC: Body size and risk of breast cancer. Am J Epidemiol 1997, 145:1011–1019.

58. Hormones E, Cancer B, Group C: Body Mass Index, Serum Sex Hormones, and Breast Cancer Risk in Postmenopausal Women. J Natl Cancer Inst 2003, 95:1218–1226.

59. Pierobon M, Frankenfeld CL: Obesity as a risk factor for triple-negative breast cancers: A systematic review and meta-analysis. Breast Cancer Res Treat 2013, 137:307–314.

60. Protani M, Coory M, Martin JH: Effect of obesity on survival of women with breast cancer: Systematic review and meta-Analysis. Breast Cancer Res Treat 2010, 123:627–635.

61. Brown KA: Impact of obesity on mammary gland inflammation and local estrogen production. J Mammary Gland Biol Neoplasia 2014, 19:183–189.

62. Zahid H, Simpson ER, Brown KA: Inflammation, dysregulated metabolism and aromatase in obesity and breast cancer. Curr Opin Pharmacol 2016, 31:90–96.

63. Cleary MP, Grossmann ME: Minireview: Obesity and breast cancer: The estrogen connection. Endocrinology 2009, 150:2537–2542.

64. Cleary MP, Grossmann ME, Ray A: Effect of obesity on breast cancer development. Vet Pathol 2010, 47:202–213.

65. Divoux A, Tordjman J, Veyrie N, Hugol D, Poitou C, Aissat A, Basdevant A, Zucker J, Bedossa P, Cle K: Fibrosis in Human Adipose Tissue : Composition , Distribution , and Link With Lipid Metabolism and Fat. Diabetes 2010, 59:2817–2825.

66. Henegar C, Tordjman J, Achard V, Lacasa D, Cremer I, Guerre-Millo M, Poitou C, Basdevant A, Stich V, Viguerie N, Langin D, Bedossa P, Zucker JD, Clement K: Adipose tissue transcriptomic signature highlights the pathological relevance of extracellular matrix in human obesity. Genome Biol 2008, 9:1–32.

67. Wentworth JM, Naselli G, Brown WA, Doyle L: Pro-inflammatory CD11c+ CD206+ adipose tissue macrophages are associated with insulin resistance in human obesity. Diabetes 2010, 59:1648–1656.

68. Zeyda M, Farmer D, Todoric J, Aszmann O, Speiser M, Györi G, Zlabinger GJ, Stulnig TM: Human adipose tissue macrophages are of an anti-inflammatory phenotype but capable of excessive pro-inflammatory mediator production. Int J Obes 2007, 31:1420–1428.

69. Journal H, Medicina F De: Picrosirius staining plus polarization microscopy , a specific method for collagen detection in tissue sections. 1979, 11:447–455.

70. Newman AM, Liu CL, Green MR, Gentles AJ, Feng W, Xu Y, Hoang CD, Diehn M, Alizadeh AA: Robust enumeration of cell subsets from tissue expression profiles. Nat Methods 2015, 12:453–457.

71. Olefsky JM, Glass CK: Macrophages, inflammation, and insulin resistance. Annu Rev Physiol 2010, 72:219–246.

72. Coffelt SB, Lewis CE, Naldini L, Brown JM, Ferrara N, De Palma M: Elusive identities and overlapping phenotypes of proangiogenic myeloid cells in tumors. Am J Pathol 2010, 176:1564–1576.

73. Sousa S, Brion R, Lintunen M, Kronqvist P, Sandholm J, Mönkkönen J, Kellokumpu-Lehtinen P-L, Lauttia S, Tynninen O, Joensuu H, Heymann D, Määttä JA.: Human breast cancer cells educate macrophages toward the M2 activation status. Breast Cancer Res 2015, 17:101.

74. Hill DA, Lim H-W, Kim YH, Ho WY, Foong YH, Nelson VL, Nguyen HCB, Chegireddy K, Kim J, Habertheuer A, Vallabhajosyula P, Kambayashi T, Won K-J, Lazar MA: Distinct macrophage populations direct inflammatory versus physiological changes in adipose tissue. Proc Natl Acad Sci USA 2018, 115:E5096-E5105

75. Italiani P, Boraschi D: From monocytes to M1/M2 macrophages: Phenotypical vs. functional differentiation. Front Immunol 2014, 5:1–22.

76. Murray PJ, Allen JE, Biswas SK, Fisher EA, Gilroy DW, Goerdt S, Gordon S, Hamilton JA, Ivashkiv LB, Lawrence T, Locati M, Mantovani A, Martinez FO, Mege JL, Mosser DM, Natoli G, Saeij JP, Schultze JL, Shirey KA, Sica A, Suttles J, Udalova I, vanGinderachter JA, Vogel SN, Wynn TA: Macrophage Activation and Polarization: Nomenclature and Experimental Guidelines. Immunity 2014, 41:14–20.

77. Klein-Wieringa IR, Andersen SN, Kwekkeboom JC, Giera M, de Lange-Brokaar BJE, van Osch GJVM, Zuurmond A-M, Stojanovic-Susulic V, Nelissen RGHH, Pijl H, Huizinga TWJ, Kloppenburg M, Toes REM, Ioan-Facsinay A: Adipocytes Modulate the Phenotype of Human Macrophages through Secreted Lipids. J Immunol 2013, 191:1356–1363.

78. Curat CA, Miranville A, Sengenès C, Diehl M, Tonus C, Busse R, Bouloumié A: From Blood Monocytes to Adipose Tissue-Resident Macrophages: Induction of Diapedesis by Human Mature Adipocytes. Diabetes 2004, 53:1285–1292.

79. Sun K, Kusminski CCM, Scherer PEP: Adipose tissue remodeling and obesity. J Clin Invest 2011, 121:2094–2101.

80. Meng FW, Slivka PF, Dearth CL, Badylak SF: Solubilized extracellular matrix from brain and urinary bladder elicits distinct functional and phenotypic responses in macrophages. Biomaterials 2015, 46:131–140.

81. Franz S, Allenstein F, Kajahn J, Forstreuter I, Hintze V, Möller S, Simon JC: Artificial extracellular matrices composed of collagen I and high-sulfated hyaluronan promote phenotypic and functional modulation of human pro-inflammatory M1 macrophages. Acta Biomater 2013, 9:5621–5629.

82. Boyd NF, Lockwood GA, Byng JW, Tritchler DL, Yaffe MJ: Mammographic densities and breast cancer risk. Cancer Epidemiol Biomarkers Prev 1998, 7:1133–1144.

83. Coussens LM, Werb Z. Inflammation and Cancer. Nature 2002, 420:860-867.

84. Pesic M, Greten FR: Inflammation and cancer: tissue regeneration gone awry. Curr Opin Cell Biol 2016, 43:55–61.

85. Wu Y, Antony S, Meitzler JL, Doroshow JH: Molecular mechanisms underlying chronic inflammation-associated cancers. Cancer Lett 2014, 345:164–173.

86. Neuhouser ML, Aragaki AK, Prentice RL, Manson JE, Chlebowski R, Carty CL, Ochs-Balcom HM, Thomson CA, Caan BJ, Tinker LF, Urrutia RP, Knudtson J, Anderson GL: Overweight, Obesity, and Postmenopausal Invasive Breast Cancer Risk. JAMA Oncol 2015, 1:611.

87. Yang L, Zhang Y: Tumor-associated macrophages: from basic research to clinical application. J Hematol Oncol 2017, 10:58.

88. Xu X, Grijalva A, Skowronski A, Van Eijk M, Serlie MJ, Ferrante AW: Obesity activates a program of lysosomal-dependent lipid metabolism in adipose tissue macrophages independently of classic activation. Cell Metab 2013, 18:816–830.

89. Kratz M, Coats BR, Hisert KB, Hagman D, Mutskov V, Peris E, Schoenfelt KQ, Kuzma JN, Larson I, Billing PS, Landerholm RW, Crouthamel M, Gozal D, Hwang S, Singh PK, Becker L: Metabolic Dysfunction Drives a Mechanistically Distinct Proinflammatory Phenotype in Adipose Tissue Macrophages. Cell Metab 2014, 20:614–625.

90. Fujisaka S, Usui I, Bukhari A, Ikutani M, Oya T, Kanatani Y, Tsuneyama K, Nagai Y, Takatsu K, Urakaze M, Kobayashi M, Tobe K: Regulatory mechanisms for adipose tissue M1 and M2 macrophages in diet-induced obese mice. Diabetes 2009, 58:2574–2582.

91. Lumeng CN, Liu J, Geletka L, Delaney C, Delproposto J, Desai A, Oatmen K, Martinez-Santibanez G, Julius A, Garg S, Yung RL: Aging Is Associated with an Increase in T Cells and Inflammatory Macrophages in Visceral Adipose Tissue. J Immunol 2011, 187:6208–6216.

92. Fujii M, Inoguchi T, Batchuluun B, Sugiyama N, Kobayashi K, Sonoda N, Takayanagi R: CTLA-4Ig immunotherapy of obesity-induced insulin resistance by manipulation of macrophage polarization in adipose tissues. Biochem Biophys Res Commun 2013, 438:103–109.

93. Huo CW, Chew G, Hill P, Huang D, Ingman W, Hodson L, Brown KA, Magenau A, Allam AH, Mcghee E, Timpson P, Henderson MA: High mammographic density is associated with an increase in stromal collagen and immune cells within the mammary epithelium. Breast Cancer Res 2015, 17:1–20.

94. Lapeire L, Hendrix A, Lambein K, Van Bockstal M, Braems G, Van Broecke R Den, Limame R, Mestdagh P, Vesompele J, Vanhove C, Maynard D, Lehuédé C, Muller C, Valet P, Gespach CP, Bracke M, Cocquyt V, Denys H, De Wever O: Cancer-associated adipose tissue promotes breast cancer progression by paracrine oncostatin M and Jak/STAT3 signaling. Cancer Res 2014, 74:6806-

6819.

95. Lore L, An H, Evelyne L, Mieke VB, Jo V, Dawn M, Geert B, Rudy V den B, Cathérine M, Marc B, Véronique C, Hannelore D, Olivier DW: Secretome analysis of breast cancer-associated adipose tissue to identify paracrine regulators of breast cancer growth. Oncotarget 2017, 8:47239–47249.

96. Himbert C, Delphan M, Scherer D, Bowers LW, Hursting S, Ulrich CM: Signals from the adipose microenvironment and the obesity-cancer link-a systematic review. Cancer Prev Res 2017, 10:494–506.

97. Wagner M, Bjerkvig R, Wiig H, Melero-Martin JM, Lin RZ, Klagsbrun M, Dudley AC: Inflamed tumor-associated adipose tissue is a depot for macrophages that stimulate tumor growth and angiogenesis. Angiogenesis 2012, 15:481–495.

98. Hinz B, Phan SH, Thannickal VJ, Galli A, Bochaton-Piallat M-L, Gabbiani G: The myofibroblast: one function, multiple origins. Am J Pathol 2007, 170:1807–1816.

99. Headland SE, Norling LV: The resolution of inflammation: Principles and challenges. Semin Immunol 2015, 27:149–160.

100. Dvorak HF: Tumors: wounds that do not heal. N Engl J Med 1986, 315:1650–1659.

101. Tanaka M, Ikeda K, Suganami T, Komiya C, Ochi K, Shirakawa I, Hamaguchi M, Nishimura S, Manabe I, Matsuda T, Kimura K, Inoue H, Inagaki Y, Aoe S, Yamasaki S, Ogawa Y: Macrophage-inducible C-type lectin underlies obesity-induced adipose tissue fibrosis. Nat Commun 2014, 5:4982.

102. Wynn TA, Barron L: Macrophages: master regulators of inflammation and fibrosis. Semin Liver Dis 2010, 30:245–257.

103. Wynn TA, Vannella KM: Macrophages in Tissue Repair, Regeneration, and Fibrosis. Immunity 2016, 44:450–462.

104. Gruber E, Heyward C, Cameron J, Leifer C: Toll-like receptor signaling in macrophages is regulated by extracellular substrate stiffness and Rho-associated coiled-coil kinase (ROCK1/2). Int Immunol 2018, 30:267–278.

105. Lourenço BN, Springer NL, Ferreira D, Oliveira C, Granja PL, Fischbach C: CD44v6 increases gastric cancer malignant phenotype by modulating adipose stromal cell-mediated ECM remodeling. Integr Biol 2018, 10:145–158.

106. Crapo PM, Gilbert TW, Badylak SF: An overview of tissue and whole organ decellularization processes. Biomaterials 2011, 32:3233–3243.

107. Badylak SF: Decellularized Allogeneic and Xenogeneic Tissue as a Bioscaffold for Regenerative Medicine: Factors that Influence the Host Response. Ann Biomed Eng 2014, 42:1517–1527.

108. Dontu G, Ince TA: Of Mice and Women: A Comparative Tissue Biology Perspective of Breast Stem Cells and Differentiation. J Mammary Gland Biol Neoplasia 2015, 20:51–62.

109. Jain N, Vogel V: Spatial confinement downsizes the inflammatory response of macrophages. Nat Mater 2018, 17:1134–1144.

110. McCoy MG, Wei JM, Choi S, Goerger JP, Zipfel W, Fischbach C: Collagen Fiber Orientation Regulates 3D Vascular Network Formation and Alignment. ACS Biomater Sci Eng 2018, 4:2967–2976.

111. Buxboim A, Ivanovska IL, Discher DE: Matrix elasticity, cytoskeletal forces and physics of the nucleus: how deeply do cells “feel” outside and in? J Cell Sci 2010, 123:297–308.

112. Barth KA, Waterfield JD, Brunette DM: The effect of surface roughness on RAW 264.7 macrophage phenotype. J Biomed Mater Res - Part A 2013, 101 A:2679–2688.

113. Li X, Huang Q, Elkhooly TA, Liu Y, Wu H, Feng Q, Liu L, Fang Y, Zhu W, Hu T: Effects of titanium surface roughness on the mediation of osteogenesis via modulating the immune response of macrophages. Biomed Mater, 2018, 13:045013.

114. Garg K, Pullen NA, Oskeritzian CA, Ryan JJ, Bowlin GL: Macrophage functional polarization (M1/M2) in response to varying fiber and pore dimensions of electrospun scaffolds. Biomaterials, 2013, 34:4439–4451.

115. Wang Z, Cui Y, Wang J, Yang X, Wu Y, Wang K, Gao X, Li D, Li Y, Zheng XL, Zhu Y, Kong D, Zhao Q: The effect of thick fibers and large pores of electrospun poly(ε-caprolactone) vascular grafts on macrophage polarization and arterial regeneration. Biomaterials 2014, 35:5700–5710.

116. Kubow KE, Klotzsch E, Smith ML, Gourdon D, Little WC, Vogel V: Crosslinking of cell-derived 3D scaffolds up-regulates the stretching and unfolding of new extracellular matrix assembled by reseeded cells. Integr Biol, 2009, 1:635–648.

117. Baker BM, Trappmann B, Wang WY, Sakar MS, Kim IL, Shenoy VB, Burdick JA, Chen CS: Cell-mediated fibre recruitment drives extracellular matrix mechanosensing in engineered fibrillar microenvironments. Nat Mater 2015, 14:1262–1268.

118. Hashimoto D, Chow A, Noizat C, Teo P, Beasley MB, Leboeuf M, Becker CD, See P, Price J, Lucas D, Greter M, Mortha A, Boyer SW, Forsberg EC, Tanaka M, van Rooijen N, García-Sastre A, Stanley ER, Ginhoux F, Frenette PS, Merad M: Tissue-resident macrophages self-maintain locally throughout adult life with minimal contribution from circulating monocytes. Immunity 2013, 38:792–804.

119. Gomez Perdiguero E, Klapproth K, Schulz C, Busch K, Azzoni E, Crozet L, Garner H, Trouillet C, De Bruijn MF, Geissmann F, Rodewald HR: Tissue-

resident macrophages originate from yolk-sac-derived erythro-myeloid progenitors. Nature 2015, 518:547–551.

120. Arendt LM, McCready J, Keller PJ, Baker DD, Naber SP, Seewaldt V, Kuperwasser C: Obesity promotes breast cancer by CCL2-mediated macrophage recruitment and angiogenesis. Cancer Res 2013, 73:6080–6093.
121. Eccles S: Tumor-associated macrophages in breast cancer: distinct subets, distinct functions. Int J Dev Biol 2011, 55:719–729.

122. Hanahan D, Coussens LM: Accessories to the Crime: Functions of Cells Recruited to the Tumor Microenvironment. Cancer Cell, 2012, 21:309–322.

123. Afik R, Zigmond E, Vugman M, Klepfish M, Shimshoni E, Pasmanik-Chor M, Shenoy A, Bassat E, Halpern Z, Geiger T, Sagi I, Varol C: Tumor macrophages are pivotal constructors of tumor collagenous matrix. J Exp Med 2016, 213:2315–2331. 124. Pinto ML, Rios E, Silva AC, Neves SC, Caires HR, Pinto AT, Durães C, Carvalho FA, Cardoso AP, Santos NC, Barrias CC, Nascimento DS, Pinto-do-Ó P, Barbosa MA, Carneiro F, Oliveira MJ: Decellularized human colorectal cancer matrices polarize macrophages towards an anti-inflammatory phenotype promoting cancer cell invasion via CCL18. Biomaterials 2017, 124:211–224.

125. Medrek C, Ponten F, Jirstrom K, Leandersson K: The presence of tumor associated macrophages in tumor stroma as a prognostic marker for breast cancer patients. BMC Cancer 2012, 12:306.

126. Lin L, Chen YS, Yao YD, Chen JQ, Chen JN, Huang SY, Zeng YJ, Yao HR, Zeng SH, Fu YS, Song EW: CCL18 from tumor-associated macrophages promotes angiogenesis in breast cancer. Oncotarget 2015, 6:34758-34773.

127. Anders S, Pyl PT, Huber W: HTSeq-A Python framework to work with high-throughput sequencing data. Bioinformatics 2015, 31:166–169.

128. Love MI, Huber W, Anders S: Moderated estimation of fold change and dispersion for RNA-seq data with DESeq2. Genome Biol 2014, 15:1–21.

129. Subramanian A, Tamayo P, Mootha V: GSEA : Gene set enrichment analysis Gene set enrichment analysis : A knowledge-based approach for interpreting genome-wide expression profiles. Proc Natl Acad Sci USA 2005, 102:15545-15550.

130. Liberzon A, Subramanian A, Pinchback R, Thorvaldsdóttir H, Tamayo P, Mesirov JP: Molecular signatures database (MSigDB) 3.0. Bioinformatics 2011, 27:1739–1740.

131. Kuleshov MV, Jones MR, Rouillard AD, Fernandez NF, Duan Q, Wang Z, Kolev S, Jenkins SL, Jagodnik KM, Lachmann A, McDermott MG, Montiero CD, Gundersen GW, Ma'ayan A: Enrichr: a comprehensive gene set enrichment analysis web server 2016 update. Nucleic Acids Res 2016, 44:W90–W97.

132. Chen EY, Tan CM, Kou Y, Duan Q, Wang Z, Meirelles GV, Clark NR,

Ma'ayan A: Enrichr: interactive and collaborative HTML5 gene list enrichment analysis tool. BMC Bioinformatics 2013, 14:1471–2105.

133. Ojalvo LS, King W, Cox D, Pollard JW: High-Density Gene Expression Analysis of Tumor-Associated Macrophages from Mouse Mammary Tumors. Am J Pathol 2009, 174:1048–1064.

134. Fang Z, Wen C, Chen X, Yin R, Zhang C, Wang X, Huang Y: Myeloid-derived suppressor cell and macrophage exert distinct angiogenic and immunosuppressive effects in breast cancer. Oncotarget 2017, 8:54173–54186.
135. Lu H, Clauser KR, Tam WL, Fröse J, Ye X, Eaton EN, Reinhardt F, Donnenberg VS, Bhargava R, Carr SA, Weinberg RA: A breast cancer stem cell niche supported by juxtacrine signalling from monocytes and macrophages. Nat Cell Biol 2014, 16:1105-1117.

136. Gu P, Xu A: Interplay between adipose tissue and blood vessels in obesity and vascular dysfunction. Rev Endocr Metab Disord 2013, 14:49–58.
137. Carmeliet P, Jain RK: Angiogenesis in cancer and other diseases. Nature 2000, 407:249–257.

138. Hanahan D, Weinberg RA: Hallmarks of cancer: The next generation. Cell 2011, 144:646–674.

139. Lewis CE, Pollard JW: Distinct role of macrophages in different tumor microenvironments. Cancer Res 2006, 66:605–612.

140. Tariq M, Zhang J, Liang G, Ding L, He Q, Yang B: Macrophage Polarization: Anti-Cancer Strategies to Target Tumor-Associated Macrophage in Breast Cancer. J Cell Biochem 2017, 118:2484–2501.

141. Spiller KL, Anfang RR, Spiller KJ, Ng J, Nakazawa KR, Daulton JW, Vunjak-Novakovic G: The role of macrophage phenotype in vascularization of tissue engineering scaffolds. Biomaterials 2014, 35:4477–4488.

142. Sridharan R, Cameron AR, Kelly DJ, Kearney CJ, O'Brien FJ: Biomaterial based modulation of macrophage polarization: A review and suggested design principles. Mater Today 2015, 18:313–325.

143. Spiller KL, Koh TJ: Macrophage-based therapeutic strategies in regenerative medicine. Adv Drug Deliv Rev 2017, 122:74–83.

144. Petrosyan A, Da Sacco S, Tripuraneni N, Kreuser U, Lavarreda-Pearce M, Tamburrini R, De Filippo RE, Orlando G, Cravedi P, Perin L: A step towards clinical application of acellular matrix: A clue from macrophage polarization. Matrix Biol 2017, 57–58:334–346.

145. Truong D, Puleo J, Llave A, Mouneimne G, Kamm RD, Nikkhah M: Breast cancer cell invasion into a three dimensional tumor-stroma microenvironment. Sci Rep 2016, 6:1–18.

146. Han S, Shin Y, Jeong HE, Jeon JS, Kamm RD, Huh D, Sohn LL, Chung S: Constructive remodeling of a synthetic endothelial extracellular matrix. Sci Rep

2015, 5:18290.

147. Li R, Hebert JD, Lee TA, Xing H, Boussommier-Calleja A, Hynes RO, Lauffenburger DA, Kamm RD: Macrophage-secreted TNFα and TGFβ1 influence migration speed and persistence of cancer cells in 3D tissue culture via independent pathways. Cancer Res 2017, 77:279–290.

148. Shevde LA, Samant RS: Role of osteopontin in the pathophysiology of cancer. Matrix Biol 2014, 37:131–141.

149. Kiefer FW, Zeyda M, Todoric J, Huber J, Geyeregger R, Weichhart T, Aszmann O, Ludvik B, Silberhumer GR, Prager G, Stulnig TM: Osteopontin expression in human and murine obesity: Extensive local up-regulation in adipose tissue but minimal systemic alterations. Endocrinology 2008, 149:1350–1357.

150. Nomiyama T, Perez-Tilve D, Ogawa D, Gizard F, Zhao Y, Heywood EB, Jones KL, Kawamori R, Cassis LA, Tschop MH, Bruemmer D: Osteopontin mediates obesity-induced adipose tissue macrophage infiltration and insulin resistance in mice. J Clin Invest 2007, 117:2877-2888.

151. Tardelli M, Zeyda K, Moreno-Viedma V, Wanko B, Grün NG, Staffler G, Zeyda M, Stulnig TM: Osteopontin is a key player for local adipose tissue macrophage proliferation in obesity. Mol Metab 2016, 5:1131–1137.

152. Cheng J, Huo DH, Kuang DM, Yang J, Zheng L, Zhuang SM: Human macrophages promote the motility and invasiveness of osteopontin-knockdown tumor cells. Cancer Res 2007, 67:5141–5147.

153. Kale S, Raja R, Thorat D, Soundararajan G, Patil TV, Kundu GC: Osteopontin signaling upregulates cyclooxygenase-2 expression in tumor-associated macrophages leading to enhanced angiogenesis and melanoma growth via α9β1 integrin. Oncogene 2014, 33:2295-2306.

154. Esbona K, Yi Y, Saha S, Yu M, Van Doorn RR, Conklin MW, Graham DS, Wisinski KB, Ponik SM, Eliceiri KW, Wilke LG, Keely PJ: The Presence of Cyclooxygenase 2, Tumor-Associated Macrophages, and Collagen Alignment as Prognostic Markers for Invasive Breast Carcinoma Patients. Am J Pathol 2018, 188:559–573.

155. Maury E, Ehala-Aleksejev K, Guiot Y, Detry R, Vandenhooft A, Brichard SM: Adipokines oversecreted by omental adipose tissue in human obesity. Am J Physiol - Endocrinol Metab 2007, 293:656–665.

156. Meissburger B, Stachorski L, Röder E, Rudofsky G, Wolfrum C: Tissue inhibitor of matrix metalloproteinase 1 (TIMP1) controls adipogenesis in obesity in mice and in humans. Diabetologia 2011, 54:1468–1479.

157. Kim EJ, Hong JE, Eom SJ, Lee JY, Park JHY: Oral administration of benzyl-isothiocyanate inhibits solid tumor growth and lung metastasis of 4T1 murine mammary carcinoma cells in BALB/c mice. Breast Cancer Res Treat 2011, 130:61–71.

158. Previtera ML: Mechanotransduction in the Immune System. Cell Mol Bioeng 2014, 7:473–481.

159. Wen JH, Vincent LG, Fuhrmann A, Choi YS, Hribar KC, Taylor-Weiner H, Chen S, Engler AJ: Interplay of matrix stiffness and protein tethering in stem cell differentiation. Nat Mater 2014, 13:979–987.

160. Wang H, Tibbitt MW, Langer SJ, Leinwand L a, Anseth KS: Hydrogels preserve native phenotypes of valvular fibroblasts through an elasticity-regulated PI3K/AKT pathway. Proc Natl Acad Sci USA 2013, 110:19336–19341.

161. Chaudhuri O, Koshy ST, Branco da Cunha C, Shin J-W, Verbeke CS, Allison KH, Mooney DJ: Extracellular matrix stiffness and composition jointly regulate the induction of malignant phenotypes in mammary epithelium. Nat Mater 2014, 13:970–978.

162. Rubashkin MG, Cassereau L, Bainer R, DuFort CC, Yui Y, Ou G, Paszek MJ, Davidson MW, Chen YY, Weaver VM: Force engages vinculin and promotes tumor progression by enhancing PI3K activation of phosphatidylinositol (3,4,5)-triphosphate. Cancer Res 2014, 74:4597–4611.

163. Vergadi E, Ieronymaki E, Lyroni K, Vaporidi K, Tsatsanis C: Akt Signaling Pathway in Macrophage Activation and M1/M2 Polarization. J Immunol 2017, 198:1006–1014.

164. Blakney AK, Swartzlander MD, Bryant SJ: The effects of substrate stiffness on the in vitro activation of macrophages and in vivo host response to poly(ethylene glycol)-based hydrogels. J Biomed Mater Res 2012, 100A:1375–1386.

165. Zandi S, Nakao S, Chun K-H, Fiorina P, Sun D, Arita R, Zhao M, Kim E, Schueller O, Campbell S, Taher M, Melhorn MI, Schering A, Gatti F, Tezza S, Xie F, Vergani A, Yoshida S, Ishikawa K, Yamaguchi M, Sasaki F, Schmidt-Ullrich R, Hata Y, Enaida H, Yuzawa M, Yokomizo T, Kim Y-B, Sweetnam P, Ishibashi T, Hafezi-Moghadam A: ROCK-Isoform-Specific Polarization of Macrophages Associated with Age-Related Macular Degeneration. Cell Rep, The Authors, 2015, 10:1173–1186.

166. Rocher C, Singla DK: SMAD-PI3K-Akt-mTOR pathway mediates BMP-7 polarization of monocytes into M2 macrophages. PLoS One 2013, e84009.

167. Klingberg F, Chow ML, Koehler A, Boo S, Buscemi L, Quinn TM, Costell M, Alman B a, Genot E, Hinz B: Prestress in the extracellular matrix sensitizes latent TGF-B1 for activation. J Cell Biol 2014, 207:283–297.

168. Ferrante CJ, Leibovich SJ: Regulation of Macrophage Polarization and Wound Healing. Adv Wound Care 2012, 1:10–16.

169. Young DA, Choi YS, Engler AJ, Christman KL: Stimulation of adipogenesis of adult adipose-derived stem cells using substrates that mimic the stiffness of adipose tissue. Biomaterials 2013, 34:8581–8588.

170. Pelham Jr. RJ, Yu-Li W: Cell locomotion and focal adhesions are regulated by substrate flexibility. Proc Natl Acad Sci USA 1997, 94:13661–13665.

171. Khetan S, Guvendiren M, Legant WR, Cohen DM, Chen CS, Burdick JA: Degradation-mediated cellular traction directs stem cell fate in covalently crosslinked three-dimensional hydrogels. Nat Mater 2013, 12:458–465.

172. Kloxin AM, Tibbitt MW, Anseth KS: Synthesis of photodegradable hydrogels as dynamically tunable cell culture platforms. Nat Protoc 2010, 5:1867–1887.

173. Owen SC, Fisher S a., Tam RY, Nimmo CM, Shoichet MS: Hyaluronic acid click hydrogels emulate the extracellular matrix. Langmuir 2013, 29:7393–7400.

174. Nguyen D-HT, Stapleton SC, Yang MT, Cha SS, Choi CK, Galie PA, Chen CS: Biomimetic model to reconstitute angiogenic sprouting morphogenesis in vitro. Proc Natl Acad Sci USA 2013, 110:6712–6717.

175. Yang C, Tibbitt MW, Basta L, Anseth KS: Mechanical memory and dosing influence stem cell fate. Nat Mater 2014, 13:645–652.

176. Patterson J, Hubbell JA: Enhanced proteolytic degradation of molecularly engineered PEG hydrogels in response to MMP-1 and MMP-2. Biomaterials, 2010, 31:7836–7845.

177. Chwalek K, Tsurkan M V, Freudenberg U, Werner C: Glycosaminoglycan-based hydrogels to modulate heterocellular communication in in vitro angiogenesis models. Sci Rep 2014, 4:4414.

178. Highley CB, Rodell CB, Kim IL, Wade RJ, Burdick JA: Ordered, adherent layers of nanofibers enabled by supramolecular interactions. J Mater Chem B Mater Biol Med 2014, 2:8110–8115.

179. Baker BM, Trappmann B, Wang WY, Sakar MS, Kim IL, Shenoy VB, Burdick JA, Chen CS: Cell-mediated fibre recruitment drives extracellular matrix mechanosensing in engineered fibrillar microenvironments. Nat Mater 2015, 14:1262-1268.

180. Brownfield DG, Venugopalan G, Lo A, Mori H, Tanner K, Fletcher DA, Bissell MJ: Patterned collagen fibers orient branching mammary epithelium through distinct signaling modules. Curr Biol 2013, 23:703–709.

181. Panzetta V, Fusco S, Netti PA: Cell mechanosensing is regulated by substrate strain energy rather than stiffness. Proc Natl Acad Sci USA 2019, 116:22004-22013.

182. Li R, Serrano JC, Xing H, Lee TA, Azizgolshani H, Zaman M, Kamm RD: Interstitial flow promotes macrophage polarization toward an M2 phenotype. Mol Biol Cell 2018, 29:1927–1940.

183. Morgan JP, Delnero PF, Zheng Y, Verbridge SS, Chen J, Craven M, Choi NW, Diaz-Santana A, Kermani P, Hempstead B, López JA, Corso TN, Fischbach C,

Stroock AD: Formation of microvascular networks in vitro. Nat Protoc 2013, 8:1820–1836.

184. Miller JS, Stevens KR, Yang MT, Baker BM, Nguyen D-HT, Cohen DM, Toro E, Chen AA, Galie PA, Yu X, Chaturvedi R, Bhatia SN, Chen CS: Rapid casting of patterned vascular networks for perfusable engineered three-dimensional tissues. Nat Mater 2012, 11:768–774.

185. Ragelle H, Naba A, Larson BL, Zhou F, Prijić M, Whittaker CA, Del Rosario A, Langer R, Hynes RO, Anderson DG: Comprehensive proteomic characterization of stem cell-derived extracellular matrices. Biomaterials 2017, 128:147–159.

186. Calle EA, Hill RC, Leiby KL, Le A V., Gard AL, Madri JA, Hansen KC, Niklason LE: Targeted proteomics effectively quantifies differences between native lung and detergent-decellularized lung extracellular matrices. Acta Biomater 2016, 46:91–100.

187. Kuljanin M, Brown CFC, Raleigh MJ, Lajoie GA, Flynn LE: Collagenase treatment enhances proteomic coverage of low-abundance proteins in decellularized matrix bioscaffolds. Biomaterials 2017, 144:130–143.

188. Pinto ML, Rios E, Silva AC, Neves SC, Caires HR, Pinto AT, Durães C, Carvalho FA, Cardoso AP, Santos NC, Barrias CC, Nascimento DS, Pinto-do-Ó P, Barbosa MA, Carneiro F, Oliveira MJ: Decellularized human colorectal cancer matrices polarize macrophages towards an anti-inflammatory phenotype promoting cancer cell invasion via CCL18. Biomaterials 2017, 124:211–224.

189. Magno V, Friedrichs J, Weber HM, Prewitz MC, Tsurkan M V., Werner C: Macromolecular crowding for tailoring tissue-derived fibrillated matrices. Acta Biomater 2017, 55:109–119.

190. Tsai CK, Chen YS, Wu PC, Hsieh TY, Liu HW, Yeh CY, Lin WL, Chia JS, Liu TM: Imaging granularity of leukocytes with third harmonic generation microscopy. Biomed Opt Express 2012, 3:2234.

191. Chen C-K, Liu T-M: Imaging morphodynamics of human blood cells in vivo with video-rate third harmonic generation microscopy. Biomed Opt Express 2012, 3:2860.

192. Wu PC, Hsieh TY, Tsai ZU, Liu TM: In vivo Quantification of the Structural Changes of Collagens in a Melanoma Microenvironment with Second and Third Harmonic Generation Microscopy. Sci Rep 2015, 5:34–38.

193. Shapouri-Moghaddam A, Mohammadian S, Vazini H, Taghadosi M, Esmaeili SA, Mardani F, Seifi B, Mohammadi A, Afshari JT, Sahebkar A: Macrophage plasticity, polarization, and function in health and disease. J Cell Physiol 2018, 233:6425–6440.

194. Jablonski KA, Amici SA, Webb LM, Ruiz-Rosado JDD, Popovich PG, Partida-Sanchez S, Guerau-De-arellano M: Novel markers to delineate murine M1 and M2 macrophages. PLoS One 2015, 10:5–11.

195. Kratz M, Coats BR, Hisert KB, Hagman D, Mutskov V, Peris E, Schoenfelt KQ, Kuzma JN, Larson I, Billing PS, Landerholm RW, Crouthamel M, Gozal D, Hwang S, Singh PK, Becker L: Metabolic dysfunction drives a mechanistically distinct proinflammatory phenotype in adipose tissue macrophages. Cell Metab 2014, 20:614–625.

196. Brake DK, Smith CW: Flow cytometry on the stromal-vascular fraction of white adipose tissue. Methods Mol Biol 2008, 456:221–229.

197. Cho KW, Morris DL, Lumeng CN: Flow cytometry analyses of adipose tissue macrophages. Methods Enzymol 2014, 537:297–314.

198. Dixon AR, Bathany C, Tsuei M, White J, Barald KF, Takayama S: Recent developments in multiplexing techniques for immunohistochemistry. Expert Rev Mol Diagn 2015, 15:1171–1186.

199. Lee SSY, Bindokas VP, Lingen MW, Kron SJ: Nondestructive, multiplex three-dimensional mapping of immune infiltrates in core needle biopsy. Lab Investig 2019, 99:1400–1413.

200. Blom S, Paavolainen L, Bychkov D, Turkki R, Mäki-Teeri P, Hemmes A, Välimäki K, Lundin J, Kallioniemi O, Pellinen T: Systems pathology by multiplexed immunohistochemistry and whole-slide digital image analysis. Sci Rep 2017, 7:1–13.

201. Liu H, McDowell TL, Hanson NE, Tang X, Fujimoto J, Rodriguez-Canales J: Laser Capture Microdissection for the Investigative Pathologist. Vet Pathol 2014, 51:257–269.

202. Xu K, Tian X, Oh SY, Movassaghi M, Naber SP, Kuperwasser C, Buchsbaum RJ: The fibroblast Tiam1-osteopontin pathway modulates breast cancer invasion and metastasis. Breast Cancer Res 2016, 18:1–15.

203. Sharon Y, Raz Y, Cohen N, Ben-Shmuel A, Schwartz H, Geiger T, Erez N: Tumor-derived osteopontin reprograms normal mammary fibroblasts to promote inflammation and tumor growth in breast cancer. Cancer Res 2015, 75:963–973.

204. Arwert EN, Harney AS, Entenberg D, Wang Y, Sahai E, Pollard JW, Condeelis JS: A Unidirectional Transition from Migratory to Perivascular Macrophage Is Required for Tumor Cell Intravasation. Cell Rep 2018, 23:1239–1248.

205. Qian BZ, Li J, Zhang H, Kitamura T, Zhang J, Campion LR, Kaiser EA, Snyder LA, Pollard JW: CCL2 recruits inflammatory monocytes to facilitate breast-tumour metastasis. Nature 2011, 475:222–225.

206. Rossi EL, De Angel RE, Bowers LW, Khatib SA, Smith LA, Van Buren E, Bhardwaj P, Giri D, Estecio MR, Troester MA, Hair BY, Kirk EL, Gong T, Shen J, Dannenberg AJ, Hursting SD: Obesity-associated alterations in inflammation, epigenetics, and mammary tumor growth persist in formerly obese mice. Cancer Prev Res 2016, 9:339–348.

207. Cousminer DL, Berry DJ, Timpson NJ, Ang W, Thiering E, Pouta A, Das S, Lagou V, Power C, Prokopenko I: Genome-wide association and longitudinal analyses reveal genetic loci linking pubertal height growth, pubertal timing and childhood adiposity. 2013, 22:2735–2747.

208. Izquierdo AG, Crujeiras AB: Obesity-Related Epigenetic Changes After Bariatric Surgery. Front Endocrinol 2019, 10:1–12.

209. Wen LM, Rissel C, He G: The Effect of Early Life Factors and Early Interventions on Childhood Overweight and Obesity. J Obes 2017;3642818.

210. Pérez LM, Pareja-Galeano H, Sanchis-Gomar F, Emanuele E, Lucia A, Gálvez BG: 'Adipaging': ageing and obesity share biological hallmarks related to a dysfunctional adipose tissue. J Physiol 2016, 594:3187–3207.

211. Mikuła-Pietrasik J, Uruski P, Tykarski A, Książek K: The peritoneal "soil" for a cancerous "seed": a comprehensive review of the pathogenesis of intraperitoneal cancer metastases. Cell Mol Life Sci 2018, 75:509–525.

212. Liu Y, Cao X: Characteristics and Significance of the Pre-metastatic Niche. Cancer Cell 2016, 30:668–681.

213. Gandellini P, Andriani F, Merlino G, D'Aiuto F, Roz L, Callari M: Complexity in the tumour microenvironment: Cancer associated fibroblast gene expression patterns identify both common and unique features of tumour-stroma crosstalk across cancer types. Semin Cancer Biol 2015, 35:96–106.

214. Friedl P, Alexander S: Cancer invasion and the microenvironment: Plasticity and reciprocity. Cell 2011, 147:992–1009.

215. Dehne N, Mora J, Namgaladze D, Weigert A, Brüne B: Cancer cell and macrophage cross-talk in the tumor microenvironment. Curr Opin Pharmacol 2017, 35:12–19.

216. Varol C, Sagi I: Phagocyte-extracellular matrix crosstalk empowers tumor development and dissemination. FEBS J 2018, 285:734–751.

217. Kennedy PJ, Sousa F, Ferreira D, Pereira C, Nestor M, Oliveira C, Granja PL, Sarmento B: Fab-conjugated PLGA nanoparticles effectively target cancer cells expressing human CD44v6. Acta Biomater 2018, 81:208–218.

218. Pathi SP, Kowalczewski C, Tadipatri R, Fischbach C: A novel 3-D mineralized tumor model to study breast cancer bone metastasis. PLoS One 2010, 5:1–10.

219. Infanger DW, Cho YJ, Lopez BS, Mohanan S, Liu SC, Gursel D, Boockvar JA, Fischbach C: Glioblastoma stem cells are regulated by interleukin-8 signaling in a tumoral perivascular niche. Cancer Res 2013, 73:7079–7089.

220. Hu M, Yao J, Carroll DK, Weremowicz S, Chen H, Carrasco D, Richardson A, Violette S, Nikolskaya T, Nikolsky Y, Bauerlein EL, Hahn WC, Gelman RS, Allred C, Bissell MJ, Schnitt S, Polyak K: Regulation of In Situ to Invasive Breast Carcinoma Transition. Cancer Cell 2008, 13:394–406.

221. Clevers H: The cancer stem cell: premises, promises and challenges. Nat Med, Nature Publishing Group, 2011, 17:313–319.

222. Zheng Q, Banaszak L, Fracci S, Basali D, Dunlap SM, Hursting SD, Rich JN, Hjlemeland AB, Vasanji A, Berger NA, Lathia JD, Reizes O: Leptin receptor maintains cancer stem-like properties in triple negative breast cancer cells. Endocr Relat Cancer 2013, 20:797–808.

223. Al-Hajj M, Wicha MS, Benito-Hernandez A, Morrison SJ, Clarke MF: Prospective identification of tumorigenic breast cancer cells. Proc Natl Acad Sci USA 2003, 100:3983–3988.

224. Jeter CR, Badeaux M, Choy G, Chandra D, Patrawala L, Liu C, Calhoun-Davis T, Zaehres H, Daley GQ, Tang DG: Functional evidence that the self-renewal gene NANOG regulates human tumor development. Stem Cells 2009, 27:993–1005.

225. Sampieri K, Fodde R: Cancer stem cells and metastasis. Semin Cancer Biol, 2012, 22:187–193.

226. Brabletz T, Jung A, Spaderna S, Hlubek F, Kirchner T: Opinion: migrating cancer stem cells - an integrated concept of malignant tumour progression. Nat Rev Cancer 2005, 5:744–749.

227. Begum A, Ewachiw T, Jung C, Huang A, Norberg KJ, Marchionni L, McMillan R, Penchev V, Rajeshkumar NV, Maitra A, Wood L, Wang C, Wolfgang C, Dejesus-Acosta A, Laheru D, Shapiro IM, Padval M, Pachter JA, Weaver DT, Rasheed ZA, Matsui W: The extracellular matrix and focal adhesion kinase signaling regulate cancer stem cell function in pancreatic ductal adenocarcinoma. PLoS One 2017, 12:1–21.

228. Northey JJ, Przybyla L, Weaver VM: Tissue force programs cell fate and tumor aggression. Cancer Discov 2017, 7:1224–1237.

229. Thiagarajan PS, Hitomi M, Hale JS, Alvarado AG, Otvos B, Sinyuk M, Stoltz K, Wiechert A, Mulkearns-Hubert E, Jarrar A, Zheng Q, Thomas D, Egelhoff T, Rich JN, Liu H, Lathia JD, Reizes O: Development of a Fluorescent Reporter System to Delineate Cancer Stem Cells in Triple-Negative Breast Cancer. Stem Cells 2015, 33:2114-2125.

230. Springer NL, Iyengar NM, Bareja R, Verma A, Jochelson M, Giri DD, Zhou XK, Elemento O, Dannenberg AJ, Fischbach C: Obesity-Associated Extracellular Matrix Remodeling Promotes a Macrophage Phenotype Similar to Tumor-Associated Macrophages. Am J Pathol 2019, 189:2019–2035.